# STEREOCHEMISTRY AS A MECHANISTIC PROBE IN PHOTOAQUATION OF CHROMIUM(III) COMPLEXES

by

Sellapperumage Rupasiri Lakshman Fernando

B.Sc., University of Colombo, Sri Lanka, 1985

A Dissertation Submitted in Partial Fulfillment of the

Requirements for the Degree of

DOCTOR OF PHILOSOPHY

in the Department of Chemistry

We accept this dissertation as confirming to the required standard

Dr. Alexander D. Kirk, Supervisor (Department of Chemistry)

Dr. David A. Harrington (Department of Chemistry)

Dr. Peter C. Wan (Department of Chemistry)

Dr. George A. Beer (Department of Physics)

Dr. Ross H. Hill, External Examiner (Simon Fraser University)

Name

*Dissertation Abstracts International* is arranged by broad, general subject categories. Please select the one subject which most nearly describes the content of your dissertation. Enter the corresponding four digit code in the spaces provided.

SUBJECT TERM

SUBJECT CODE

U·M·I

## Subject Categories

# THE HUMANITIES AND SOCIAL SCIENCES

### COMMUNICATIONS AND THE ARTS

Architecture 0729
Art History 0377
Cinema 0900
Dance 0378
Fine Arts 0357
Information Science 0723
Journalism 0391
Library Science 0399
Mass Communications 0708
Music 0413
Speech Communication 0459
Theater 0465

### EDUCATION

General 0515
Administration 0514
Adult and Continuing 0516
Agricultural 0517
Art 0273
Bilingual and Multicultural 0282
Business 0688
Community College 0275
Curriculum and Instruction 0727
Early Childhood 0518
Elementary 0524
Finance 0277
Guidance and Counseling 0519
Health 0680
Higher 0745
History of 0520
Home Economics 0278
Industrial 0521
Language and Literature 0279
Mathematics 0280
Music 0522
Philosophy of 0998
Physical 0523

Psychology 0525
Reading 0535
Religious 0527
Sciences 0714
Secondary 0533
Social Sciences 0534
Sociology of 0340
Special 0529
Teacher Training 0530
Technology 0710
Tests and Measurements 0288
Vocational 0747

### LANGUAGE, LITERATURE AND LINGUISTICS

Language
General 0679
Ancient 0289
Linguistics 0290
Modern 0291
Literature
General 0401
Classical 0294
Comparative 0295
Medieval 0297
Modern 0298
African 0316
American 0591
Asian 0305
Canadian (English) 0352
Canadian (French) 0355
English 0593
Germanic 0311
Latin American 0312
Middle Eastern 0315
Romance 0313
Slavic and East European 0314

### PHILOSOPHY, RELIGION AND THEOLOGY

Philosophy 0422
Religion
General 0318
Biblical Studies 0321
Clergy 0319
History of 0320
Philosophy of 0322
Theology 0469

### SOCIAL SCIENCES

American Studies 0323
Anthropology
Archaeology 0324
Cultural 0326
Physical 0327
Business Administration
General 0310
Accounting 0272
Banking 0770
Management 0454
Marketing 0338
Canadian Studies 0385
Economics
General 0501
Agricultural 0503
Commerce-Business 0505
Finance 0508
History 0509
Labor 0510
Theory 0511
Folklore 0358
Geography 0366
Gerontology 0351
History
General 0578

Ancient 0579
Medieval 0581
Modern 0582
Black 0328
African 0331
Asia, Australia and Oceania 0332
Canadian 0334
European 0335
Latin American 0336
Middle Eastern 0333
United States 0337
History of Science 0585
Law 0398
Political Science
General 0615
International Law and Relations 0616
Public Administration 0617
Recreation 0814
Social Work 0452
Sociology
General 0626
Criminology and Penology 0627
Demography 0938
Ethnic and Racial Studies 0631
Individual and Family Studies 0628
Industrial and Labor Relations 0629
Public and Social Welfare 0630
Social Structure and Development 0700
Theory and Methods 0344
Transportation 0709
Urban and Regional Planning 0999
Women's Studies 0453

# THE SCIENCES AND ENGINEERING

### BIOLOGICAL SCIENCES

Agriculture
General 0473
Agronomy 0285
Animal Culture and Nutrition 0475
Animal Pathology 0476
Food Science and Technology 0359
Forestry and Wildlife 0478
Plant Culture 0479
Plant Pathology 0480
Plant Physiology 0817
Range Management 0777
Wood Technology 0746
Biology
General 0306
Anatomy 0287
Biostatistics 0308
Botany 0309
Cell 0379
Ecology 0329
Entomology 0353
Genetics 0369
Limnology 0793
Microbiology 0410
Molecular 0307
Neuroscience 0317
Oceanography 0416
Physiology 0433
Radiation 0821
Veterinary Science 0778
Zoology 0472
Biophysics
General 0786
Medical 0760

### EARTH SCIENCES

Biogeochemistry 0425
Geochemistry 0996

Geodesy 0370
Geology 0372
Geophysics 0373
Hydrology 0388
Mineralogy 0411
Paleobotany 0345
Paleoecology 0426
Paleontology 0418
Paleozoology 0985
Palynology 0427
Physical Geography 0368
Physical Oceanography 0415

### HEALTH AND ENVIRONMENTAL SCIENCES

Environmental Sciences 0768
Health Sciences
General 0566
Audiology 0300
Chemotherapy 0992
Dentistry 0567
Education 0350
Hospital Management 0769
Human Development 0758
Immunology 0982
Medicine and Surgery 0564
Mental Health 0347
Nursing 0569
Nutrition 0570
Obstetrics and Gynecology 0380
Occupational Health and Therapy 0354
Ophthalmology 0381
Pathology 0571
Pharmacology 0419
Pharmacy 0572
Physical Therapy 0382
Public Health 0573
Radiology 0574
Recreation 0575

Speech Pathology 0460
Toxicology 0383
Home Economics 0386

### PHYSICAL SCIENCES

#### Pure Sciences

Chemistry
General 0485
Agricultural 0749
Analytical 0486
Biochemistry 0487
Inorganic 0488
Nuclear 0738
Organic 0490
Pharmaceutical 0491
Physical 0494
Polymer 0495
Radiation 0754
Mathematics 0405
Physics
General 0605
Acoustics 0986
Astronomy and Astrophysics 0606
Atmospheric Science 0608
Atomic 0748
Electronics and Electricity 0607
Elementary Particles and High Energy 0798
Fluid and Plasma 0759
Molecular 0609
Nuclear 0610
Optics 0752
Radiation 0756
Solid State 0611
Statistics 0463

#### Applied Sciences

Applied Mechanics 0346
Computer Science 0984

Engineering
General 0537
Aerospace 0538
Agricultural 0539
Automotive 0540
Biomedical 0541
Chemical 0542
Civil 0543
Electronics and Electrical 0544
Heat and Thermodynamics 0348
Hydraulic 0545
Industrial 0546
Marine 0547
Materials Science 0794
Mechanical 0548
Metallurgy 0743
Mining 0551
Nuclear 0552
Packaging 0549
Petroleum 0765
Sanitary and Municipal 0554
System Science 0790
Geotechnology 0428
Operations Research 0796
Plastics Technology 0795
Textile Technology 0994

### PSYCHOLOGY

General 0621
Behavioral 0384
Clinical 0622
Developmental 0620
Experimental 0623
Industrial 0624
Personality 0625
Physiological 0989
Psychobiology 0349
Psychometrics 0632
Social 0451

Supervisor: Dr. A. D. Kirk

## Abstract

The unifying theme of this dissertation is the use of stereochemistry as a probe of mechanism in Cr(III) photosubstitution reactions.

Mechanistic stereochemical change has been shown to be a requirement for axial photoaquation reactions of Cr(III) complexes but the situation for equatorial ligand loss is less clear. To explore this, *trans*-[Cr(2,3,2-tet)$(CN)_2$]$(ClO_4)$, (2,3,2-tet = N,N'-Bis(2-aminoethyl)-1,3-propanediamine) was prepared and characterized. It was photo-labile with a proton uptake quantum yield of 0.09 ± 0.01 in acidic aqueous solution. No detectable amount of $CN^-$ was photoreleased ($\Phi_{CN^-} \leq 0.02$) and the major photoproduct was Cr(2,3,2-tetH)$(H_2O)(CN)_2^{2+}$. In neutral or basic media this product exhibited rapid ($t_{1/2}$ = 8 min in pH 6 at 25°C) thermal recoordination of the dangling amine ligand giving Cr(2,3,2-tet)$(CN)_2^+$. HPLC study of the stereochemistry of this recoordination and the ligand field analysis of the visible spectrum showed that the photoproduct was *trans*-Cr(2,3,2-tetH)$(H_2O)(CN)_2^{2+}$. Flash photolysis experiments with conductivity detection showed that the reaction goes completely via the doublet state. The thermal and emission properties were also investigated.

In the $^4B_{2g}$ lowest energy state of the molecule the ligand motion required for *trans* attack in the equatorial plane is obstructed by the 2,3,2-tet ligand. If stereochemical change is a requirement for substitution from this state it should therefore be photo-inert . The higher energy $^4E_g$ state could be photoactive but the photoproduct would be expected to be *cis*-Cr(2,3,2-tetH)$(H_2O)(CN)_2^{2+}$. Since the *trans* product was observed we conclude that

mechanistic stereochemical change is not a requirement for photoaquation of *trans*-$Cr(2,3,2\text{-tet})(CN)_2^+$. This complete stereoretentive photoreaction observed is unusual and is discussed in terms of existing theoretical models.

For studies of wavelength dependence of products and their stereochemistry, the compound *trans*-$[Cr(tn)_2(CN)_2]ClO_4$, was prepared and characterized (tn = 1,3-diaminopropane). Both cyanide and tn of the molecule were photoaquated. The proton uptake measurements showed that the photolysis behavior was nonlinear owing to quenching of the photoreactant doublet state by photoproducts. The total product quantum yields were therefore based on the zero time slopes of the proton uptake data. Quantum yields are; (irradiation wavelength, nm): $\Phi(CN^-)$, $\Phi(tnH^+)$; 436: 0.035 ± 0.004, 0.048 ± 0.005; 458: 0.023 ± 0.004. 0.052 ± 0.004. Loss of cyanide is not predicted by photochemical theory and its occurrence is attributed to the role of ligand interactions in directing photoaquation modes. The quenching by photoproducts, however, made *trans*-$Cr(tn)_2(CN)_2^+$ unsuitable for the wavelength dependence studies.

Wavelength dependence of the product distribution in the prompt photoaquation of $Cr(tn)_3^{3+}$ has previously been reported. The commonly used quenchers in such studies of excited state reactivity are $OH^-$, $Cr(CN)_6^{3-}$ and $Cr(ox)_3^{3-}$. They have not been suitable in all instances due to various problems such as reactive quenching, instability of compounds in base, precipitation of highly charged cationic complexes, significant absorption of visible light or solubility problems in aqueous solutions. We report the synthesis and characterization of $Na[Cr(tn)(CN)_4]$. This compound showed the necessary thermo ($t_{1/2} \approx 5$ hours in pH 2 at 20°C) and photo ($\Phi_{tot} = 0.04 \pm 0.01$) stability and was free from the above problems.

The wavelength effect in $Cr(tn)_3^{3+}$ was reinvestigated and the percentage *cis*-$Cr(tn)_2(tnH)(H_2O)^{4+}$ product found was 38 ± 1% for the unquenched reaction and 47% for the prompt reaction, whether the quencher was $Cr(tn)(CN)_4^-$ or $OH^-$. These percentages differ from the values reported previously and the implications of these new results are discussed.

Examiners:

Dr. Alexander D. Kirk, Supervisor (Department of Chemistry)

Dr. David A. Harrington (Department of Chemistry)

Dr. Peter C. Wan (Department of Chemistry)

Dr. George A. Beer (Department of Physics)

Dr. Ross H. Hill, External Examiner (Simon Fraser University)

## Table of Contents

# List of Tables

## List of Figures

## List of Abbreviations

| | |
|---|---|
| bipy | 2,2'-bipyridine |
| cyclam | 1,4,8,11-tetraazacyclotetradecane |
| en | 1,2-diaminoethane |
| phen | 1,10-phenanthroline |
| tn | 1,3-diaminopropane |
| tacn | 1,4,7-triazacyclononane |
| 2,3,2-tet | N,N'-Bis(2-aminoethyl)-1,3-propanediamine |
| 3,2,3-tet | N,N'-Bis(3-aminoprpyl)-1,2-ethylenediamine |
| teta | 5,12-meso-5,7,7,12,14,14-hexamethyl-1,4,8,11-tetraazacyclotetradecane |
| | |
| am(m)ine | amine and/or ammine |
| A | Ammonia |
| AOM | Angular Overlap Model |
| ax | axial |
| *c* | *cis* |
| CF | Crystal Field |
| D | Doublet |
| dc | direct current |
| DMF | dimethylformamide |
| DMSO | dimethylsulphoxide |
| eq | equatorial |
| h | hour |
| HPLC | High Pressure Liquid Chromatography |
| $I^*$ | Excited state bond energy |
| IE | Ion Exchange |
| I/O | Input/Output |
| IP | Ion Pair |
| IR | Infra Red |
| L | Ligand |

| | |
|---|---|
| LF | Ligand Field |
| MO | Molecular Orbital |
| N | coordinated nitrogen of an am(m)ine |
| nm | nanometre |
| ns | nanosecond |
| Q | Quartet |
| RB | Round Bottom |
| RP | Reversed Phase |
| s | second |
| SP | Square Pyramidal |
| *t* | *trans* |
| TBP | Trigonal bipyramidal |
| TM | transition metal |
| UV/Vis | Ultra Violet and Visible |
| V | Volts |
| VB | Valence Bond |
| VC | Vanquickenborne and Ceulemans |
| W | Water |

| | |
|---|---|
| $\varepsilon$ | molar absorptivity |
| $\Phi$ | quantum yield |
| $\lambda$ | wavelength |
| $\mu$ | micro |
| $\tau$ | lifetime |

## Acknowledgments

I wish to express my sincere gratitude to my research supervisor Dr. A. D. Kirk for his help and guidance throughout the course of this work, and for permitting me to use several figures created by him. I am thankful to Dr. D. A. House for his assistance with the synthetic aspects and helpful ideas. I owe a word of appreciation to the technical staff in the instrument, mechanical and glass shops for their kind assistance during this work.

I express my appreciation to all the members of the department of chemistry especially to fellow graduate students, past and present, for generating a wonderful working environment.

This dissertation is dedicated

to my beloved father and mother

# CHAPTER ONE

## Introduction

## 1.1 General

Photochemistry is a branch of science dealing with the interaction of light with matter. "Photochemistry is likely the key for the origin of life on the earth, played a fundamental role in life evolution, and it is responsible, through the photosynthetic process that takes place in green plants, for the maintenance of all living organisms."[1] Photochemistry is important in many biological and environmental processes such as vision and control of ozone in the upper atmosphere. Practical applications of photochemistry include solar energy conversion, imaging, photography and chemical synthesis.

Photochemistry of transition metal complexes is of fundamental importance in a variety of contexts including various applications,[2, 3] and it has been the subject of many reviews [3-5] Cr(III) complexes are among the most extensively studied systems.[6-13] The important reasons[6] for this are the availability of a large variety of relatively thermally stable complexes, their interesting and fairly well understood absorption and emission spectroscopy, the comparative efficiency of their photochemical reactions and the fact that many of these molecules emit under room temperature solution conditions, permitting simultaneous studies of photochemistry and photophysics. The present work deals with the understanding of the stereochemical aspects of photoprocesses of Cr(III) complexes. To begin this dissertation some basic concepts relevant to photochemistry and photophysics of Cr(III) complexes are described.

## 1.2 Theoretical Approaches to the Electronic Structure of Transition Metal Complexes

The best approach to the electronic structure of complexes is provided by the molecular orbital (MO) theory. In order to obtain quantitative results using this theory, however, a great deal of computational effort is required.[13] As a consequence, more convenient, alternative theories have frequently been used to describe the bonding and structure of complexes. They are mainly valence bond (VB) theory, crystal field (CF) theory and ligand field (LF) theory.

VB theory is substantially inadequate for describing the electronic structure of transition metal (TM) complexes. Moreover, this theory does not take the existence of electronic excited states into account. CF theory, on the other hand, has been remarkably successful in explaining many features of transition metal complexes and historically, it has been the driving force for the development of the entire field of inorganic coordination chemistry.[14] Despite its striking results, this purely electrostatic model is unsatisfactory in explaining many features of TM complexes.

LF theory preserves all the conceptual and computational advantages of the simple CF theory and includes the covalent character between the metal ligand bonds. Therefore LF theory is superior to CF theory and enjoys a wide application in TM complexes.

In LF theory, the energy gap between $t_{2g}$ and $e_g$ set of orbitals of an octahedral complex is designated as $\Delta$, whereas in CF theory, it is 10Dq. In recent literature, however, 10Dq has been considered as an experimentally determined parameter and therefore $\Delta$ and 10Dq are equal. In this dissertation, we also continue this usage.

Several semi-empirical MO approaches which incorporate some metal ligand overlap have been reported.[14] Even though they have not been widely used, they led to the development of a powerful analytical procedure, the orbital angular overlap model (section 1.2.1). This model has been successfully used in developing photochemical theories of Cr(III) complexes (sections 1.5 and 1.6) and it is important to discuss its basis.

### 1.2.1 Angular Overlap Model (AOM)

In this model the energy levels of a complex molecule $ML_n$ are obtained simply by summing the perturbation of each ligand L on the five d orbitals of the central metal ion, carefully taking into account their geometric relationship to each other.[14] The sigma and pi bonding effect of each ligand L is specified with AOM parameters, $\sigma_L$ and $\pi_L$.

The z axis of each ligand is retained collinear with its metal ligand bond and pointing towards the metal. The z axis of the metal is defined to be collinear with one of the metal ligand bonds in turn, and then the other metal ligand bonds lie along or between other axes. The ligand on the z axis yields a $\sigma$ interaction with the $d_{z2}$ orbital and $\pi$ interactions with the $d_{xz}$ and $d_{yz}$ orbitals. The contribution of each ligand to the energies of all five d orbitals is calculated and the total perturbation energy of each orbital is obtained by taking the summation.

The energies of d orbitals calculated in the above manner for hexacoordinated complexes with tetragonal symmetry are given by the following equations.[14]

$$E(z^2) = 2\sigma_{ax} + \sigma_{eq} \quad (1.2.1)$$

$$E(x^2 - y^2) = 3\sigma_{eq} \quad (1.2.2)$$

$$E(xz) = 2\pi_{ax} + 2\pi_{eq} \quad (1.2.3)$$

$$E(yz) = 2\pi_{ax} + 2\pi_{eq} \quad (1.2.4)$$

$$E(xy) = 4\pi_{eq} \quad (1.2.5)$$

where $\sigma_{ax}$ , $\sigma_{eq}$ , $\pi_{ax}$ and $\pi_{eq}$ represent the average axial and equatorial $\sigma$ and $\pi$ parameters. While usually $\sigma > 0$, $\pi$ values may be >0 or <0 depending whether the ligand is a $\pi$ donor or a $\pi$ acceptor.

In the case of an $O_h$ symmetry molecule, the axial and equatorial parameters are equal and then the above equations show that the energy difference between the $t_{2g}$ and $e_g$ sets of orbitals is $3\sigma - 4\pi$. Therefore the correlation between AOM parameters and LF theory parameters can be written as follows.

$$10Dq = 3\sigma - 4\pi \quad (1.2.6)$$

The similar relationships for tetragonal symmetry molecules can be represented by the following equations.

$$10Dq_{ax} = 3\sigma_{ax} - 4\pi_{ax} \quad (1.2.7)$$

$$10Dq_{eq} = 3\sigma_{eq} - 4\pi_{eq} \quad (1.2.8)$$

AOM and LF theory relationships and expressions for orbital energies for complexes with other symmetries can be derived.[14]

## 1.3 Electronic States and Spectra of Cr(III) Complexes

Cr(III) ion has a $d^3$ ground state electronic configuration ($t_{2g}^3 e_g^0$) with three unpaired electrons. Therefore the ground state is a quartet, in contrast to singlets in the majority of molecules.

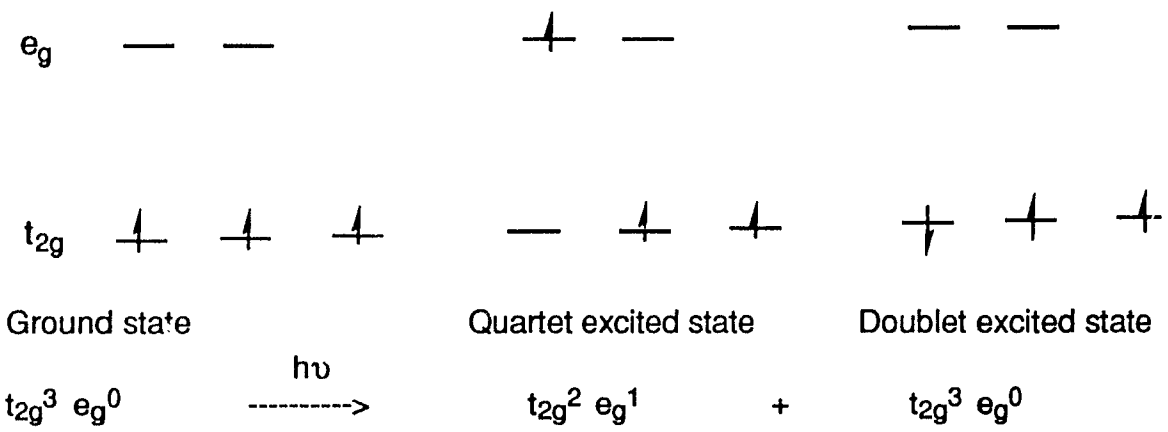


**Fig. 1.3.1** A simple Ligand Field Theory representation of the orbital electron distribution in ground state, and doublet and quartet excited states.

Electronic excitation produces an excited quartet state with $t_{2g}^2\ e_g^1$ configuration. This can convert by intersystem crossing (section 1.4) to a doublet excited state with spin paired $t_{2g}^3\ e_g^o$ configuration. Fig. 1.3.1 shows a simple LF theory representation of the orbital electron distribution, corresponding to these states of an octahedral complex.

The group theoretical term symbols for these states of an $O_h$ molecule are $^4A_{2g}$, $^4T_{2g}$ and $^2E_g$ (Fig. 1.3.2). In the electronic spectra of $O_h$ Cr(III) complexes, the lowest energy bands correspond to the $^4T_{2g}$ <--- $^4A_{2g}$ transition in the quartet absorption and $^4A_{2g}$ <--- $^2E_g$ in doublet emission. The former transition is equivalent to a 45° rotation of charge density in one of the three orthogonal planes (xy, xz or yz) since the appropriate orbitals involved are $d_{xy}$ ---> $d_{x^2-y^2}$, $d_{xz}$ ---> $d_{x^2-z^2}$ and $d_{yz}$ ---> $d_{y^2-z^2}$, where $d_{x^2-z^2}$ and $d_{y^2-z^2}$ are linear combinations of the $d_{z^2}$ and $d_{x^2-y^2}$ orbitals.

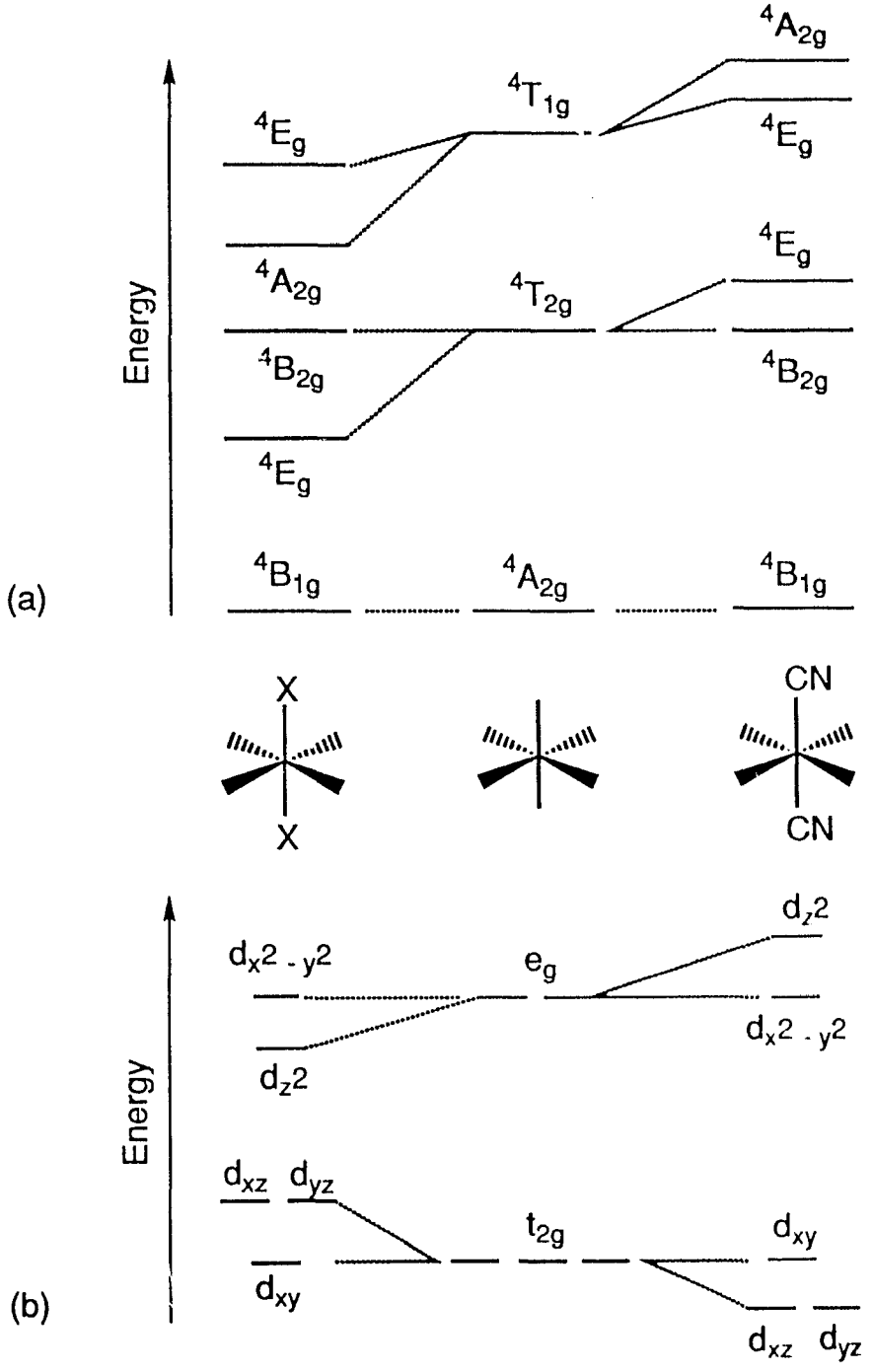


**Fig. 1.3.2** Schematic (a) state and (b) orbital energy-level diagram for *trans*-$CrN_4(CN)_2^+$ type complexes.

N = am(m)ine, X = ligands of lower 10Dq values than am(m)ine (e.g. $Cl^-$). The center vertical part and edges represent $O_h$ and $D_{4h}$ complexes respectively.

For Cr(III) complexes, the energies of the doublet and quartet states are dependent on the nature of ligands. The relative variation of the doublet excited state energy is expressed in the Nephelauxetic Series whereas that of the quartet is expressed in the Spectrochemical Series. For instance, cyanide takes the top position among common acido ligands in both series. Therefore, having more cyanide ligands in a complex will decrease the doublet state (D) energy and increase the quartet state (Q) energy, overall increasing the D/Q energy gap. The highest D/Q energy gap of common Cr(III) complexes is expected for $Cr(CN)_6^{3-}$ and this is experimentally observed.[15] However, it should be noted that the spectroscopically determined D/Q energy gap can be altered by the interaction of molecules with solvent.[6, 16]

If the symmetry of a molecule is lowered to $D_{4h}$ as in *trans*-$CrL_4X_2$, the $^4T_{2g}$ state splits into $^4E_g$ and $^4B_{2g}$ components. The relative energy ordering of these states[17] for *trans*-diacidotetraam(m)ine Cr(III) complexes are shown in Fig. 1.3.2. It shows that the lowest energy excited quartet state of *trans*-$CrN_4(CN)_2^+$ is $^4B_{2g}$. Since the appropriate orbital electron density change to populate this state is $d_{xy}$ ---> $d_{x^2-y^2}$, the electronic transition is confined to the xy plane. Similarly, if the excitation is to the higher energy $^4E_g$ component, the electronic transition will be confined to xz and yz planes. Therefore, the lowest energy quartet band of LF absorption spectrum of a $D_{4h}$ complex is split into two components corresponding to $^4B_{2g}$ <--- $^4A_{2g}$ and $^4E_g$ <--- $^4A_{2g}$ transitions. This splitting is, however, not always resolved in an experimental spectrum.

According to LF theory, the $^4B_{2g}/^4E_g$ energy gap can be expressed by the following equation.[18]

$$E(^4B_{2g}) - E(^4E_g) = 1/2\ (10Dq_{eq} - 10Dq_{ax}) \qquad (1.3.1)$$

where $10Dq_{eq}$ and $10Dq_{ax}$ corresponds to the average equatorial and axial 10Dq values respectively. Therefore once 10Dq values are known the lowest energy quartet state can be determined and the energy gap calculated using equation 1.3.1.

In this dissertation, we will be referring to these spectroscopic state symbols only as convenient labels, and will be considering only the micro symmetry of the coordinating atoms. Therefore, the subscript "g", required when there is a true center of inversion, will usually be omitted.

## 1.4 Excited State Processes of Cr(III) Complexes

Typical excited state processes of Cr(III) complexes are represented in Fig. 1.4.1. Excitation to Franck-Condon (FC) states, quickly decays by internal conversion to the zero vibrational level of the electronically excited quartet state, $Q_1{}^0$. Intersystem crossing to the doublet state $D_1$ can compete with FC ---> $Q_1{}^0$ relaxation or from $Q_1{}^0$. The former process is called prompt intersystem crossing. Both $D_1{}^0$ and $Q_1{}^0$ states lead to the processes of radiative emission (Phosphorescence or Fluorescence respectively) and non radiative decay. According to Kasha's rule, all photoprocesses should originate from $D^0$ and/or $Q_1{}^0$ states. Experimentally, the state(s) from which a chemical reaction originates seems to be more subtle and will be discussed in section 1.8.

Unlike the FC state, molecules in the $D_1{}^0$ and $Q_1{}^0$ excited states are thermally equilibrated. Therefore these states are called "Thermally equilibrated excited states" or "thexi" states.[19]

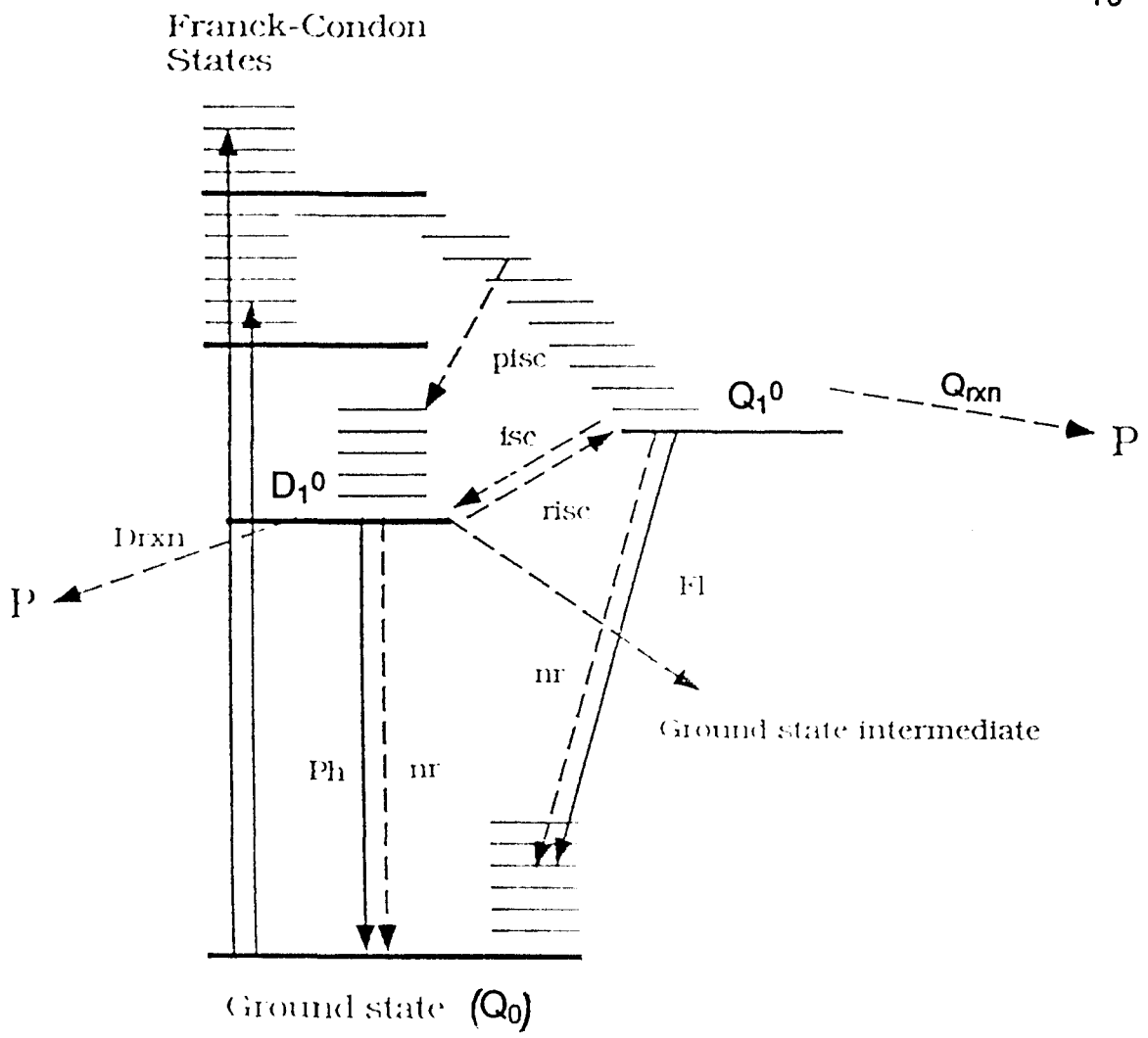


**Fig. 1.4.1** A schematic representation of excited state processes of Cr(III) complexes.

**Key** : $Q_0$ = ground state, $D_1^0$ and $Q_1^0$ = zero vibrational level of the lowest energy doublet and quartet excited states. Fl = Fluorescence, Ph = Phosphorescence,

nr = nonradiative decay, isc = inter system crossing, pisc = prompt intersystem crossing, risc = reverse intersystem crossing, Drxn = doublet reaction, Qrxn = quartet reaction, P = products. Solid arrows => radiative processes, dotted arrows => nonradiative processes.

The lifetimes of the doublet excited states are relatively long, usually in the region of μs, but the lifetime of the quartet state is much shorter, and believed to be in the picosecond or sub-picosecond domain. The doublet deactivation processes are therefore quenchable with suitable quenchers, but the quartet processes are not. The early work, which identified this behavior, is summarized in section 1.13.3.

Photoreactions that go via the doublet state are called "quenchable" or "slow" reactions, whereas, those originating directly from the quartet are called "unquenchable", "fast" or "prompt" reactions. Photoreactions of Cr(III) am(m)ine and cyanoam(m)ine complexes usually show both the "slow" and "fast" components. The distribution of a reaction between these two components is determined by

(a) measuring the quantum yield of a reaction with and without a suitable quencher

(b) following the change in conductivity of the solution on the time scale of the doublet lifetime (see section 3.2.7).

The other key features associated with photoreactions of Cr(III) complexes are the photoreaction modes, stereochemistry and the nature of intermediates formed during the reaction. The present understanding of these features is described in sections 1.5, 1.6 and 1.7.

## 1.5 Photoreaction Modes of Cr(III) Complexes

Upon irradiation of transition metal complexes in the ligand field region of their UV/Vis spectrum the photochemical reaction modes did not, in many cases, coincide with thermal reaction modes. Typical examples were

acidopentammine complexes, such as $Cr(NH_3)_5(NCS)^{2+}$.[20] This complex thermally aquates thiocyanate whereas the photochemically dominant mode is ammonia loss. This type of result led Adamson to propose rules (section 1.5.1).

### 1.5.1 Adamson's Rules

The photochemistry of Cr(III) complexes made a significant advancement following the proposal of these rules,[21] that rationalize the photoreaction modes of mixed-ligand Cr(III) complexes.

**Rule 1**: "Consider the six ligands to lie in pairs at the ends of three mutually perpendicular axes. That axis having the weakest average crystal field will be the one labilized."

**Rule 2:** "If the labilized axis contains two different ligands, then the ligand of greater field strength preferentially aquates."

For instance, the weakest average ligand field in $Cr(NH_3)_5Cl^{2+}$ is on the Cl-Cr-$NH_3$ axis and therefore the predicted leaving ligand is the $NH_3$ trans to $Cl^-$. Experimentally $NH_3$ loss was observed.[22] In this case, however, it is not clear whether the observed ammonia originated on the Cl-Cr-$NH_3$ axis. Later, work by Kirk, Zinato, Adamson, Balzani and their coworkers unambiguously established the overall validity of both of Adamson's rules, as described in section 1.6. Since then ligand labilization of many Cr(III) complexes has been studied.

While these rules are very successful for many Cr(III) complexes, there are exceptions especially in compounds containing $F^-$ ligands. The major reaction mode of both *cis* and *trans* isomers of $Cr(NH_3)_4F_2^{2+}$ and $Cr(en)_2F_2^{2+}$ is ammonia loss[23, 24] while Adamson's rules predict fluoride loss.

Subsequently, Zink[25, 26] and Wrighton et al.[27] realized that a possible basis for Adamson's rules could reside in the preferential location of the quartet state σ antibonding electron density on the weak field axis, accompanied by destabilization or stabilization by π donor or acceptor ligands respectively. Zink developed a model based on molecular orbital theory calculations to estimate the M-L bond strengths in the excited state and obtained generally satisfactory agreement with experimental results.[28] Building on this background, Vanquickenborne and Ceulemans (VC) presented their theory of ligand labilization (section 1.5.2) that does not require extensive molecular orbital calculations.

### 1.5.2 Vanquickenborne and Ceulemans Theory of Ligand Labilization

This readily applicable semi-empirical theory[18, 29] of ligand labilization is based on the Angular Overlap Model (section 1.2.1) in which the ground and excited state bond energies are expressed in terms of ligand field σ and π parameters. This theory, more general than Adamson's rules, is currently the most successful method for predicting the leaving ligand. The reactive state is assumed to be the lowest energy quartet excited state of the split $^4T_{2g}$ level and this assignment can be determined using 10Dq values (equation 1.3.1). Also assuming a dissociative mechanism, it calculates the excited state bond strength of each ligand and the leaving ligand is the one with the lowest excited state bond strength.

The calculations of the energy of d orbitals in tetragonal symmetry were described in section 1.2.1. The M-L bond energy will depend on electron occupancy in each orbital. The total bond energy ($I_T$) is defined by the equation

$$I_T = \Sigma\, h_i E_i \qquad (1.5.1)$$

where the summation runs over the five d orbitals, $h_i$ and $E_i$ are respectively the number of holes and the destabilization energies (given by equations 1.2.1 to 1.2.5) of the $i^{th}$ d orbital. Because of the additive postulate of AOM, this quantity can be partitioned into individual ligand contributions. For instance, in the case of an $O_h$ molecule

$$I\,(M\text{-}L) = I_T/6 \qquad (1.5.2)$$

Thus energy expressions for $I\,(M\text{-}L)$ values can be derived for any given electronic configuration. To illustrate this, consider the $^4B_2$ state of a tetragonal complex. The d electronic configuration is $(xz)^1$, $(yz)^1$, $(x^2 - y^2)^1$. Therefore, each one of these orbitals has one hole, and the other two orbitals have two holes. The total bond energy (eq. 1.5.1) of the state is given by

$$I^*(^4B_2) = E(xz) + E(yz) + 2E(xy) + E(x^2 - y^2) + 2E(z^2) \qquad (1.5.3)$$
$$= 4\sigma_{ax} + 4\pi_{ax} + 5\sigma_{eq} + 12\pi_{eq}$$

Since the complex has two axial and four equatorial ligands

$$I^*(M\text{-}L_{ax} : {}^4B_2) = 2\sigma_{ax} + 2\pi_{ax} \qquad (1.5.4)$$

$$I^*(M\text{-}L_{eq} : {}^4B_2) = 5/4\sigma_{eq} + 3\pi_{eq} \qquad (1.5.5)$$

In the case of excitation to the $^4E$ state corrections for mixing of the $^4E(^4T_{2g})$ and $^4E(^4T_{1g})$ states are necessary in the energy expressions. By using these expressions and known ligand field parameters, $I^*(M\text{-}L)$ values can be calculated. The leaving ligand is the one with the lowest value of $I^*(M\text{-}L)$. The results of a sample calculation of this type for *trans*-$Cr(NH_3)_4(CN)_2^+$ are given in Table 1.5.1.

The major reaction modes of most Cr(III) complexes are in accordance with the VC theory predictions including the complexes containing $F^-$ ligands. The deviation of fluoro compounds from Adamson's rule is attributed to the fact

that $F^-$ is a strong $\pi$ donor besides being a strong $\sigma$ donor. The VC calculations for $Cr(en)_2F_2^+$ show the excitation does destabilize the Cr-F axis more than the Cr-N axis but because the ground state I(Cr-F) is much larger than I (Cr-N), the final $I^*(Cr\text{-}F) > I^*(Cr\text{-}N)$.

There are, however, several exceptions to VC theory of ligand labilization. One contrasting example is *trans*-$Cr(NH_3)_4(Cl)(CN)^+$,[30] where the theory predicts ammonia loss while the observed major reaction mode is cyanide release.

**Table 1.5.1** Excited state bond strengths of *trans*-$Cr(NH_3)_4(CN)_2^+$, calculated on the basis of Vanquickenborne and Ceulemans theory of ligand labilization.

| Bond | Energy ($\mu m^{-1}$) | |
|---|---|---|
| | $^4B_{2g}$ | $^4E_g$ |
| $I^*$ (Cr-CN) | 1.9 | 1.3 |
| $I^*$ (Cr-$NH_3$) | 0.9 | 1.1 |

$E(^4E_g) - E(^4B_{2g}) = 0.25\ \mu m^{-1}$. $\sigma_{NH_3} = 7.18$, $\pi_{NH_3} = 0$, $\sigma_{CN^-} = 8.48$, $\pi_{CN^-} = -290\ \mu m^{-1}$.

## 1.6 Photostereochemistry of Cr(III) complexes

After formulation of the rules for ligand labilization, the question arose whether these rules had any stereochemical implications.[31,32] It was already established that photoaquation reactions of Cr(III) complexes exhibit stereochemical change.[33] Photolysis of *trans*-$Cr(en)_2Cl_2^+$ produced *cis*-$Cr(en)_2(H_2O)Cl^{2+}$ as the major (≥70%) photoproduct.[33] (later shown to be

≥99%)[34] while *trans*-$Cr(en)_2(NCS)Cl^{+}$[35] produced predominantly *cis*-$Cr(en)_2(H_2O)Cl_2^{+}$, even though the latter case is complicated by strong temperature dependence of the product yield. These two results originally produced evidence for stereochemical change as well as for Adamson's rules. With the gathering of more evidence the stereochemical behavior was rationalized into a single rule[36] (section 1.6.1). After several years Vanquickenborne and Ceulemans developed the first theory of photostereochemistry[29, 37, 38] (section 1.6.2). More recently they presented a Jahn-Teller type treatment for photostereochemistry[39] (section 1.6.3). Details of these approaches are given below.

### 1.6.1 Kirk's Rule

This rule[36] rationalizes the stereochemistry of Cr(III) photosubstitution reactions in aqueous solutions.

**Rule:** "The entering ligand will stereospecifically occupy a position corresponding to entry into the coordination sphere trans to the leaving ligand."

The rule predicts that once a ligand is lost, one of its adjacent ligands ("cis") takes up its position and the substituting ligand occupies the vacated position (Fig. 1.6.1). This specific movement of ligand taking place in any one of the three orthogonal planes within the coordination sphere of the molecule is also known as the "Edge displacement mechanism." Mechanistically the rule implies an associative (or interchange associative) pathway and essentially complete stereomobility[29]. It also shows that the ligand motion is confined to one plane. The rule, however, does not identify the original plane of excitation and as a consequence there are some reported exceptions to predictions based on this rule.[11] For example, the photolysis of *cis*-$Cr(NH_3)_4F_2^{+}$ produces

*mer*-FWF and *mer*-WFF as major products.[23] The rule predicts *fac*-WFF as the major product while experimentally it is only a minor product. The VC theory of photostereochemistry (section 1.6.2) identifies a particular plane of photoreaction and the above exceptions disappear if the rule is then applied.

Elegant experiments on *trans*-$Cr(NH_3)_4(^{15}NH_3)Cl_2^{+}$,[40] and *trans*-$Cr(en)_2(NH_3)Cl^{2+}$,[41] unambiguously established the validity of both Kirk's and Adamson's rules. Stereochemical change associated with many Cr(III) complexes has since been demonstrated[6] and in many systems it approaches 100%.

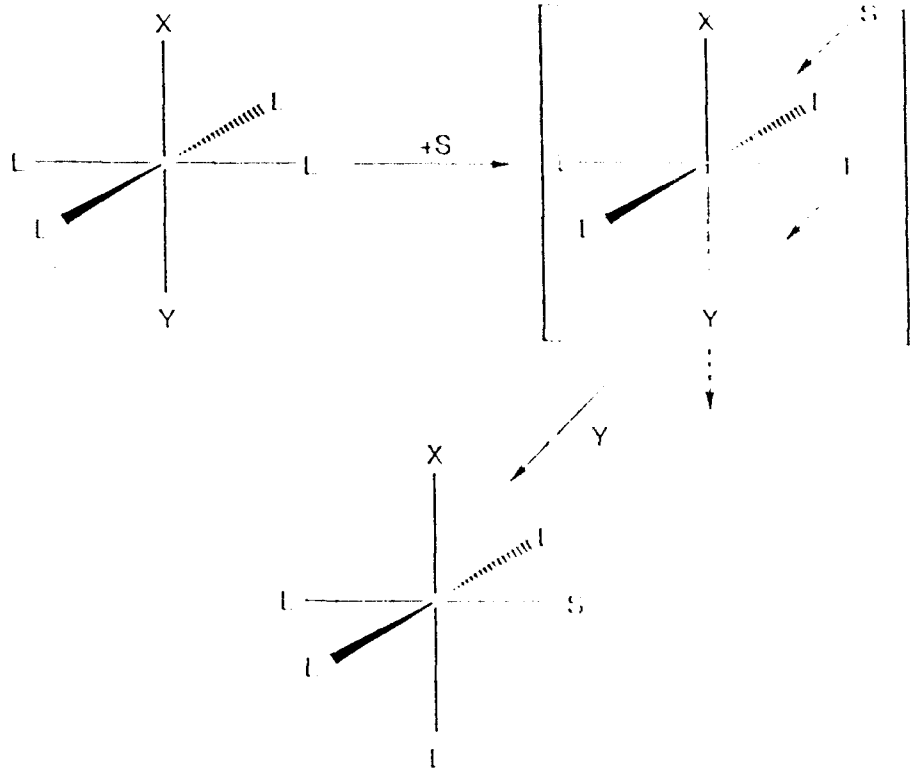


**Fig. 1.6.1** Kirk's rule interpretation of the photosubstitution reactions of Cr(III) complexes in aqueous solutions.

*trans*-$CrL_4XY$ + S ———> *cis*-$CrL_4XS$ + Y

There are several complexes which show stereoretentive reactions with very small quantum yields. They were originally considered as exceptions to the rule of complete stereochemical change. Later their behavior has been reinterpreted in favor of the stereochemical change (see section 1.13.2).

It is notable that all the observations that unambiguously established the stereochemical change of the photoreactions have been associated with axial ligand loss. The stereochemical aspect of equatorial ligand loss is not so clear cut (section 3.1) even though the photosubstitution of many such complexes in the literature is consistent with stereochemical change.

### 1.6.2 Vanquickenborne and Ceulemans Theory of Photostereochemistry

Vanquickenborne and Ceulemans extended their application of the AOM to calculate the energetics of various reaction pathways leading to an elegant theory of photostereochemistry for Cr(III) [and Co(III)] complexes.[29, 37] This model assumes that the photoreactive state is the lowest energy quartet excited state and photoreaction involves the following steps.

(a) dissociation of a ligand to form a five coordinated square pyramidal (SP) intermediate.

(b) isomerization of the SP intermediate to yield a trigonal bipyramidal (TBP) intermediate

(c) association of the isomerized TBP intermediate with the entering ligand.

These three processes will actually proceed in a more or less concerted way, and not simply consecutively.[37] The above processes are governed by the following electronic and symmetry selection rules.

**Rule 1:** "Consider the plane of excitation. In the lowest excited quartet, this is the plane formed by the two axes of weakest average field. Upon removal of the leaving ligand from this plane, the resulting T shape structure will rearrange to an equilateral triangle ($\Delta$). The perpendicular axis is conserved. If there are two equivalent weak-field planes, the rule yields the same result when applied to either one of them."

**Rule 2:** "If the rearrangement T ---> $\Delta$ does not conserve symmetry elements other than the plane in which the motion takes place ($C_s$ only), the TBP will be reached in its first excited state. If the motion has $C_{2V}$ symmetry, a $^4B_2$ is reached. This will be the ground or excited state depending whether the ligand on the diagonal axis has the weakest field or not."

**Rule 3:** "If the TBP is in its ground state, an incoming nucleophile has preferential access trans to the strongest equatorial ligands. The excited state favors attack on the complementary site."

The above rules can be elaborated as follows.

The excitation to the lowest excited quartet state corresponds to an in-plane rotation of electron density (section 1.3). This plane of the molecule is the one having the lowest $\Sigma$10Dq value. The excitation populates antibonding orbitals and destabilizes all 4 ligands. If all four ligands are not the same, the electron distribution between the orbital lobes will not be equal and therefore the different ligands will be labilized to different extents depending on their LF strengths. The loss of the ligand with lowest excited state bond energy forms an excited SP intermediate. The remaining ligands will then rearrange to minimize the energy with the assistance of the interaction of the vacant $t_{2g}$ orbital. The

importance of this vacant $t_{2g}$ orbital for stereochemical change was originally pointed out by Kirk[36] and Zink.[28] Out of plane rotations are orbitally forbidden since the other two $t_{2g}$ electrons occupy the available space. Following these restrictions, the SP intermediate isomerises to a TBP intermediate. All these facts are incorporated in "Rule 1."

Now consider the electronic and geometric structure of the TBP formed. State and orbital correlation diagrams derived[37] by VC show that it has frontier orbitals one of which is occupied. If all the ligands are the same ($D_{3h}$ symmetry), the two orbitals are degenerate giving rise to a $^4E'$ ground state. If there is a hetero-atom (say X) on the equatorial triangle ($C_{2V}$), these two orbitals are not degenerate and the $^4E'$ state splits into $^4B_2$ and $^4A_1$ components. Now $^4B_2$ corresponds to the occupation of the orbital directed towards X while $^4A_1$ corresponds to the occupation of the orbital directed towards other two ligands (Fig. 1.6.2). The energy spacing between $^4B_2$ and $^4A_1$ is also determined by 10Dq values as given by the following equation.[29]

$$E(^4A_1) - E(^4B_2) = 1/4\ (10Dq_L - 10Dq_X) \qquad (1.9.1)$$

Now "Rule 2" determines which one of the components will be reached; a result depending on the symmetry of the ligand movement within the plane of the triangle, independent of the axial ligands.

The TBP could isomerise further to the complementary SP ground state but at the same time it is susceptible to nucleophilic attack. Even though in a recent paper[42], the first process is adopted, it was previously assumed the substitution originates at the TBP intermediate. In the $^4B_2$ state of the TBP structure, the vacant d orbital attracts the incoming ligand to enter trans to the lost ligand whereas from $^4A_1$ state the preferential attack is from the direction from which the lost ligand was originally present, cis to the leaving ligand (see

arrows in Fig 1.6.2. Thus the "Rule 3" summarizes the preferential direction of attack.

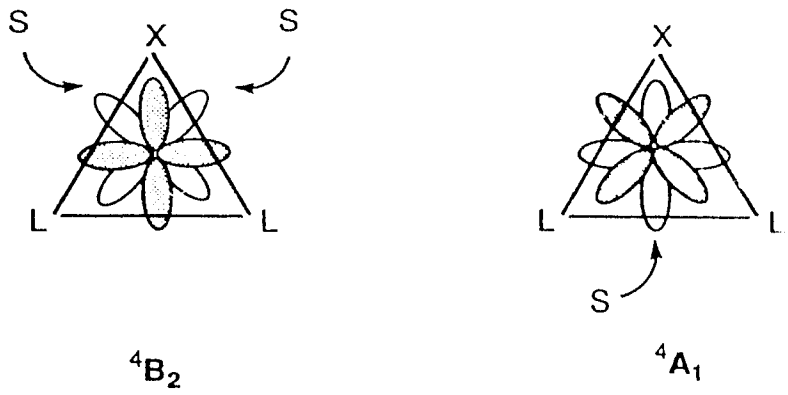


**Fig. 1.6.2** An orbital representation of the TBP intermediates for $^4B_2$ and $^4A_1$ states, described in Vanquickenborne and Ceulemans theory of photostereochemistry.

According to these three rules, the final product formed via the $^4B_2$ state will show a mechanistic stereochemical change whereas a product via $^4A_1$ will appear stereoretentive. These rules can account for observed photochemistry of many Cr(III) complexes. Fig. 1.6.3 describes[6] the application of the VC theory for axial ammonia loss of $Cr(NH_3)_5Cl^{2+}$.

Application of this theory for *cis*-$Cr(NH_3)_4F_2^+$, for which edge displacement mechanism was not successful, clearly shows that the *fac*-WFF product is not predicted. This is because the plane corresponding to the lowest energy quartet state ($^4B_{2g}$) is the AAFF plane and whether the incoming group enters *trans* or *cis* to the leaving ligand, the product is a meridional isomer.

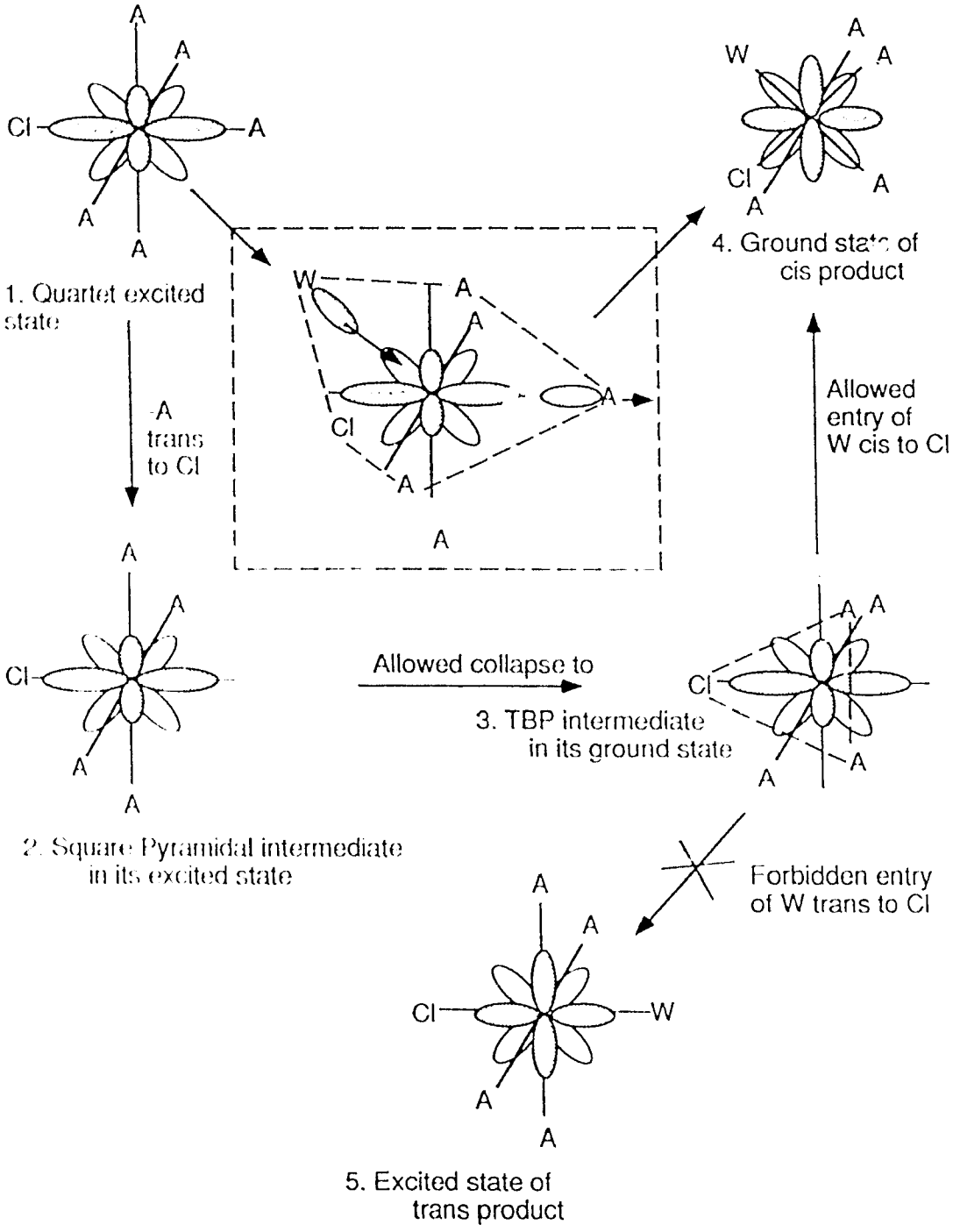


**Fig. 1.6.3** Pictorial representation of the application of Vanquickenborne and Ceulemans theory of photostereochemistry for $Cr(NH_3)_5Cl^{2+}$.

**Key :** A = $NH_3$, W = $H_2O$

VC theories on both ligand labilization and stereochemistry are based on semi-empirical methods, mainly LF models. In a recent paper VC investigated photochemistry of Cr(III) complexes by means of more rigorous ab initio calculations, again assuming a dissociative mechanism[42]. This method leads to the correct sequence of energies for all of the photoactive states used in VC theories.

Despite the great success of VC theory in explaining the stereochemistry, it is not consistent with the observations that several Cr(III) complexes show associative reaction pathways (section 1.7). It has not been possible to obtain similar theoretical predictions within a framework involving a seven coordinated intermediate species.[29] Kirk has, however indicated "it seems reasonable that the same electronic driving forces will operate to control the outcome of a substitution process independent of the exact sequence of bond breaking and bond formation."[6] Such a process is pictorially represented in the insert box of Fig. 1.6.5 that rationalizes the product formation observed.

### 1.6.3 Jahn-Teller approach to Photostereochemistry

State and orbital correlation diagrams, on which the VC theory of photostereochemistry is based, make use of one dimensional sections through the reaction surface. Recently Vanquickenborne and Ceulemans presented[39, 43] a close examination of multidimensional potential energy surfaces involved using a Jahn-Teller treatment. This method was successfully applied for $Cr(NH_3)_5F^{2+}$, and *cis*- and *trans*-$Cr(NH_3)_4F_2^+$ species. In this method VC have assumed that the TBP* intermediate formed (section 1.6.2) continues isomerization to ground state SP intermediates by Berry pseudorotation prior to substitution.

A given TBP structure can isomerise, in general, to three different SP structures while maintaining the axial ligands unchanged. VC has represented this behavior as in Fig. 1.6.4. Consequently, a given SP structure can isomerise to two more SP's via a TBP intermediate. If there is only one hetero-atom in the equatorial plane of the TBP, one $SP_{apical}$ and two $SP_{basal}$ structures will result.

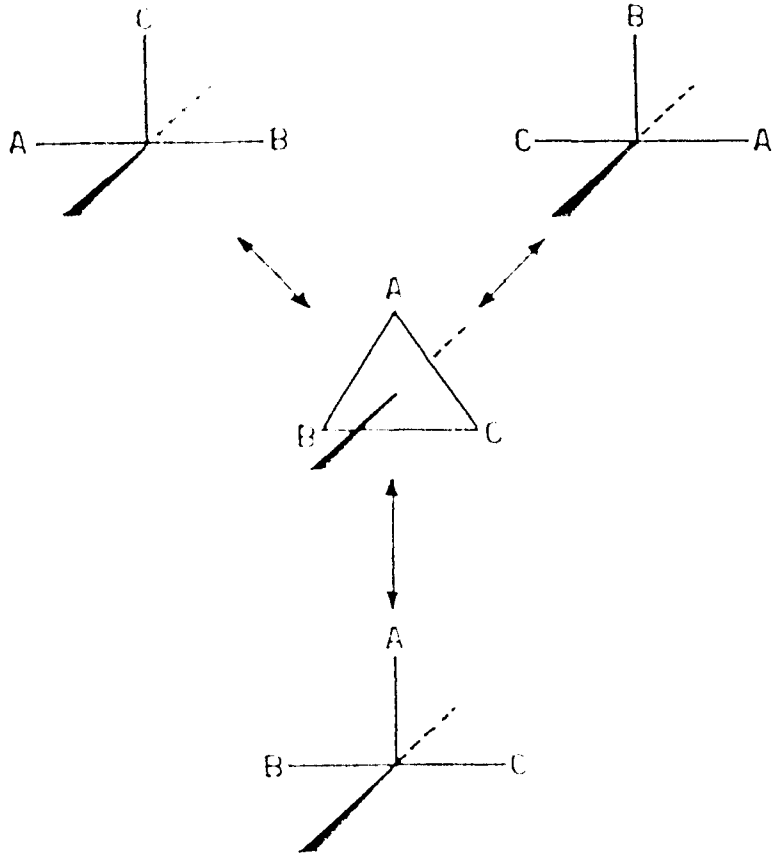


**Fig. 1.6.4** Schematic representation of the isomerization pathways of a TBP fragment.

"If all ligands are equal ($D_{3h}$ symmetry), the TBP gives rise to a $^4E'$ ground state (section 1.6.2). The potential energy surfaces of such a system appear like a Mexican hat structure with the TBP at the central pivot point and three equivalent SP fragments in three surrounding minima, as pictorially represented in Fig. 1.6.5. The structure of this surface is not greatly altered by the introduction of a hetero ligand but it removes the degeneracy of $^4E'$. The primary effect of substituents is, therefore, to displace the surface intersection point (degeneracy point) between upper and lower surfaces."[43]

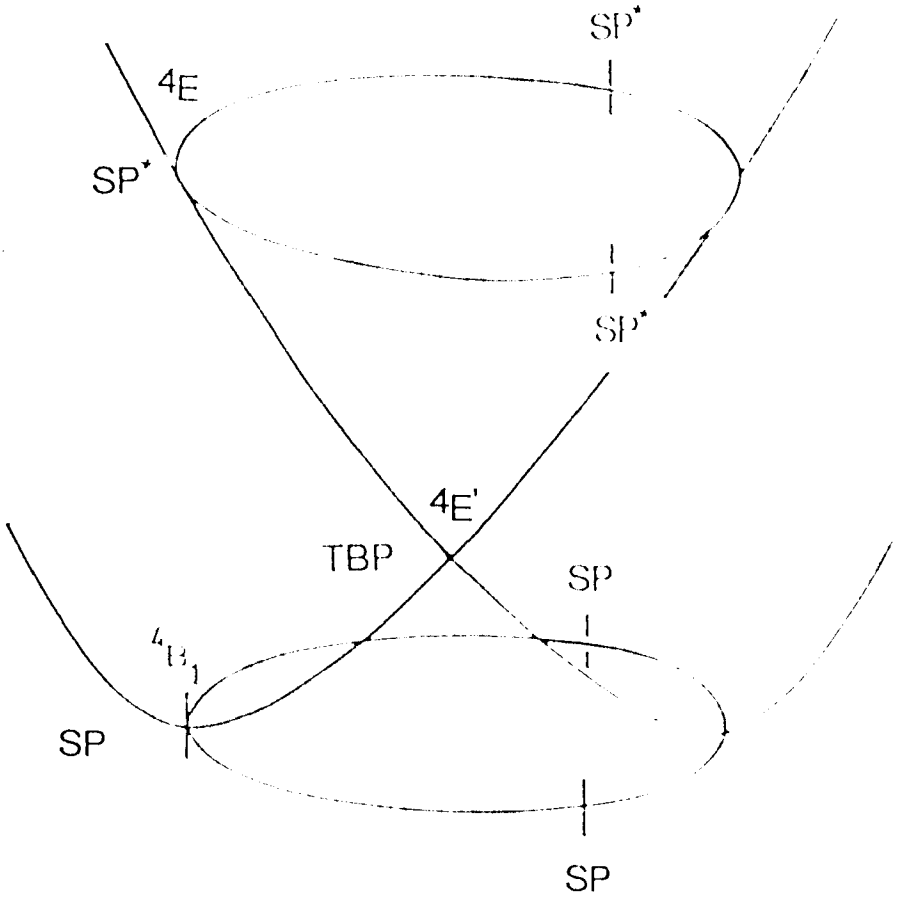


**Fig. 1.6.5** Mexican hat potential surface around a $^4E'$ state of a symmetric ($ML_5$) TBP.

"Upon ligand loss, a system will enter the upper surface at an SP structure in an excited state. Subsequent decay will populate the SP ground state wells on the lower surface. These ground states will then be trapped by solvent molecules to yield the hexacoordinated product."[39] In order to get stereochemical change, the SP intermediates on the opposite side must be populated, in other words transverse tunneling is required. VC show, however, that the efficiency of this transverse tunneling is dependent on the relationship between the excited state entrance point and the surface intersection point, as given by the following rule.[39]

**Rule:** "In all cases where the intersection point of upper and lower surface is displaced towards the excited state entrance point, the preference for transverse tunneling is most pronounced. In cases where the intersection point is displaced away from the entrance point, the directional selectivity is partly lost and a more random decay will be observed."

The above rule integrates the "Rule 2" and "Rule 3" of VC theory of photostereochemistry (section 1.6.2) and also implies that the tunneling tends to conserve nuclear momentum. Their interpretation of the product stereochemistry is given below. Text and figures were, therefore, chosen as closely as possible to the original reports.[42, 43]

For $Cr(NH_3)_4X^{2+}$ fragments, the degeneracy point is found along the $SP^*_{ap}$ ---> $TBP_{eq}$ path (see Fig. 1.6.6). In this case the intersection point is displaced towards the excited state entrance point. Therefore axial ligand losses from $CrN_5X^{2+}$ type molecules undergo efficient transverse tunneling and show complete stereochemical change, consistent with the experimental results.

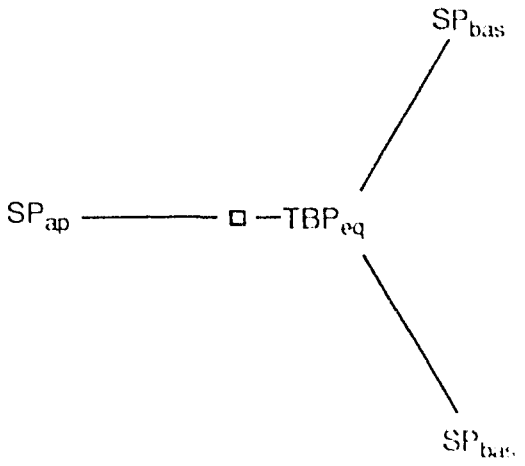


**Fig. 1.6.6** A schematic representation of the top elevation of the Jahn-Teller surface for $Cr(NH_3)_4X^{2+}$ fragment, where 10Dq ($X^-$) < 10Dq ($NH_3$).

□ = degeneracy point.

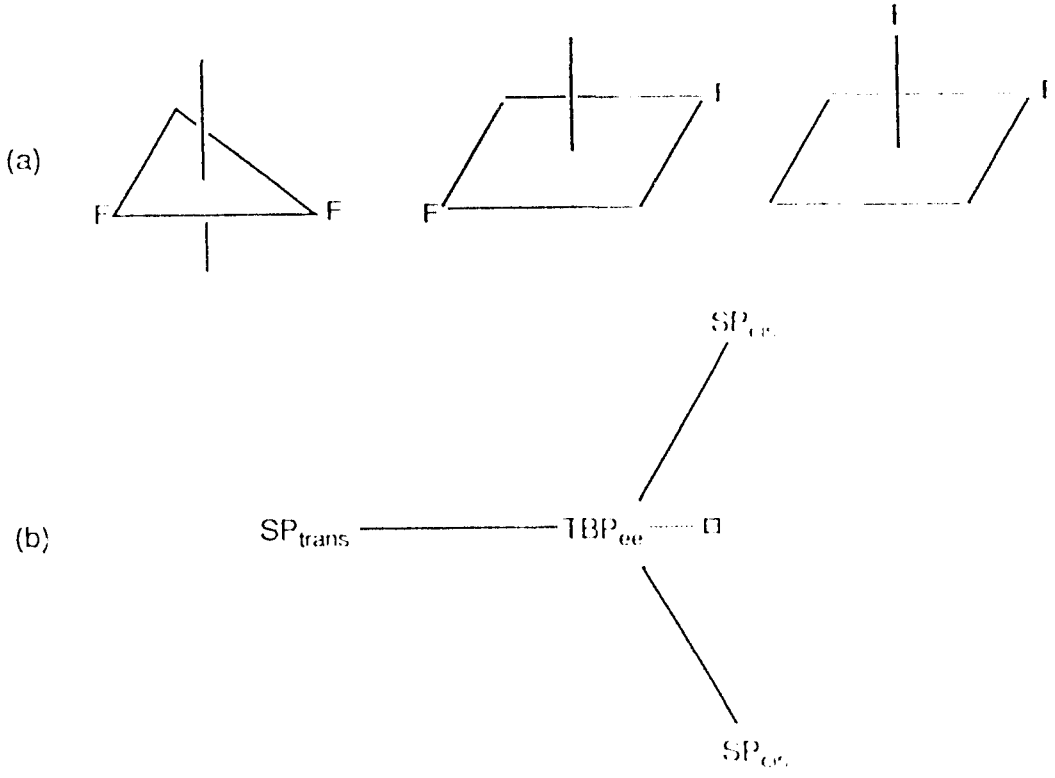


**Fig. 1.6.7** (a) TBP and SP structures of $Cr(NH_3)_3F_2^+$ species. (b) A schematic representation of the top elevation of the Jahn-Teller surface for $Cr(NH_3)_3F_2^+$ fragments. ◘ = degeneracy point.

The situation is more complicated for species like *cis*- and *trans*-$Cr(NH_3)_4F_2^+$. In both species the photoactive $N_2F_2$ plane produces a TBP with two $F^-$ ligands. The appropriate SP structures will be one $SP_{trans}$ and two $SP_{cis}$ (see Fig. 1.6.7.(a)). A schematic representation of the Jahn-Teller surface is shown in Fig. 1.6.7.(b). In the case of *trans*-$Cr(NH_3)_4F_2^+$, the entrance species is $SP^*_{trans}$ that is on the opposite side of the potential surface from the intersection point. Therefore a random population of all three SP ground state is predicted by the rule, producing 33% mer-FWF and 67% mer-FFW. This is consistent with the experimentally observed products (30% mer-FWF and 70% mer-FFW). On the other hand, the entering species of *cis*-$Cr(NH_3)_4F_2^+$ is $SP^*_{cis}$. Since the crossing point in this case is close to the entry point, transverse crossing is expected, producing both the $SP_{cis}$ and $SP_{trans}$. This would lead to a 50 : 50 mixture of two meridional products, which is indeed close to the observed results (45% mer-FWF and 55% mer FFW).

## 1.7 Intermediates in Cr(III) Photoreactions

The mechanism of thermal substitution reactions of Cr(III) complexes are usually associative, via a seven coordinated intermediate. This raises the question whether photoaquation reactions are also associative in nature. Some experimental results addressing this question are presented below.

Krause and Wasgestian studied the competition between chloride photoanation and photoaquation of $Cr(NH_3)_6^{3+}$,[44,45]. The total quantum yield for ammonia loss was remarkably constant over the whole range of $Cl^-$ concentration. Based on this result a mechanism assuming a trigonal prismatic transition state was proposed. "One might be inclined to interpret this independence of entering ligand as an indication in favor of a primary

dissociative step."[29] A similar study for the photoanation of $Cr(DMSO)_6^{3+}$ by $N_3^-$ and $CSN^-$ by Langford and Tong however showed that the quantum yield for azide anation was distinctly larger than those for thiocyanate.[46] This result was ascribed to an associative mechanism, with a cautionary note that the role of an entering ligand in a photoreaction would be different from its behavior in a thermal activation process and probably more subtle than experience with thermal reactions has revealed.

More definite results were obtained with volume of activation measurements. The photosubstitution of $NH_3$ by $H_2O$ in $Cr(NH_3)_6^{3+}$ and $Cr(NH_3)_5X^{2+}$ ($X = Cl^-$, $Br^-$ and $NCS^-$) shows negative activation volumes, about -6 $cm^3\ mol^{-1}$, independent of the complex.[47] On this basis, an associative ($I_a$) mechanism was proposed. On the other hand photoaquation of $Cr(NCS)_6^{3-}$ and $Cr(CN)_6^{3-}$ showes positive activation volumes, about +2 $cm^3\ mol^{-1}$, and the results were attributed to a dissociative mechanism.[48] In the $Cr(NH_3)_6^{3+}$ case, exchange of neutral ligands is involved which are not complicated by electrostriction effects and therefore the results provide more definitive information than values reported for photoaquation of negatively charged ligands.

Recent work by Waltz et. el. on *cis*-$Cr(cyclam)(NH_3)_2^{3+}$ provided direct evidence for formation of a seven coordinate intermediate,[49] by the flash photolysis method with conductivity detection. In this experiment, at pH values between 4.0 and 5.4, the system showed an initial increase in conductivity preceeding the decay whereas no such initial increase was observed at lower pH values. This result was interpreted in terms of formation of seven coordinated intermediate containing a coordinated water molecule with $pK_a \approx 4.6$.

Even though this section does not provide a comprehensive account of all the data, most of the experimental results support an associative type mechanism for the photoaquation of Cr(III) complexes.

## 1.8 Excited State(s) Responsible for Photoreaction of Cr(III) Complexes

The prompt reaction of Cr(III) complexes has been unanimously assigned to the short lived quartet state. This reaction is proposed to initiate either from the $Q_1^0$ state or from vibrationally excited quartet states, in violation of Kasha's rule. This aspect will be discussed separately in section 1.13.3.

For the reaction via the doublet state ("slow" component), three hypotheses have been proposed.

(a) Direct doublet reaction

(b) Reverse intersystem crossing followed by quartet reaction

(c) Crossing to a reactive ground state intermediate.

Most of the results available by now are against (a) above. Present literature on photoprocesses of Cr(III) complexes has, however, been divided between (b) and (c), mostly supporting (b) which include recent spectroscopic[16] and activation energy[50] data.

A good criterion to distinguish (b) from (c) [and (a)] is the stereochemistry of photoproducts. Photoaquation of Cr(III) complexes usually occurs with stereochemical change (section 1.6). The quartet state with a vacant $t_{2g}$ orbital can facilitate such a stereochemical change. A reaction from a ground state intermediate [or directly from the doublet] is expected to show similar stereochemistry to the ground state (thermal) reactions which are

stereoretentive in nature. Therefore, (c) [and (a)] above cannot easily account for the observed stereochemical change. Thus the stereochemical results favour (b). Therefore, as a working hypothesis in this dissertation, we assume the mechanism of the pathway via the doublet state involves reverse intersystem crossing followed by quartet reaction.

## 1.9 Significance of Cr(III) Cyanoam(m)ine Complexes

Cr(III) cyanoam(m)ine complexes were unknown until 1975. This is presumably due to the difficulties in synthesis. These complexes show unique features due to the following properties of $CN^-$ ligands.[15]

(a) great stability of the metal ligand bond

(b) $\pi$ acceptor character

(c) high basicity

(d) the top spectrochemical position

(e) the large nephelauxetic effect

(f) the considerable trans effect

(g) the bridging ability

Photochemistry of a variety of Cr(III) cyanoam(m)ine complexes has been reported since ~1980, mainly by Zinato, Riccieri and coworkers. These complexes provide important test cases for mechanistic aspects of Cr(III) photochemistry due tothe following features.[15]

(a) The uncommon ordering of the LF energy levels ($^4B_2 <$ [illegible] which enables full access to a state that in other acidoam(m)ines can be populated to limited extent, at most.

(b) The fairly intense long lived doublet excited state under photolysis conditions.

(c) The relatively wide gap between the doublet and the quartet states.

The photochemical, photophysical and thermal properties of these complexes are described in sections 1.10, 1.11 and 1.12.

## 1.10 Photoaquation of Cr(III) Cyanoam(m)ine Complexes

Quantum yields for LF substitution reactions of Cr(III) cyanoam(m)ine complexes[15] are listed in Table 1.10.1. This includes the references for complexes discussed below.

**Table 1.10.1** Quantum yields for ligand field photoaquation of Cr(III) cyanoam(m)ine complexes in room-temperature solutions.

| Complex | $\Phi_{am(m)ine}$ | $\Phi_{CN^-}$ | Ref. |
|---|---|---|---|
| $Cr(NH_3)_5(CN)^{2+}$ | 0.33 | < 0.0005 | 51 |
| *trans*-$Cr(NH_3)_4(CN)_2^+$ | 0.28 | <0.005 | 52 |
| *cis*-$Cr(NH_3)_4(CN)_2^+$ | 0.26[a] | 0.02[a] | 52 |
| *trans*-$Cr(en)_2(CN)_2^+$ | 0.6 | <0.002 | 53 |
| *cis*-$Cr(en)_2(CN)_2^+$ | 0.51[a] | 0.1[a] | 53 |
| *trans*-Cr(cyclam)$(CN)_2^+$ | $< 10^{-5}$ | $< 10^{-5}$ | 54 |
| *trans*-Cr(teta)$(CN)_2^+$ | $< 10^{-5}$ | $< 10^{-5}$ | 55 |
| $Cr(NH_3)(CN)_5^{2-}$ | 0.08 | 0.06 | 56 |

[a] Some wavelength dependence is reported.

$Cr(NH_3)_5(CN)^{2+}$ undergoes exclusive $NH_3$ aquation. The general problem with pentaammines, however, is that the original location of the displaced $NH_3$ is unknown. The products were, *cis*-$Cr(NH_3)_4(H_2O)(CN)_2^{2+}$ (70%) and *trans*-$Cr(NH_3)_4(H_2O)(CN)_2^{2+}$ (30%).

In agreement with all the theories (section 1.5) the dominant reaction mode of *trans*-$Cr(N)_4(CN)_2^+$ complexes is loss of equatorial am(m)ine. This is clear cut for the $N_4 = (NH_3)_4$ and $(en)_2$ cases. For $N_4$ = cyclam or teta, however, the molecules are photoinert, which was attributed to steric constraints of the amine ligands. This effect will be discussed in section 1.13.2. Stereochemistry of photoproducts was investigated for $N_4 = (NH_3)_4$. The photoproducts were *mer*-1,6-CN-$Cr(NH_3)_3(H_2O)(CN)_2^+$ (70%) and *mer*-1,2-CN-$Cr(NH_3)_3(H_2O)(CN)_2^+$ (30%). The absence of the facial isomer shows that the photoreaction is stereospecific. While the 1,2-CN product is a result of the stereochemical change, the 1,6-CN product is silent about the mechanistic photostereochemistry (section 3.1).

In *cis*-$Cr(N)_4(CN)_2^+$ complexes, ($^4E < {}^4B_2$ in energy), the major photoreaction mode for both $N_4 = (NH_3)_4$ and $(en)_2$ involves am(m)ine loss which is in accordance with the theories (section 1.5). In addition to this mode, however, an appreciable amount of $CN^-$ is also released. The major photoproducts consist of *fac*-1,2-CN-$Cr(NH_3)_3(H_2O)(CN)_2^+$ and *mer*-1,6-CN-$Cr(NH_3)_3(H_2O)(CN)_2^+$, and their proportion is 2 : 1 or 1 : 1 depending on whether the first or second LF band is irradiated.

$Cr(NH_3)(CN)_5^{2-}$ produces $NH_3$ as the major product but a comparable amount of $CN^-$ is also released. Photochemistry of many Cr(III) cyanoam(m)ine complexes with acido ligands has also been reported, mainly the *trans*-$Cr(NH_3)_4X(CN)^{n+}$ series, where $X = Cl^-$ [30, 57], $F^-$ [57, 58], $NCS^-$ [57, 58] and $H_2O$ [58].

## 1.11 Photophysics of Cr(III) Cyanoam(m)ine Complexes

Photophysics of Cr(III) complexes, in general, has been extensively studied.[59, 60] Initially, some rules were proposed to predict the relative variation of lifetimes of complexes[61], but they were not as successful as those for photochemistry.

Data relevant to Cr(III) cyanoam(m)ino complexes are listed in Table 1.11.1. A few scattered results on intersystem crossing efficiencies are also found in the literature.[15] The notable feature relevant to the present work is that most of them show strong emission with long lifetimes in room-temperature aqueous solutions, compared to other Cr(III) complexes.

According to our hypothesis that the doublet deactivation processes involve reverse intersystem crossing to the quartet state, the activation energy values reported correspond to the effective D/Q energy gap. This energy gap can be altered from the spectroscopically determined values, due to the interaction of solvents with excited molecules and such a solvent assisted process has been called "Nucleophile-assisted reverse intersystem crossing"[6]. This behavior has been underlined in favor of the reverse intersystem crossing to the quartet excited state pathway for the doublet decay.[62]

**Table 1.11.1** Emission lifetimes and their apparent activation energies, and emission peak maxima of some Cr(III) am(m)ine, cyanoam(m)ine and cyano complexes.

| Complex | Solvent | $\lambda_{max}$ (nm) | $\tau$ (μs)[a] | E (kJ mol$^{-1}$)[b] | Ref. |
|---|---|---|---|---|---|
| $Cr(NH_3)_6^{3+}$ | $H_2O$ | 654 | 1.6 | | 63 |
| $Cr(en)_3^{3+}$ | $H_2O$ | 670 | 1.7 | | 64 |
| $Cr(tn)_3^{3+}$ | $H_2O$ | 666 | 2.6 | | 63 |
| $Cr(NH_3)_5(CN)^{2+}$ | $H_2O$ | 680 | 22 | 47 | 65 |
| | DMSO | 682 | 35 | 55 | 65 |
| | DMF | 682 | 20 | 53 | 65 |
| *trans*-$Cr(NH_3)_4(CN)_2^{+}$ | $H_2O$ | 700 | 40 | 28 | 52 |
| | DMSO | 701 | 19 | 55 | 52 |
| | DMF | 699 | 10 | 36 | 52 |
| *cis*-$Cr(NH_3)_4(CN)_2^{+}$ | $H_2O$ | 701 | 26 | 27 | 52 |
| | DMSO | 703 | 71 | 30 | 52 |
| | DMF | 702 | 33 | 25 | 52 |
| *trans*-$Cr(en)_2(CN)_2^{+}$ | $H_2O$ | | 1 | | 66 |
| | DMSO | | 1 | | 66 |
| | -[c] | 703 | | | 66 |
| *cis*-$Cr(en)_2(CN)_2^{+}$ | $H_2O$ | | 2 | | 66 |
| | DMSO | | 9 | | 66 |
| | -[c] | 705 | | | 66 |
| *trans*-Cr(cyclam)$(CN)_2^{+}$ | $H_2O$ | 720 | 335 | 38 | 54 |
| | DMSO | | 330 | | 54 |
| *trans*-Cr(teta)$(CN)_2^{+}$ | $H_2O$ | 715 | 395 | | 55 |

**Table 1.11.1** (Continued)

| Complex | Solvent | $\lambda_{max}$ (nm) | $\tau$ ($\mu$s)[a] | E (kJ/mol)[b] | Ref. |
|---|---|---|---|---|---|
| $Cr(NH_3)_5(CN)^{2+}$ | DMSO | 777 | 32 | | 65 |
| | DMF | 777 | | | 65 |
| $Cr(CN)_6^{3-}$ | DMSO | 800 | | | 56 |
| | DMF | 803 | | | 56 |
| *trans*-$Cr(2,3,2\text{-tet})(CN)_2^{+}$ | $H_2O$ | 705 | 30 | 38 | e,67 |
| | DMSO | 705 | | | e |
| *trans*-$Cr(tn)_2(CN)_2^{+}$ | $H_2O$ | 703 | 185 | | e,68 |
| | DMSO | 705 | | | e |
| $Cr(tn)(CN)_4^{-}$ | DMSO | 748 | 4 | | e |
| | DMSO | 749[d] | | | e |
| | DMF | 747 | 17 | | e |

[a] At or close to 20 °C. [b] Around room temperature. [c] DMSO / $CF_3SO_3H$.

[d] Estimated value (see section 4.3.2). [e] This work.

## 1.12 Thermoaquation of Cr(III) Cyanoam(m)ine Complexes

Thermal reactions of Cr(III) complexes, in general, are extensively studied and have frequently been reviewed[69-72] while those relevant to cyanoam(m)ine complexes in particular have been reviewed only recently.[15]

Two notable features of the solution behavior of Cr(III) cyanoam(m)ine complexes are

(i) high lability of $CN^-$ in acidic aqueous solutions.

(ii) high inertness in neutral or basic aqueous media (and in aprotic solvents)

The acid-catalyzed aquation of $CN^-$ has been investigated in detail for $Cr(NH_3)_5(CN)^{2+}$,[73] and $Cr(NH_3)_4(CN)_2^+$,[74, 75] complexes. In these cases $CN^-$ loss is proposed to take place via two parallel pathways as shown in the following scheme.[15, 75]

$$CrN_4X(CN)^{n+} + 2H_2O \xrightarrow{k_0} CrN_4X(H_2O)^{(n+1)+} + HCN + OH^-$$

$$\Big\Vert \; H^+$$

$$CrN_4X(CNH)^{(n+1)+} + H_2O \xrightarrow{k_H} CrN_4X(H_2O)^{(n+1)+} + HCN$$

where x = $NH_3$ or CN, $k_0$ and $k_H$ are rate constants for acid-independent and acid-dependent pathways. The equilibrium constant for protonation of cyanide ligand is K.

For these complexes, the pseudo-first-order rate constants, $k_{obsd}$, have been found to fit the general expression[15, 75]

$$k_{obsd} = (k_0 + k_H K[H^+]) / (1 + K[H^+]) \qquad (1.12.1)$$

The $k_0$ value is usually several orders of magnitude smaller than $k_H$. For instance, the $k_0$ and $k_H$ values for $Cr(NH_3)_5(CN)^{2+}$ are $1 \times 10^{-7}$ $s^{-1}$ and $1.5 \times 10^{-2}$ $s^{-1}$ respectively. Therefore under ordinary conditions, the contribution of the unprotonated forms to reactivity is generally unimportant. The enhancement of the lability of cyanide upon protonation has been attributed to the decrease in nucleophilicity and increase in ligand repulsion consequent to removal of the negative charge.[15]

Another notable feature in acid catalyzed cyanide aquation reactions is that *trans*-dicyano complexes aquate faster than *cis* isomers,[15] in contrast to the usual behavior of the *cis*- and *trans*-diacidotetram(m)ine pairs.[69, 76] For instance, the $k_HK$ value of *trans*-$Cr(NH_3)_4(CN)_2^+$ is about $10^2$ greater than that for *cis*-$Cr(NH_3)_4(CN)_2^+$,[77]. It is also notable that *trans*-$CrN_4(CN)_2^+$ complexes aquate faster than $CrN_5(CN)^{2+}$ complexes. As an example the $k_H$ value of *trans*-$Cr(NH_3)_4(CN)_2^+$ is about seven times greater than that for $Cr(NH_3)_5(CN)^{2+}$. The high rate constants for *trans*-dicyano complexes have been attributed to a thermodynamic trans effect.[15]

It is well established that thermal substitution reactions of Cr(III) complexes in aqueous solutions are stereoretentive. For instance, cyanide aquation reactions of *trans*-$CrN_4(CN)_2^+$ complexes, where $N_4 = (NH_3)_4$[77], cyclam[78] and tetā[55], were found to aquate with complete retention of configuration.

## 1.13 Mechanistic Significance of Stereochemical Results

### 1.13.1 Evidence for Photoreaction Pathways

As discussed in section 1.8, the stereochemical change associated with the photosubstitution processes of Cr(III) complexes allows us to infer that the doublet excited state deactivation pathway involves reverse intersystem crossing to the quartet excited state. Thus stereochemical results provide mechanistic details about the pathway of the excited state reaction.

### 1.13.2 Hindrance of Photoreaction by Stereochemical Constraints

Several Cr(III) complexes have been found to be photoinert ($\Phi_{total} < 1 \times 10^{4}$). Interestingly all these complexes are of the *trans*-Cr(cyclam)$(X)_2$ type (see Table 1.13.1) whereas their analogs are photoactive.

Data relevant to this behavior was first obtained by Kutal and Adamson[79] who found that the quantum yield for $Cl^-$ release upon irradiation in the quartet excited state of *trans*-Cr(cyclam)$(Cl)_2^+$ ($\phi_{Cl^-} = 3.3 \times 10^{-4}$) is three orders of magnitude less than that found for electronically and geometrically similar *trans*-$Cr(NH_3)_4Cl_2^+$ ($\phi_{Cl^-} = 0.44$) and *trans*-$Cr(en)_2Cl_2^+$ ($\phi_{Cl^-} = 0.32$) compounds (Table 1.13.1). Also the analogous *trans*-Cr(2,3,2-tet)$Cl_2^+$ complex, in which there is no complete ring in the equatorial plane, is photo active ($\phi_{Cl^-} = 0.06$) although with a reduced yield compared with am(m)ine analogous.[80] In the case of *trans*-Cr(cyclam)$(Cl)_2^+$ the photoreaction is stereoretentive giving *trans*-Cr(cyclam)$(H_2O)(Cl)^{2+}$ whereas the latter complexes photoaquate with stereochemical change giving *cis*-$CrN_4(H_2O)Cl^{2+}$ products. The drastic drop of quantum yield due to the incorporation of the cyclam ligand was attributed to the stereochemical constraint of the macrocyclic ligand. The quantum yield value of

*trans*-$Cr(2,3,2\text{-tet})Cl_2^+$ is in between *trans*-$Cr(cyclam)(Cl)_2^+$ and *trans*-$Cr(en)_2Cl_2^+$. This is consistent with the fact that 2,3,2-tet lies between those of cyclam and en in the degree of chelation or ring structure about the metal center.[80] The product stereochemistry of the *trans*-$Cr(cyclam)(Cl)_2^+$, regarded by some as an exception to Kirk's rule[81], was later rationalized as follows. The blocking of the usual pathway of photoreaction by the ligand constraint has revealed a residual, inefficient retentive pathway parallel to that for Co(III) complexes, and which is normally hidden under the efficient pathway.[6]

**Table 1.13.1** Reaction quantum yields for some Cr(III) am(m)ine and chloroam(m)ine complexes in room-temperature aqueous solutions.

| Compound | $\Phi_{amine}$ | $\Phi_{NH_3}$ | $\Phi_{Cl^-}$ | Ref. |
|---|---|---|---|---|
| $Cr(NH_3)_6^{3+}$ | | 0.46 | | 63, 82 |
| $Cr(tn)_3^{3+}$ | 0.14 | | | 63, 82 |
| $Cr(en)_3^{3+}$ | 0.45 | | | 83 |
| *trans*-$Cr(en)_2(NH_3)_2^{3+}$ | 0.40 | 0.06 | | 84 |
| *cis*-$Cr(en)_2(NH_3)_2^{3+}$ | 0.37 | 0.07 | | 84 |
| *trans*-$Cr(cyclam)(NH_3)_2^{3+}$ | | $<10^{-4}$ | | 85 |
| *cis*-$Cr(cyclam)(NH_3)_2^{3+}$ | | 0.15 | | 85, 88 |
| *trans*-$Cr(NH_3)_4Cl_2^+$ | | $< 3 \times 10^{-3}$ | 0.44 | 86 |
| *trans*-$Cr(en)_2Cl_2^+$ | | | 0.32 | 87 |
| *trans*-$Cr(2,3,2\text{-tet})Cl_2^+$ | | $< 7 \times 10^{-3}$ | 0.06 | 80 |
| *trans*-$Cr(cyclam)Cl_2^+$ | | $< 6 \times 10^{-4}$ | $< 3 \times 10^{-4}$ | 79 |

More evidence of this behavior was observed with cyclambisammine systems.[85] *Trans*-Cr(cyclam)$(NH_3)_2^{3+}$ was photoinert ($\phi_{NH_3} < 1 \times 10^{-4}$) while the cis isomer photoaquates ammonia ($\phi_{NH_3} = 0.15$) producing *cis*-Cr(cyclam)$(NH_3)(H_2O)^{3+}$. Ammonia is a weaker ligand than the cyclic amine and therefore theory (section 1.5) predicts preferential $NH_3$ photolabilization for the trans complex. The photoinertness of this complex in fluid solution was again attributed to the presence of cyclam ligand that could seriously restrict the trans ----> cis isomerization. For the $NH_3$ loss of the cis complex to produce *cis*-Cr(cyclam)$(NH_3)(H_2O)^{3+}$, however, no such motion is required by the cyclam ligand. This product may have occurred by stereoretentive substitution of $NH_3$ by $H_2O$. It is, however, consistent with a reaction with stereochemical change.[88]

All the above results show that incorporation of a cyclam ligand, which restricts trans ----> cis isomerization has suppressed the photoreaction of axial ligand labilization of complexes. The important feature of all the above is that for axial ligand loss these results support the claim that stereochemical change is not just a normal accompaniment of Cr(III) photoaquation, but is a requirement of the reaction via the excited state.[6]

### 1.13.3 Evidence for the Competition of Photoreaction with Vibrational Relaxation

In the conventional view of the photosubstitution of Cr(III) complexes, the photoreaction originates from a "thexi" state. In 1981, Hollebone, Langford and Serpone introduced the contrasting new idea that the photoprocesses can exhibit non-equilibrium dynamics.[10] In this view, the photoprocess are thought

to occur at a very fast time scale, originating from upper vibrational levels. This limit mechanism is called the DOSENCO (decay on selected nuclear coordinates) theory. In addition, theoretical selection rules for the DOSENCO coordinates were derived.[89] In the case of the $^4T_{2g}$ <--- $^4A_{2g}$ excitation of an $O_h$ Cr(III) complex, the selected reactive coordinate was assigned as a highly excited $t_{1u}$ buckle mode.[10] Decay along this mode could expose the metal ion stretched faces of the octahedral complex leading to an associative ligand replacement. In this model, the route via the "thexi" state was identified as the DERCOS (decay via random coordinate selection) limit mechanism.[89]

This theory arose out of a number of early experimental results and some of them are summarized below.

Many experiments, mostly done by Porter, Langford, Kane-Maguire, Balzani, Wasgestian and coworkers, established[90-93] that there exist pathways for quartet reactions determined prior to intersystem crossing to the doublet. Subsequently, wavelength dependence studies[94] established that intersystem crossing competes with vibrational relaxation and picosecond pulsed experiments[95] indicated that intersystem crossing indeed occurs in a few picoseconds. Since then many photochemical and photophysical experiments showing the wavelength dependence have been reported.[10]

More recent experimental results involving ultrafast laser experiments[96] and wavelength dependence studies[8] have been explained using the DOSENCO model. In 1990, it was reported that the stereochemistry of photoproducts due to the prompt reaction of $Cr(tn)_3^{3+}$ is wavelength dependent (section 4.1) in such a manner that it can be attributed the competition of photoreaction with vibrational relaxation.[97] This result shows that the

photostereochemical results can be used to provide mechanistic information on the participation of higher vibronic levels of the excited quartet states.

### 1.14 Objectives of the Present Work

In this work we will be using the stereochemical behavior of Cr(III) photoaquation reactions to investigate several mechanistic aspects of excited state processes. There are two major objectives.

(a) Photoaquation of Cr(III) complexes usually shows stereochemical change (section 1.6) providing useful mechanistic information about the excited state participation (section 1.8). This stereochemical aspect is well established for axial labilization where it is shown to be a requirement of the reaction. This behavior is, however, not established for equatorial ligand loss. Therefore, we will investigate whether stereochemical change is a requirement for equatorial ligand loss. More details of the nature of this problem, our approach to solving it and the results are discussed in chapter three, titled "Photochemistry and Photophysics of *trans*-[Cr(2,3,2-tet)$(CN)_2$]$ClO_4$. Is Stereochemical Change a Requirement for Equatorial Ligand Loss?".

(b) There are theoretical and experimental implications that excited state processes can be competitive with vibrational relaxation so that they originate from upper vibrational levels before reaching "thexi" state(s) (section 1.13.3). In a recent report, it was shown that the product stereochemistry of the photoaquation of $Cr(tn)_3^{3+}$, where the doublet pathway is quenched by $OH^-$ is wavelength dependent in such a manner, that can be attributed to the competition of the photoaquation with

vibrational relaxation (section 4.1). Therefore we will further investigate this competitive photoaquation of Cr(III) complexes, using different molecules with more reaction modes and different quenchers. More details of this behavior, our approach and results will be discussed in chapter four, titled "Wavelength dependence of prompt photoreaction in Cr(III) complexes. Is photoaquation of $Cr(tn)_3^{3+}$ competitive with vibrational relaxation?"

Our general approach can be classified as follows

(a) Synthesis and characterization of series of compounds, including several new ones

(b) Establishing the isomeric identity of new molecules and their photoproducts.

(c) Developing necessary analytical tools for quantitative and qualitative analysis of products.

(d) Carrying out necessary photochemical and photophysical measurements.

Details of all these aspects are presented in the following chapters.

# CHAPTER TWO

# Experimental

## 2.1. Synthesis

(**WARNING!** Perchlorate salts of metal complexes containing organic ligands can be dangerously explosive when shocked or heated, which we have carefully avoided.)

### 2.1.1 *trans*-Cr[(tn)$_2$F$_2$]Cl

This compound was synthesized by the literature method[98] but using 1,3-diaminopropane and with reaction overnight rather than for two hours.

A solution of 30 g of $CrCl_3.6H_2O$ in 100 mL of water was placed in a 400 mL polyethylene beaker and mixed with 21 mL of HF (48%) acid. The beaker was packed in ice and kept under efficient magnetic stirring. 132 mL of 1,3-diaminopropane was added dropwise over a period of 50 min. Then the solution was heated at 75 °C for about 16 h. The thick red solution was filtered through a large sintered glass funnel, after cooling to room temperature. The product was washed with 300 mL of 95% ethanol and 200 mL of acetone. The dry product yield was 19 g which was used without further purification.

### 2.1.2 *trans*-Cr[(tn)$_2$Br$_2$]Br

This was prepared from *trans*-Cr[(tn)$_2$F$_2$]Cl using a procedure analogous to that reported for synthesis of *trans*-Cr[(en)$_2$Br$_2$]Br [99] but with reaction overnight rather than for one hour.

8 g of *trans*-Cr[(tn)$_2$F$_2$]Cl was taken into a 250 mL of RB flask and mixed with 95 mL of 48% HBr acid. The solution was kept in the dark and stirred at room temperature for about 16 h. The green product was filtered and washed with 100 mL of 95% ethanol and air dried. The yield was 9 g.

### 2.1.3 *cis*- and *trans*-$Cr[(tn)_2(H_2O)_2](NO_3)_3$

These were prepared exactly as described in the literature.[100]

### 2.1.4 *trans*-$[Cr(tn)_2(CN)_2]ClO_4$

1.8 g (37 mmol) of finely ground NaCN (vacuum dried) was dissolved in 20 mL of DMSO (dried over 4A molecular sieves) by heating to 60-62°C in a 100 mL RB flask. Then 2 g (4.5 mmol) of *trans*-$Cr[(tn)_2Br_2]Br$ (green) was added to the solution, which quickly (< 5 min) turned dark red. As a precaution, the neck of the flask was kept closed whenever possible to minimize exposure to atmospheric moisture. On heating at 60-62°C with vigorous magnetic stirring for 140 min, the solution gradually turned orange in color and the UV/Vis spectrum shifted to the blue, at which time the heating was stopped. The two ligand field band maxima of this solution were close to the expected wavelengths for the product, $Cr(tn)_2(CN)_2^+$. The cooled reaction mixture was then added to 400 mL of ice cold 0.5 M $NaClO_4$ in dry ethanol. On standing on ice for two hours, a yellow precipitate formed which was filtered off with a sintered-glass funnel. The crude product yield was about 1 g (65% of theoretical).

500 mg of the crude product was dissolved in 250 mL of distilled water and placed on a 10 (in water) x 3 (o.d.) cm SP-Sephadex C-25 cation exchange resin column, giving a yellow band, about 2 cm wide. At flow rates of about 20 mL $min^{-1}$ the column was washed with 200 mL of distilled water and then eluted with 350 mL of 0.03 M aqueous $NaClO_4$. The initial and final pale-yellow fractions, about 50 mL each, were discarded, while the middle yellow fraction was collected and rotary evaporated to dryness at 50-55°C. Then 15 mL of dry ethanol was added to obtain a concentration of $NaClO_4$ of about 0.5 M. The

slurry was stirred thoroughly, allowed to stand for 1 hour and filtered off using a medium-porosity glass sintered funnel. The solid complex remaining was washed with 20 mL portions of dry ethanol and acetone, and vacuum dried to yield 400 mg of product (overall yield of 50%). The compound was recrystallized from a minimum amount of room temperature water by dropwise addition of 8 M $NaClO_4$ solution and cooling.

The compound is a bright yellow crystalline material and has a solubility of about 60 mg $mL^{-1}$ in water at room temperature, decreasing to 5 mg $mL^{-1}$ in 2 M $NaClO_4$ . It is readily soluble in DMSO but insoluble in methanol, ethanol, acetone, ether, acetonitrile, ethylacetate, chloroform and methylene chloride.

### 2.1.5 Na[Cr(tn)(CN)$_4$]

3.2 g (65 mmol) of finely ground NaCN (vacuum dried) was dissolved in 40 mL of DMSO (dried over 4A molecular sieves) by heating to 78-80°C in a ¬B flask. Then 1.2 g (2.7 mmol) of *trans*-Cr[(tn)$_2$Br$_2$]Br (green) was added to the solution, which immediately turned dark red. As a precaution, the neck of the flask was kept closed whenever possible to minimize exposure to atmospheric moisture. On heating at 78-80°C with magnetic stirring for 120 min, the solution gradually turned yellow and the UV/Vis spectrum shifted to the blue, at which time the heating was stopped. The two ligand field band maxima of this solution were close to the expected wavelengths for the product. The solution was allowed to cool and excess NaCN was filtered off through a sintered-glass funnel.

The filtrate was diluted to 1.6 L with distilled water and placed on a 16 (in water) x 3 (o.d.) cm Sephadex-QAE A-25 anion exchange resin column, giving a yellow band, about 3 cm wide. At flow rates of about 11 mL $min^{-1}$ the

column was washed with 200 mL of distilled water and then eluted with 0.02 M aqueous $NaClO_4$. Two distinct yellow bands were separated. Passing 1 L of eluents moved the fast moving band to the bottom of the column. The following 340 mL fraction containing this first band was collected and rotary evaporated to dryness at 50-55°C. Then about 15-20 mL of dry ethanol was added, stirred thoroughly and allowed to stand on ice for 30 min. The bright yellow product was collected by filtration through a glass sintered funnel, washed with 20 mL portions of dry ethanol and acetone, and vacuum dried to yield 400 mg of product (overall yield of 60%).

The material is readily soluble in water (> 50 mg $mL^{-1}$), DMSO and DMF, moderately in pyridine and methanol but insoluble in ethanol, acetone, ether, ethylacetate, acetonitrile and methylene chloride.

The compound contains a small amount of free cyanide which was estimated to be less than 1%, based on pH measurements in aqueous solutions. Therefore, when the compound was used in experiments where exact pH of the solution was important, it was necessary to check and adjust the pH to the desired value with few µL of 1M $HClO_4$.

The slow moving band was eluted with 0.4 M aqueous $NaClO_4$ and it was found to be $Na_3[Cr(CN)_6]$.

### 2.1.6 *cis- and trans*-$[Cr(2,3,2\text{-tet})(Cl)_2]ClO_4$

These were made by the literature method[101] except that the 2,3,2-tet ligand was added slowly over 10 min. at 125°C rather than at 100°C. Also no further heating was done after adding the ligand. If the ligand was added at low temperature (80°C) only *cis*-$[Cr(2,3,2\text{-tet})(Cl)_2]Cl$ was formed rather than a mixture of cis and trans isomers.

### 2.1.7 *trans*-[Cr(2,3,2-tet)$(CN)_2$]$ClO_4$

During this synthesis the neck of the flask was kept closed whenever possible to minimize exposure to atmospheric moisture, as a precaution. 1.0 g (2.8 mmol) of *trans*-[Cr(2,3,2-tet)$(Cl)_2$]$ClO_4$ (ash green) was dissolved in 15 mL of DMSO (dried over 4A molecular sieves) by heating at 70°C for 30 min in a RB flask under efficient magnetic stirring to give a reddish purple solution. Then 1.0 g (20 mmol) of finely ground NaCN (vacuum dried) was slowly added over 10 min. The solution turned to a yellow orange color. Heating was continued at 70°C for 1 h. The solution gradually turned yellow and a yellow solid precipitated out. This hot slurry was filtered through a medium glass sintered funnel and the crude product was washed on the filter with 25 mL portions of 2-propanol and ether to yield 0.9 g.

The crude product was dissolved in a minimum amount of water (~20 mL), a few drops of 8 M $NaClO_4$ was slowly added until crystallization just started and then the mixture was allowed to stand in the refrigerator for several hours. Bright yellow crystalline material was collected by filtration through a medium-porosity glass sintered funnel, washed with 25 mL portions of 2-propanol and ether, and vacuum dried to yield 600 mg (63% overall) of the product.

The compound is soluble readily in water, slightly in DMSO and DMF but insoluble in ethanol, methanol, acetonitrile, ethyl acetate and acetone.

In later syntheses, instead of using *trans*-[Cr(2,3,2-tet)$(Cl)_2$]$ClO_4$ its predecessor complex, the crude mixture of *cis- and trans*-[Cr(2,3,2-tet)$(Cl)_2$]Cl, was used as the starting material (see section 2.1.8).

### 2.1.8 *cis*-[Cr(2,3,2-tet)$(CN)_2$]$ClO_4$

240 mg of NaCN (vacuum dried) was dissolved in 5 mL DMSO (dried over 4A molecular sieves) in a 25 mL RB flask at 60°C and then 160 mg of *cis*-[Cr(2,3,2-tet)$(Cl)_2$]Cl was added. Continued heating at 60°C for 30 min gave a yellow solid precipitate which was removed by filtration. (see results for details of the following) This precipitate (150 mg) was crude *trans*-Cr(2,3,2-tet)$(CN)_2^+$. The filtrate was predominantly *cis*-Cr(2,3,2-tet)$(CN)_2^+$ together with minor amounts of Cr(2,3,2-tet)(Cl)$(CN)^+$ and unprecipitated *trans*-Cr(2,3,2-tet)$(CN)_2^+$. This solution was loaded on to a 4 x 1 (o.d.) cm SP-Sephadex C-25 cation exchange resin column and eluted with 0.015 M aqueous $NaClO_4$. A small fraction of pure *cis*-[Cr(2,3,2-tet)$(CN)_2$]$ClO_4$ was isolated in solution.

## 2.2 Materials

All chemicals used were analytical grade reagents, purchased from Aldrich, BDH or Fisher Scientific chemical companies. They were used without further purification except that the solvents were dried over 4A molecular sieves. Organo purewater was prepared from a Sybron / Barnstead purifying system.

## 2.3 Elemental Analysis

Elemental analysis were carried out by Canadian Microanalytical Service Ltd. (Delta, British Columbia) except for chromium. Determination of Cr in solid or solution samples was done as follows.

An accurately weighed (Perkin-Elmer AD-2 Autobalance) 5-10 mg solid sample or a suitable volume of solution containing an equivalent amount of chromium was placed in a 10 mL RB flask and digested on an oil bath with 10 drops of concentrated nitric acid for 10 min around 100°C. This solution was

allowed to cool and 2 mL of organopure water, 3 pellets of sodium hydroxide and 10 drops of 30% hydrogen peroxide were added. The solution was then digested at about 100°C for 45 min. This yellow solution was diluted to 100.0 mL (25.0 mL if less chromium is present) with organopure water. Note that the use of organopure water is crucial for accurate results. The absorbance of the resulting chromate solution was measured at 373 nm ($\varepsilon = 4.82 \times 10^3\ M^{-1}\ cm^{-1}$) and the chromium content was calculated.

## 2.4 Instruments and Techniques

### 2.4.1 UV/Vis Spectra

Phillips PU-8740 or Unicam SP8-400 scanning spectrophotometers were used except when the spectral data were to be stored on a computer disk. The latter work was done on a Cary-5 UV-Vis-NIR Spectrophotometer coupled with a Compaq Deskpro 386s micro computer. The spectral data were evaluated using the Igor Program (WaveMetrics, Inc.) run on a Macintosh IIci computer. This program was used to convert the absorbance values of a spectrum to molar absorptivity ($\varepsilon$), to calculate the spectrum of a photoproduct(s) by subtracting the spectrum of the solution before photolysis from that after the photolysis, and for gaussian analysis of a spectrum. (See section 3.2.5 for details).

### 2.4.2 IR Spectra

A Perkin-Elmer 283 spectrophotometer or Bruker IFS-25 FTIR spectrophotometer coupled with an IBM PS/2 Model 50-Z computer was used. Samples were prepared as KBr disks.

### 2.4.3 HPLC Analysis

A Varian 5000 liquid chromatograph with 25 cm octadecylsilane RP-HPLC column was employed to separate solution mixtures containing cationic or neutral complexes, by ion interaction chromatography. Eluents consisted of tetraethylammonium as the competing cation and butanesulphonate or hexanesulphonate as the anion interaction agent in methanol / water at specific pH values, usually at 3. Peaks were detected by their UV absorption at a wavelength in the 240 - 220 nm region. In this method of detection, the relative peak areas represent the actual component ratio only if the molar absorptivities of these species are equal at the wavelength of detection. Details of conditions are given where appropriate. Whenever, the percentage methanol is mentioned under HPLC conditions, it refers to the use of 90% methanol. This ion pair reversed phase HPLC technique[102] has been successfully optimized to obtain rapid separations of all the peaks of interest.

### 2.4.4 Ion Exchange Chromatography (IEC)

SP-Sephadex C-25 in $Na^+$ form and Sephadex-QAE A-25 in $ClO_4^-$ form were used as cation and anion exchange resins. The details are given under each experiment. Eluents were usually $NaClO_4$ solutions. IE columns with various dimensions were used for isolation of cationic and anionic complexes.

### 2.4.5 Emission Spectra

These were obtained with excitation by a Hanovia xenon lamp / Bausch and Lomb monochromator / infra-red filter (Balzers) source, with detection by using a Jarrel-Ash 0.25 m monochromator preceded by a Corning 3-71 red filter and a 1 cm path of concentrated potassium dichromate solution to remove light

of wavelengths shorter than about 650 nm. The detector was an RCA 31034 photomultiplier with a modified Keithley 410 electrometer. Spectra were recorded on a HP Mosely 7035B X-Y recorder.

### 2.4.6 Emission Lifetime Measurements

Thermostated (Brinckmann Lauda RC 3 thermostat) solutions, usually at 20.0 ± 0.1 °C, in 3 ml fluorescence cells were irradiated by a PTI PL 2300 Nitrogen Laser (1.5 mJ, 3 Hz, 10 nm peak-width) and the emission decay was followed by a Jarrel-Ash monochromator / Hamamatsu R928 photomultiplier / Tektronix 2230 oscilloscope system with GPIB interface to an ATARI 1040 computer. Lifetimes were evaluated[103] by weighted linear regression on log (intensity) versus time plots over 1024 channels of decay using a fitting program (written by Dr. A.D. Kirk). Lifetimes in the absence of oxygen were obtained by deaerating the solution under a slow flow of nitrogen for about 30 min just prior to the measurement.

To obtain Stern-Volmer Plots for lifetime quenching, exact volumes (micro syringe) of a standard solution of the appropriate quencher were added to the working solution. Then the lifetimes were remeasured at each quencher concentration. Note that proper thermostating is essential for accurate results since lifetime is very sensitive to temperature.

### 2.4.7 Light Intensity Measurements

Ferrioxalate actinometry[104-107] was used for light intensity measurements at 436, 406 and 365 nm wavelength photolysis. The quantum yields and the concentrations of $K_3[Fe(C_2O_4)_3]$ solutions used at these wavelength were 1.01 (0.15 M), 1.14 (0.15 M) and 1.22 (0.006 M) respectively. In order to get precise results, no background light was allowed during the

experiment. 3.0 ml of ferrioxalate in 0.05 M $H_2SO_4$ was exposed to light under magnetic stirring for about 30 seconds. Exact exposure time was set accurately using an electro-mechanical shutter. The solution was quantitatively transferred to a 25-mL actinometric volumetric flask. Then 6 ml of developer (0.1 M 1,10-phenanthroline / 0.75 M acetate / 0.2 M $H_2SO_4$) and 5 mL of 1 M NaF were added and the volume was made up to 25.0 mL with distilled water. This solution and a reagent blank were allowed to stand in dark for about 30 min. The absorbance of solutions was measured in a 1 cm plastic or quartz (no glass if $F^-$ !) cell at 510 nm where $Fe(phen)_3^{2+}$ product absorbs. The incident light intensity ($I_0$) was calculated by the following equation.

$$I_0 = [(A_P - A_D) \cdot V] / [\Phi \cdot f_a \cdot t \cdot \varepsilon \cdot l] \qquad (2.1)$$

where $A_P$ and $A_D$ are the absorbance of the photolysed solution and the reagent blank at 510 nm respectively. V is $2.5 \times 10^{-2}$ L. $\Phi$ is the quantum yield value of ferrioxalate at the appropriate wavelength. $f_a = (1 - 10^{-A})$ is the fraction of light absorbed, where A is the absorbance of the ferrioxalate solution at the wavelength of photolysis. t is the time of photolysis in seconds. $\varepsilon = 1.105 \times 10^4$ $M^{-1}$ $cm^{-1}$ is the molar absorptivity of $Fe(phen)_3^{2+}$ complex at 510 nm. l = 1 cm is the path-length of the cell.

### 2.4.8 Photolysis

Radiation at 436 (Balzers interference filter), 406 (Balzers interference filter) and 365 nm (Corning CS 7-60 colored glass filter) from a 1000 W mercury lamp (Universal Instruments AH6-1B) was passed through a 10 cm water filter to remove the infra-red components. The typical light intensities were $3 \times 10^{-8}$, $2 \times 10^{-8}$ and $8 \times 10^{-8}$ einsteins $s^{-1}$, respectively (ferrioxalate actinometer). Radiation at 455, 458, 488 and 514 nm was from a Spectraphysics 2000 Argon

ion laser. The laser beam was expanded to a diameter of about 1 cm using a beam expander in order to avoid possible errors due to local secondary photolysis. The laser output intensities were measured with a power meter (Scientific 36-0001 Disc Calorimeter and 36-5002-365 Digital Power and Energy Indicator) and the power values are given where appropriate, usually below 100 mW. The samples were usually prepared in 1 x $10^{-3}$ M $HClO_4$. The solutions were stirred efficiently by magnetic stirring and thermostated (Brinckmann Lauda RC 6 thermostat) in 1 cm path-length rectangular cuvettes (3 mL volume) or in 3 or 6 cm path-length cylindrical cells (20 or 50 mL volumes respectively).

To study quenched photolysis, exact volumes (micro syringe) of a standard solution of the appropriate quencher were added to the working solution just before starting photolysis. When $OH^-$ ion was the quencher, the solution was re-acidified to about pH 3 immediately after photolysing to the desired extent in order to minimize any base catalyzed thermal reactions of photoproducts or starting complex. Aliquots of these solutions were then chromatographed for qualitative or quantitative analysis of photoproducts.

Details for flash photolysis experiments are given in section 2.4.11.

### 2.4.9 Quantum Yield Determinations

For measurements of total quantum yield, efficiently stirred solutions [3 mL of (0.5 - 1.2) x $10^{-2}$ M complex in ~1 x $10^{-3}$ M $HClO_4$ acid and 0.05 or 0.1 M $NaClO_4$ ionic strength buffer] were irradiated at 10-15°C and the pH monitored by an Ingold LOT combination electrode interfaced to a PDP-11 computer using a program in PASCAL ("Work") written by Dr. A. D. Kirk. Standard acid was added from a 200 µL stepping motor burette, to maintain the

pH of the solution constant with recording of acid added and light intensity (see later). By this method a plot of volume of acid verses time plot can be generated, and any variation in quantum yield during the photolysis can be monitored. The $pK_a$ values of the coordinated water ligands, due to amine and cyanide loss from Cr(III) complexes can be estimated to be in the range 4.5 and 5.5, based on values reported for similar products of $Cr(tn)_3^{3+}$,[108] and $Cr(NH_3)_4(CN)_2^{+}$ [74] Solvent pH values were set between 2.9 - 3.3 which then avoids errors arising from partial dissociation of photoproducts to their conjugate base forms. This pH-stat method is therefore superior to the conventional ΔpH method.

The extent of photolysis was usually kept below ~12% to reduce secondary photolysis. With the mercury lamp, the light intensity was computer monitored continuously using the analog output from an Alphametrics 1020 photometer and silicon photo-detector. This signal was periodically calibrated with the ferrioxalate actinometer so that the integrated computer reading by the program during photolysis could be converted to integrated intensity falling on the front surface of the photolysis solution. In laser photolysis the light intensity did not fluctuate during the time scale of an experiment provided the laser was warmed up for at least 30 min and hence direct ferrioxalate measurements before and after were used. Photolysis time was controlled with high precision by the computer using an electro-mechanical shutter.

For measurements of cyanide yield, a $2 \times 10^{-2}$ M solution of complex in water was passed through a 3 (in water) x 1 (o.d.) cm, QAE-Sephadex A-25 anion-exchange resin column to remove any free cyanide present in the sample. The eluate was mixed with an equal volume of 0.1 M $KClO_4$ in 1.5 x

$10^{-3}$ M $HClO_4$ solution. One portion was photolyzed, while a second was kept in the dark at the same temperature as a thermal blank.

After photolysis, the two solutions were adjusted to pH 12 with a few µL of 1 M NaOH. The free cyanide in the solution was then measured using an ORION 94-06 cyanide / Ag / AgCl reference electrode combination with a Fisher Accumet digital pH meter. Standardization plots were constructed using freshly made KCN solution, in parallel with each analysis. These could be used directly for cyanide evaluation since tests showed that the complex did not affect the electrode readings.

### 2.4.10 Thermal Rate Constants

Pseudo-first-order thermal rate constants were determined either by the pH-stat method or by following the depletion (or increment) in absolute peak areas in chromatograms (HPLC).

### 2.4.11 Conductivity Measurements in Flash Photolysis Experiments

The excitation source was a Spectra Physics Quanta-Ray GCR-11 Neodymium-Yag laser (≤ 70 mJ $pulse^{-1}$ output power, 5-6 ns pulse-with, 1 pulse $s^{-1}$ at 355 nm). The light intensities were detected by a thermal detector (Molectron J 50) / Tektronix 2445 oscilloscope system. About 60 (≥ 30) mL of 1 x $10^{-3}$ M complex in 1 x $10^{-3}$ M $HClO_4$ solutions was used. The irradiation vessel employed was a flow-through quartz cell (0.7 x 0.7 x 3 cm) fitted with three parallel platinum wire electrodes (approximately 0.05 (d) x 0.8 cm) spaced at 1.1 cm separation. This arrangement gives two similar electrochemial compartments, the upper of which was irradiated. The laser beam irradiated a spot of ~ 0.6 cm diameter between the electrodes of the upper compartment

without illuminating the electrodes. The solution was flowed (~15 ml $min^{-1}$) upwards in the cell, so that the reference solution was unphotolyzed. The center electrode was grounded and the other two electrodes were connected in a Wheatstone bridge as input to a two-stage differential amplifier with variable output gains of 1---> 100 . A 135 V square pulse of 4 ms duration was applied to the outside electrodes and the bridge was balanced with the variable resistor so that only the signal of interest was measured. Then the conductivity change in solution induced by the laser pulse was measured as a change in voltage. The signals were captured on a Tektronix TDS-520 digital scope. Timing for laser pulsing and data acquisition were set by a custom made pulse generator and synchronizer in conjuction with a Stanford Research Systems DG-535 delay generator. The experimental set-up is integrated to a Macintosh IIci computer through a GPIB and an I/O data acquisition board (National Instruments). The programs for data acquisition and data analysis were written here using Labview 2.2. (National Instruments). The data acquisition program controls the sequence of events of the experimental set-up, such as shutters, filter wheels and pulsing of lasers, transfers data from the scope and also performs the required mathematical transformation. The data was evaluated by a fitting program based on Marquand Algorithm[109] interfaced to Labview 2.2. The construction of this apparatus was a combined effort of C. Bohne, A. D. Kirk, L. Netters with the technical assistance of T. K. Davies, T. Wiley, B. Dean, R. Bennett, R. Robinson and D. Searle.

# CHAPTER THREE

## Photochemistry and Photophysics of *trans*-[Cr(2,3,2-tet)$(CN)_2$]$ClO_4$. Is Stereochemical Change a Requirement for Equatorial Ligand Loss?

## 3.1 Introduction

Stereochemical change that accompanies photosubstitution of Cr(III) complexes is observed for many complexes studied to date (see section 1.6). It corresponds to a mechanism in which the substituting group enters the coordination sphere trans to the leaving group. This mechanistic rule is well established for axial ligand loss from $C_{4v}$ and $D_{4h}$ complexes where it is claimed to be a requirement for photoreaction (see section 1.13.2). For ligand loss from the equatorial plane, however, the situation is less clear as explained below (section 3.1.1).

### 3.1.1 Photostereochemistry of Equatorial Ligand Loss

The use of the term "equatorial labilization" may be ambiguous since it may refer either to

(i) the location of the ligand being lost (or labilized)

(ii) the plane in which labilization is considered to be occurring

We therefore prefer to use the unambigious phrase "equatorial ligand loss" to give the first meaning. Depending on the planes considered, there are two circumstances that can lead to loss of an equatorial ligand of $C_{4v}$ or $D_{4h}$ complexes, namely reaction via the $^4E_g$ or $^4B_{2g}$ states (Section 1 5.).

To illustrate the two circumstances, consider the application of the VC theory for aquation of *trans*-$CrA_4(CN)_2^+$, where A = $NH_3$, (see Fig. 3.1.1). When the $^4B_{2g}$ state is involved (case a), the equatorial plane is labilized and the loss of one of the ammonias (A*) followed by trans entry of a water molecule leads to the 1,6-CN-3-W product. On the other hand, if the $^4E_g$ state were involved (case b), excitation is now into one of the two degenerate planes

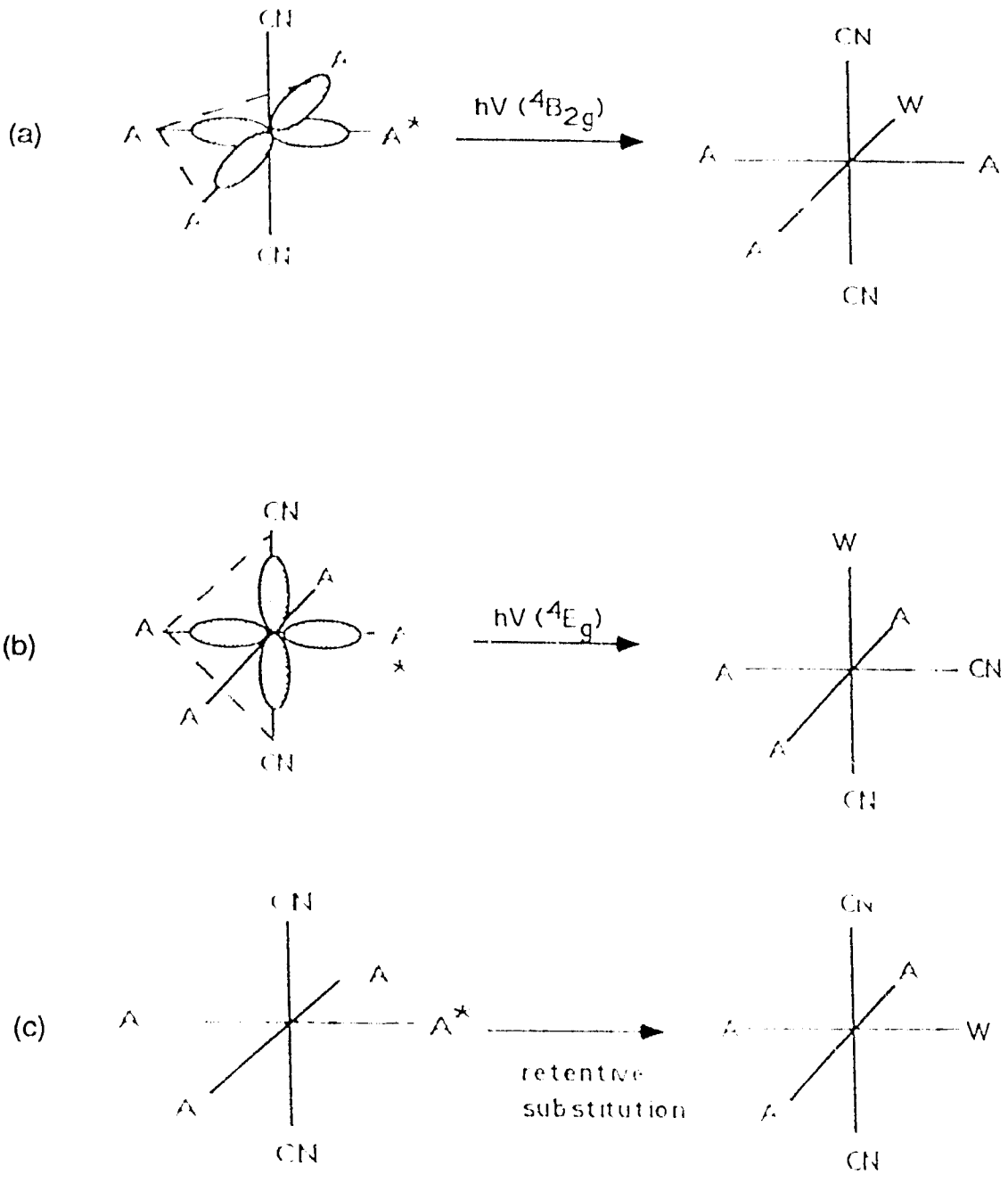


**Fig. 3.1.1** Stereochemistry of the photoaquation of ammonia in *trans*-$Cr(NH_3)_4(CN)_2^+$. Application of Vanquickenborne and Ceulemans theory for the (a) $^4B_{2g}$ state reaction. (b) $^4E_g$ state reaction. (c) stereoretentive reaction.

**Key:** A = $NH_3$, W = $H_2O$, * = leaving ligand

containing the CN-Cr-CN axis, and loss of the equatorial A* ligand would lead to the 1,2-CN-6-W product. According to VC Theory, however, the latter product is not expected in this particular molecule since the $^4E_g$ state is significantly higher in energy (0.25 $\mu m^{-1}$) than the $^4B_{2g}$ state. If, due to some reason, the photoreaction is stereoretentive (case c), the product would be 1,6-CN-3-W. That is then indistinguishable from the expected major photoproduct via the $^4B_{2g}$ state. All the examples where equatorial ligand loss was studied so far, are of this type and hence the molecular geometry of products does not distinguish whether there was a mechanistic stereochemical change associated with the photoreaction.

### 3.1.2 Recognition of Mechanistic Stereochemical Change In Equatorial Ligand Loss

*Trans*-[Cr(2,3,2-tet)$(CN)_2$]$ClO_4$ was chosen as a suitable molecule to investigate whether equatorial ligand loss is accompanied by stereochemical change. Cyanide is a stronger σ donor than amine. Therefore the trans dicyano configuration makes the $^4B_{2g}$ state lower in energy and from this state photoreaction is expected to be confined to the plane (equatorial) of 2,3,2-tet ligand (sections 1.5 and 1.6). The ligand has an ethylenediamine type end which is a good leaving group, as is evident by the relatively high (~0.6) quantum yield of *trans*-Cr$(en)_2(CN)_2^+$.[53] 2,3,2-tet would therefore allow any of the primary amine ends to come off but would inhibit the trans attack and the stereochemical change to follow. Therefore the photoreaction should be inhibited and the photoinertness of this molecule would unambiguously imply that stereochemical change is a requirement of equatorial ligand loss.

## 3.2 Results

### 3.2.1 Characterization of *trans*-$Cr(2,3,2\text{-tet})(CN)_2^+$

3.2.1a Elemental Analysis:

Analytical data were, found (calculated) : %C 29.7 (29.7), %H 5.5 (5.5), %N 22.8 (23.1), %Cr 13.9 (14.3). The results are in excellent agreement with the calculated values for $[Cr(2,3,2\text{-tet})(CN)_2]ClO_4$.

3.2.1b UV/Vis spectrum:

The compound shows two LF bands at 432 and 338 nm with $\varepsilon_{432}$ = 52.4 ± 0.9 (n = 5) $M^{-1}$ $cm^{-1}$. Spectral information on many Cr(III) complexes with the same coordinated atoms is listed in Table 3.2.1.

**Table 3.2.1** UV/Vis spectral data of some Cr(III) am(m)ine, cyanoam(m)ine, and cyano complexes.

| Complexes | Solvent | $\lambda_{max}$, nm ($\varepsilon$, $M^{-1}cm^{-1}$) | | $\varepsilon(L_1) / \varepsilon(L_2)$ | Ref. |
|---|---|---|---|---|---|
| | | $L_1$[a] | $L_2$[a] | | |
| $Cr(NH_3)_6^{3+}$ | $H_2O$ | 466 (41) | 354 (34) | | 63 |
| $Cr(en)_3^{3+}$ | $H_2O$ | 438 (72.5) | 350 (60.3) | | 69 |
| $Cr(tn)_3^{3+}$ | $H_2O$ | 464 (59) | 355 (51) | | 63 |
| $Cr(NH_3)_5(CN)^{2+}$ | $H_2O$ | 451 (42.6) | 347 (37.7) | | 73 |

**Table 3.2.1** (Continued)

| Complexes | Solvent | $\lambda_{max}$, nm (ε, $M^{-1}cm^{-1}$) | | ε($L_1$) / ε($L_2$) | Ref. |
|---|---|---|---|---|---|
| | | $L_1$[a] | $L_2$[a] | | |
| *trans*-$Cr(NH_3)_4(CN)_2^+$ | $H_2O$ | 440 (42.6) | 344 (41.5) | 1.03 | 74, 110 |
| *cis*-$Cr(NH_3)_4(CN)_2^+$ | $H_2O$ | 436 (49.0) | 342 (37.6) | 1.30 | 74 |
| *trans*-$Cr(en)_2(CN)_2^+$ | $H_2O$ | 432 (50.1) | 337 (42.7) | 1.17 | 53 |
| | $H_2O$ | 432 (49.0) | 337 (42.7) | 1.15 | 111 |
| *cis*-$Cr(en)_2(CN)_2^+$ | $H_2O$ | 433 (71) | 339 (63.1) | 1.13 | 111 |
| | $H_2O$ | 434 (70) | 339 (62.3) | 1.12 | 112 |
| | $H_2O$ | 434 (69.5) | 339 (62.2) | 1.12 | 53 |
| $Cr(NH_3)(CN)_5^{2-}$ | $H_2O$ | 397 (90) | 320 (54) | | 56 |
| | DMSO | 406 (77) | 324 (58) | | 56 |
| | DMF | 406 (72) | 316 (66) | | 56 |
| $Cr(CN)_6^{3-}$ | $H_2O$ | 377 (86) | 307 (60) | | 56 |
| | DMSO | 386 (78) | 313 (56) | | 56 |
| | DMF | 391 (78) | 317 (53) | | 56 |
| *trans*-$Cr(2,3,2\text{-tet})(CN)_2^+$ | $H_2O$ | 432 (52.4) | 338 (46.0) | 1.14 | c, 67 |
| *cis*-$Cr(2,3,2\text{-tet})(CN)_2^+$ | $H_2O$ | 435 (71) | 337 | 1.1 | c |
| $Cr(tn)_2(CN)_2^+$ | $H_2O$ | 441 (52.5) | 344 (47.5) | 1.08 | c, 68 |
| $Cr(tn)(CN)_4^-$ | $H_2O$ | 408 (55) | 329 (35) | | c |
| | $H_2O$ | 405[b] | 324[b] | | c |
| | DMSO | 414 | 333 | | c |
| | DMF | 416 | 332 | | c |

[a] $L_1$ and $L_2$ are the lowest and next highest energy bands of the UV/Vis spectrum. [b] Estimated values (see section 4.3.2). [c] This work

Among them $Cr(en)_2(CN)_2^+$ is the closest to this molecule since they both contain two en rings trans to one another, which enforces some angular distortion at Cr center in contrast to ammonia or tn ligands. The wavelengths of the peak maxima and the molar absorptivity ratio of the two bands for this complex are similar to those for both *cis*- and *trans*-$Cr(en)_2(CN)_2^+$. The absolute molar absorptivity values are, however, close to the *trans*-$Cr(en)_2(CN)_2^+$ isomer, which is distinguishable from the cis, indicating the compound is *trans*-$Cr(2,3,2\text{-tet})(CN)_2^+$.

3.2.1c Emission Spectrum:

The emission peak maximum of the complex is in the region expected for $Cr(2,3,2\text{-tet})(CN)_2^+$. (See section 3.2.6 for details.)

3.2.1d IR Spectrum:

The two very small peaks observable at 2145 and 2107 $cm^{-1}$ for the title compound (Fig. 3.2.1) were also present in the spectrum of *trans*-$Cr(2,3,2\text{-tet})Cl_2^+$ (Fig. 3.2.2), from which this compound was synthesized. Therefore, no peaks can be detected in the region corresponding to the cyanide stretch (2100 - 2200 $cm^{-1}$) of this compound. Having a very weak cyanide region is reported for many other Cr(III) cyanoam(m)ino complexes[68, 74] and therefore it cannot be used as a proof of geometric or isomeric identity.

It was, however, noted that the Cr-Cl band of *trans*-$[Cr(2,3,2\text{-tet})Cl_2]ClO_4$ which appears at 330 $cm^{-1}$ is not present in this compound, indicating the substitution of $Cl^-$ ligand during the synthesis. (This region, below 400 $cm^{-1}$, is not shown in the figures.)

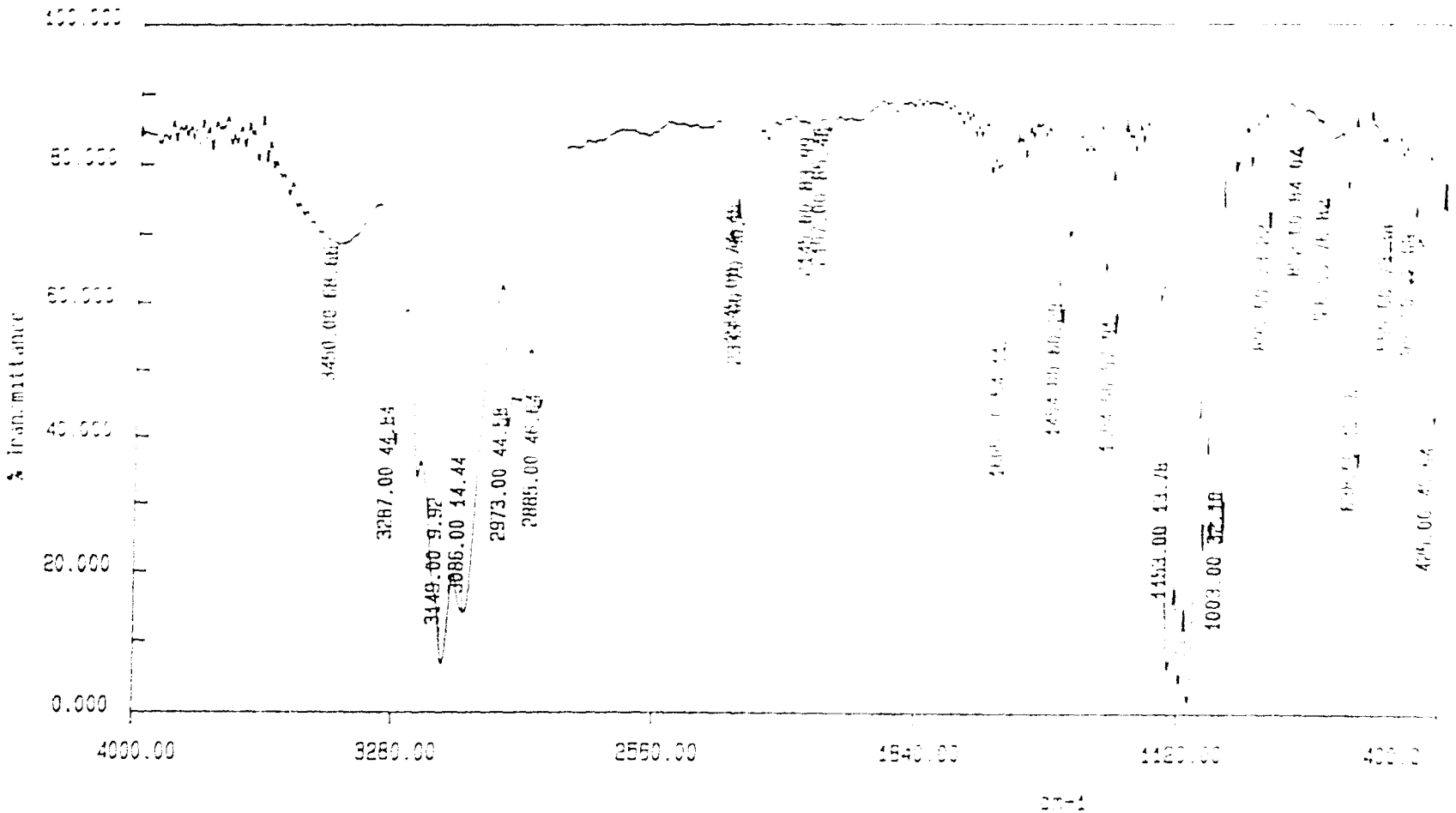


**Fig. 3.2.1** IR spectrum of *trans*-$Cr(2,3,2\text{-tet})(CN)_2](ClO_4)$.

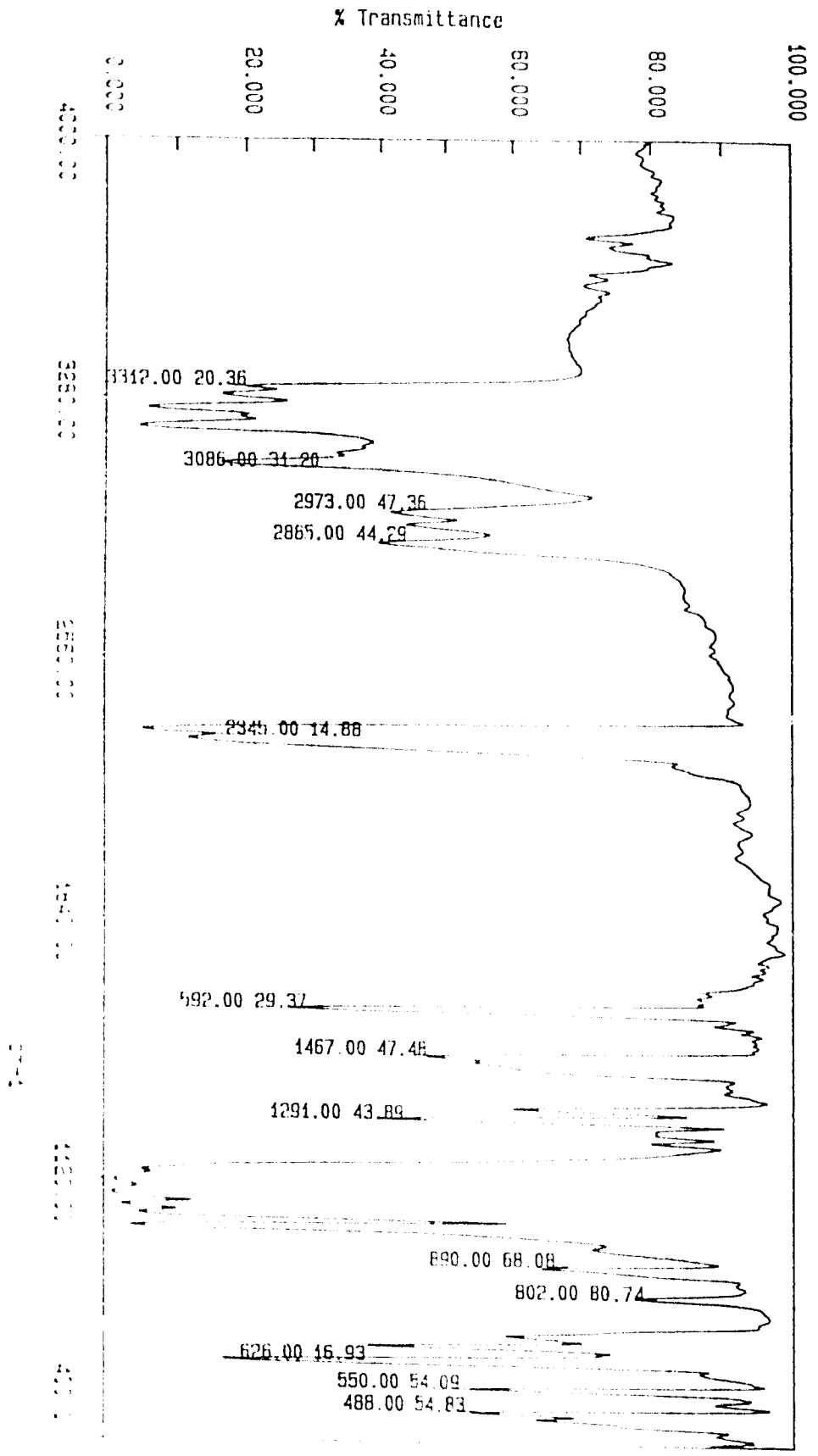


**Fig. 3.2.2** IR spectrum of *trans*-[Cr(2,3,2-tet)Cl$_2$](ClO$_4$).

3.2.1e Thermal conversion to $Cr(2,3,2\text{-tet})Cl_2^+$:

The compound was reacted with 6 M HCl for 30 min at 60°C to convert it to $Cr(2,3,2\text{-tet})(Cl)_2^+$ and the reaction was followed by UV/Vis spectroscopy and HPLC.

UV/Vis spectra of *cis*- and *trans*-$Cr(2,3,2\text{-tet})Cl_2^+$ (Fig. 3.2.3 and 3.2.4) are very different with respect to wavelengths, absolute molar absorptivities and relative molar absorptivity ratios at peak maxima [$\varepsilon(L_1)/\varepsilon(L_2)$]. The final spectrum of the solution after reacting the compound with HCl (Fig. 3.2.5) is close to the trans species indicating the product is predominantly *trans*-$Cr(2,3,2\text{-tet})Cl_2^+$. The small blue shift of the peak maxima compared to that of the authentic sample (Fig. 3.2.3), however, may be because small amounts of some aqua species are also present.

HPLC allowed us to separate $Cr(2,3,2\text{-tet})(CN)_2^+$ (S), $Cr(2,3,2\text{-tet})(H_2O)(CN)^{2+}$ (T), *cis*- (A) and *trans*-$Cr(2,3,2\text{-tet})Cl_2^+$ (B), and *cis*- (C) and *trans*-$Cr(2,3,2\text{-tet})(H_2O)Cl^{2+}$ (D) into base line resolved peaks (Fig. 3.2.6). Peaks S, A and B were confirmed with authentic samples. The assignment of peaks T (section 3.2.3), C and D were based on the thermal aquation reactions of the above species respectively. HPLC analysis of the conversion of the compound to $Cr(2,3,2\text{-tet})Cl_2^+$ shows that the reaction goes via $Cr(2,3,2\text{-tet})(H_2O)(CN)^{2+}$ and $Cr(2,3,2\text{-tet})(H_2O)Cl^{2+}$ producing *trans*-$Cr(2,3,2\text{-tet})Cl_2^+$ (B) as the major product. The final solution also contains minor components of *trans*-$Cr(2,3,2\text{-tet})(H_2O)Cl^{2+}$ (D) and *cis*-$Cr(2,3,2\text{-tet})Cl_2^+$ (A). In this solution, the peak area of A was <8% of (B + D) and no $Cr(2,3,2\text{-tet})(H_2O)(CN)^{2+}$ (T) or *cis*-$Cr(2,3,2\text{-tet})(H_2O)Cl^{2+}$ (C) was found. Since aquation and anation processes of Cr(III) complexes are sterecretentive, this result shows that the

compound is >92% trans, assuming equal molar absorptivities at the detection wavelength.

Later HPLC analysis on *cis*- and *trans*-Cr(2,3,2-tet)$(CN)_2^+$ extend these results and shows that the isomeric purity of the compound is ≥ 99% trans.

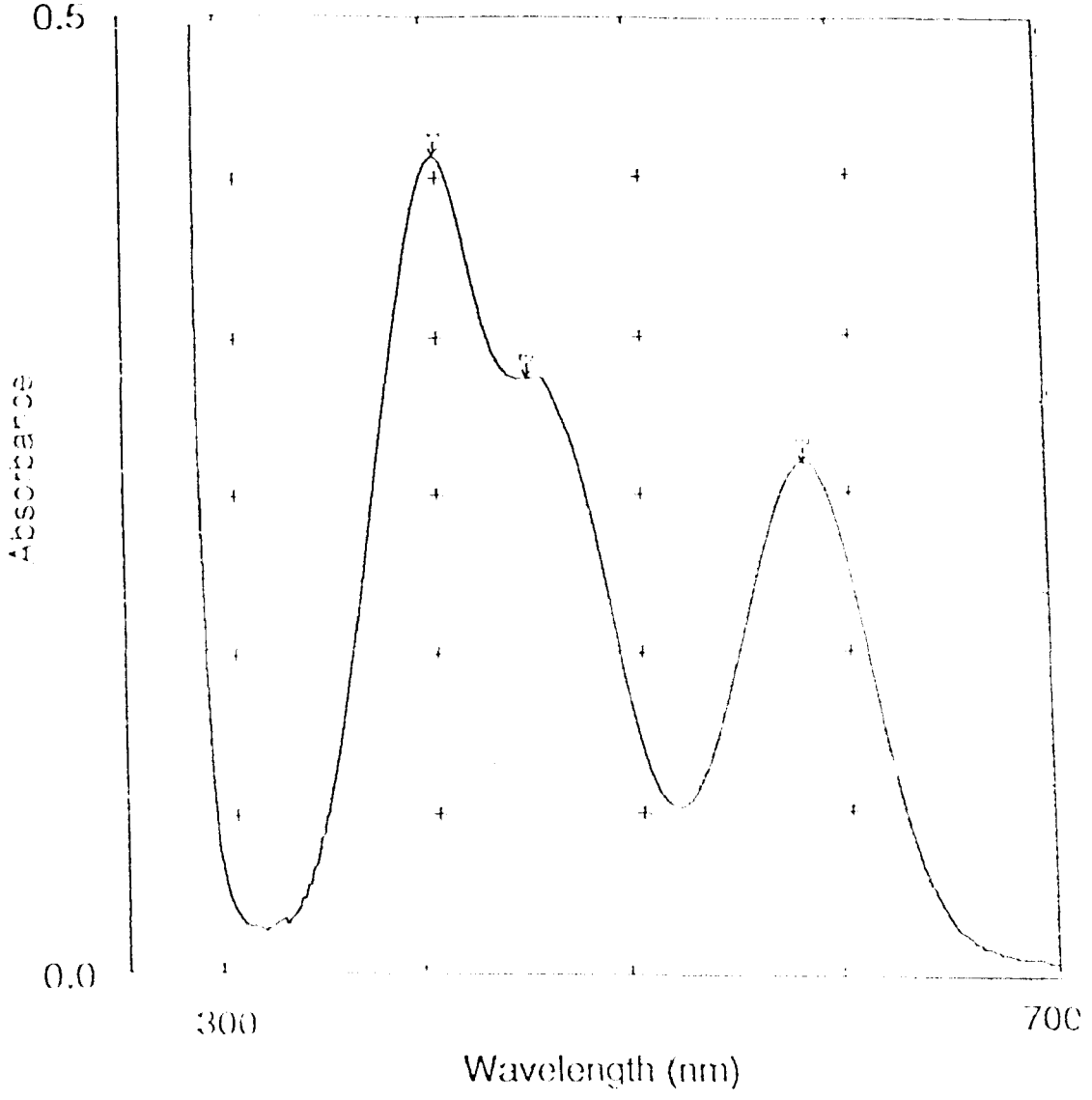


**Fig. 3.2.3** UV/Vis spectrum of *trans*-Cr(2,3,2-tet)$Cl_2^+$ in DMSO at room temperature.

($\varepsilon$ = 38 and 24 $M^{-1}$ $cm^{-1}$ at 400 and 578 nm, respectively.[80])

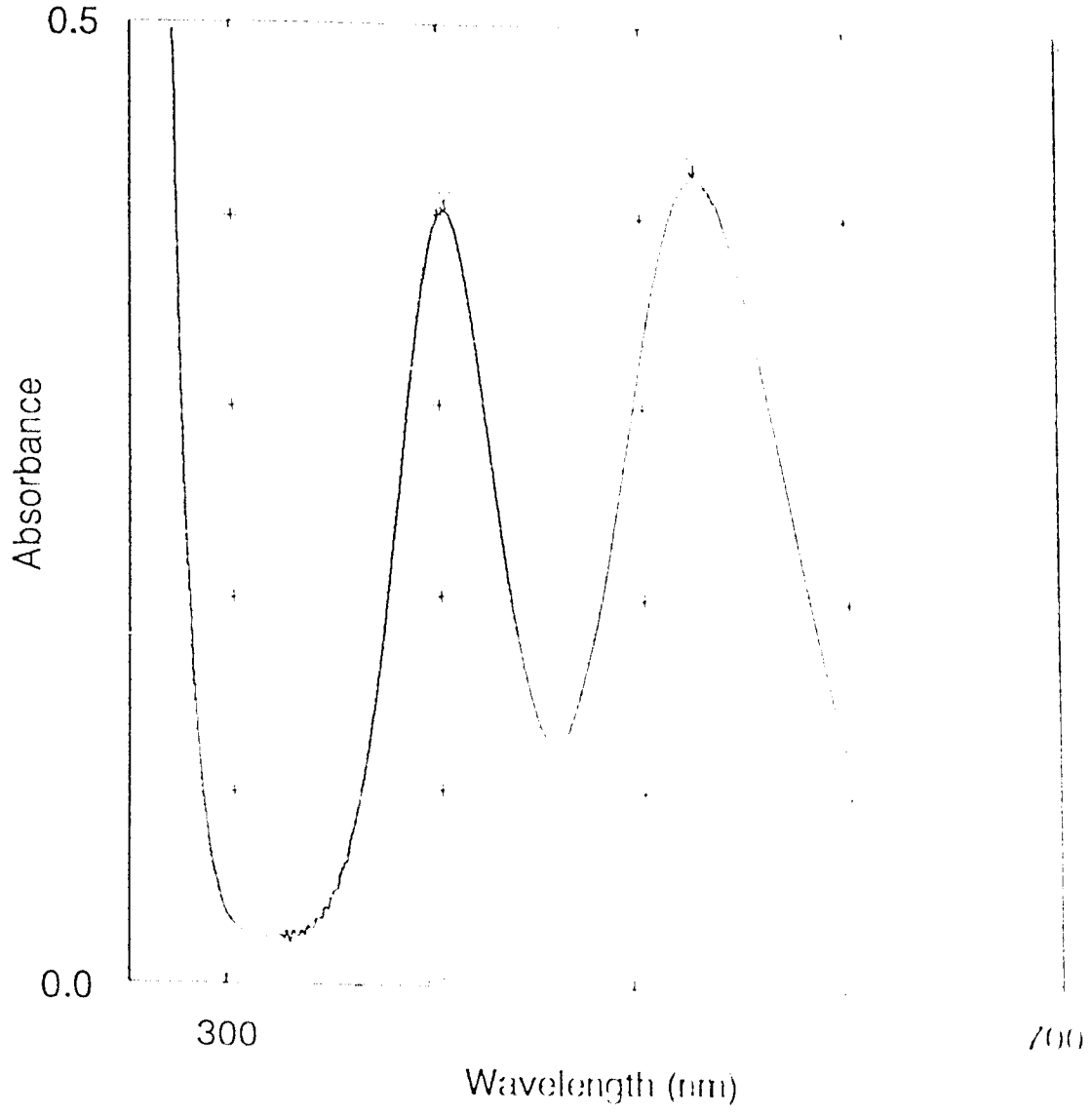


**Fig. 3.2.4** UV/Vis spectrum of *cis*-Cr(2,3,2-tet)$Cl_2^+$ in acidic aqueous solutions at room temperature.

($\varepsilon$ = 76 and 78 $M^{-1}$ $cm^{-1}$ at 404 and 527 nm, respectively.[101])

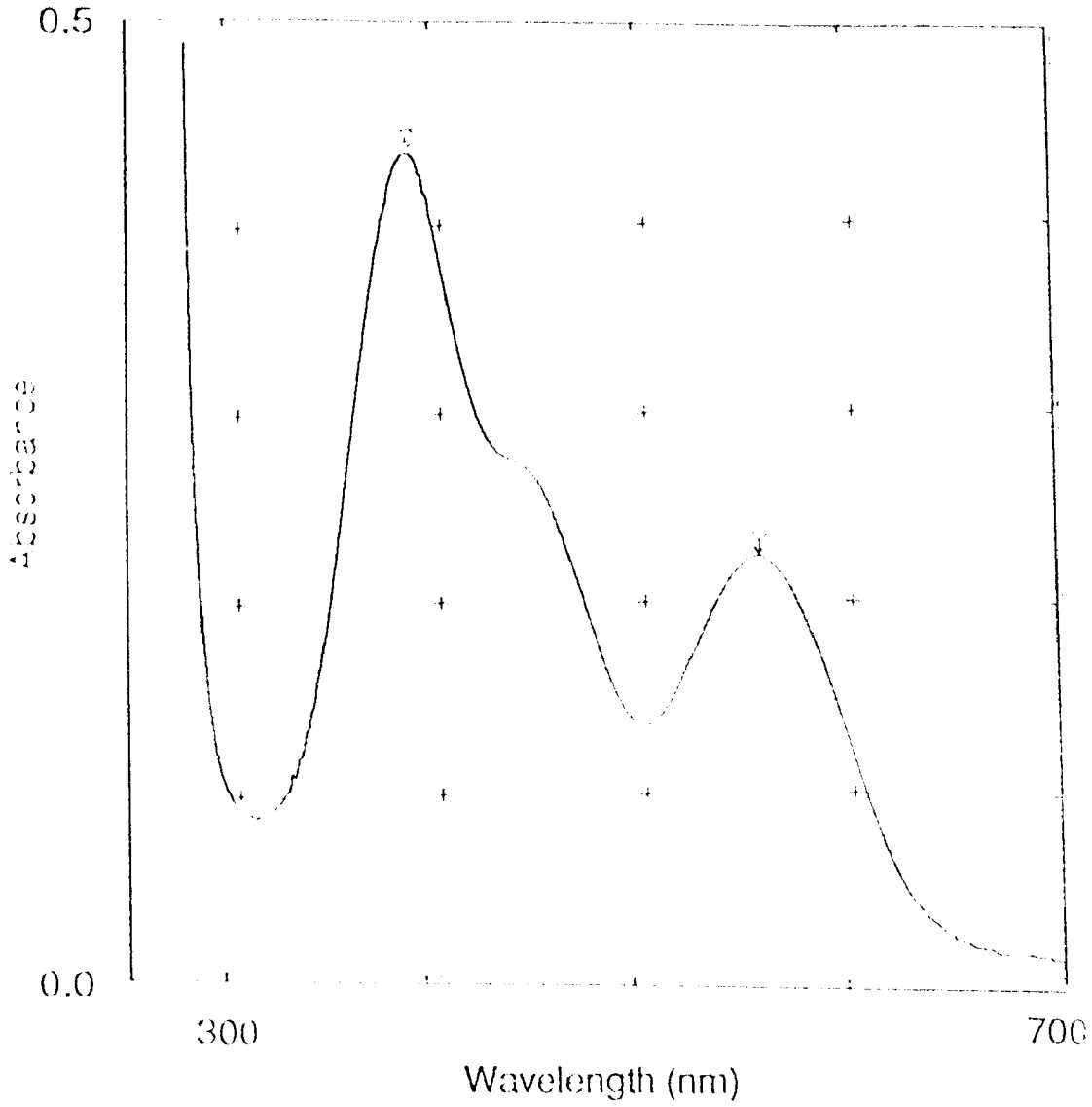


**Fig. 3.2.5** UV/Vis spectroscopic study of the thermal aquation of *trans*-Cr(2.3,2-tet)$(CN)_2^+$ : Spectrum of the product when "Cr(2,3,2-tet)$(CN)_2^+$" was reacted with 6 M HCl for 30 min at 60°C.

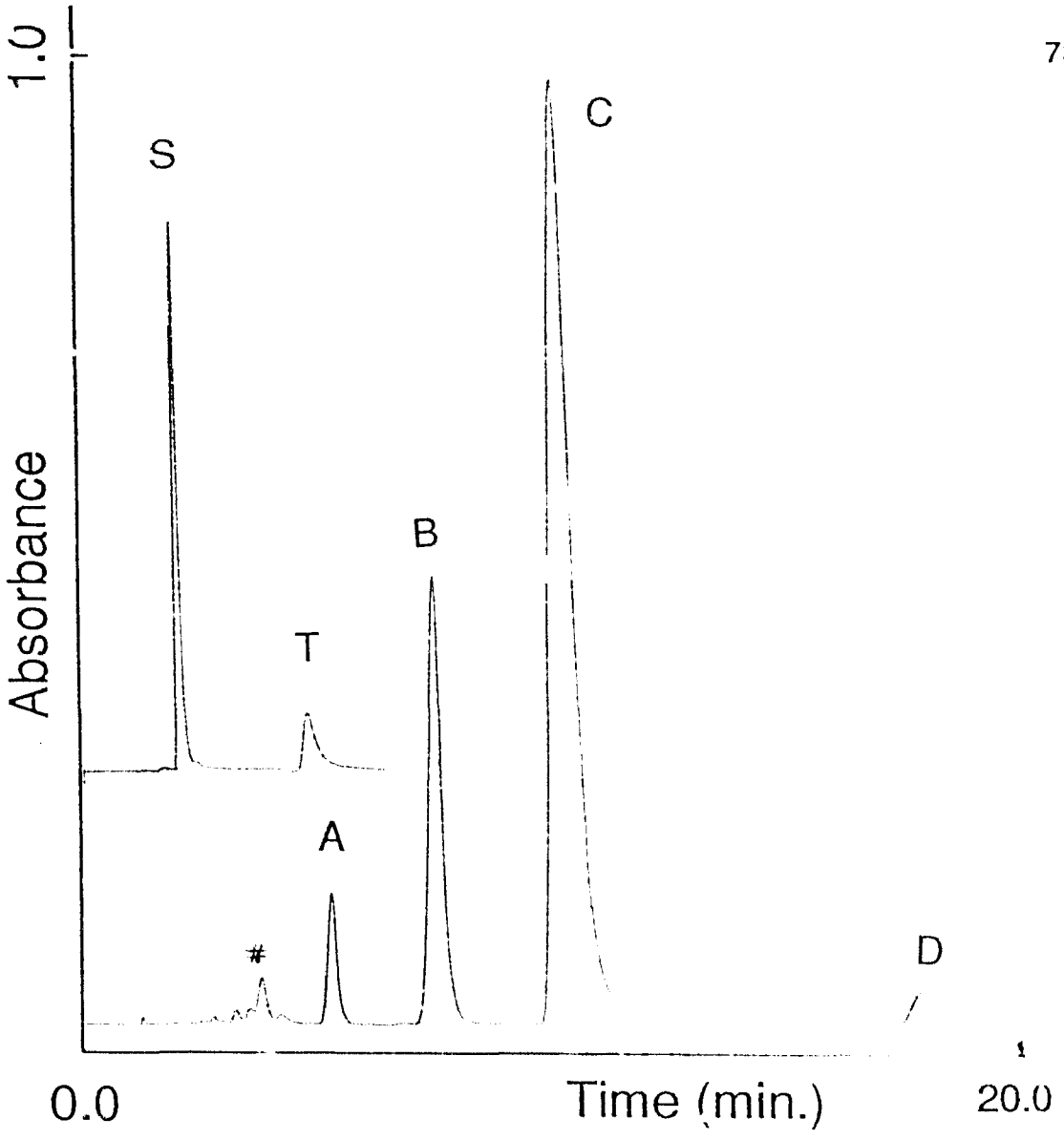


**Fig. 3.2.6** HPLC characterization of *trans*-$Cr(2,3,2\text{-tet})(CN)_2^+$ : A sample chromatogram showing the separation of $Cr(2,3,2\text{-tet})(CN)_2^+$, $Cr(2,3,2\text{-tet})Cl_2^+$ and their thermal products.

**Key :** S = $Cr(2,3,2\text{-tet})(CN)_2^+$, T = $Cr(2,3,2\text{-tet})(H_2O)(CN)^{2+}$, A = *cis*-$Cr(2,3,2\text{-tet})Cl_2^+$, B = *trans*-$Cr(2,3,2\text{-tet})Cl_2^+$, C = *cis*-$Cr(2,3,2\text{-tet})(H_2O)Cl^{2+}$, D = *trans*-$Cr(2,3,2\text{-tet})(H_2O)Cl^{2+}$. # = impurity peaks

**Conditions** : eluents; 25 mM butanesulfonate and 25 mM triethylamine in 4% methanol at pH 3.0; Flow rate 2 mL $min^{-1}$; Detection wavelength 220 nm.

### 3.2.2 Characterization of *cis*-Cr(2,3,2-tet)$(CN)_2^+$

Synthesis in DMSO starting with *cis*-Cr(2,3,2-tet)$Cl_2^+$ produced a yellow precipitate which has the same UV/Vis and IR spectra, and chromatographic retention times as *trans*-Cr(2,3,2-tet)$(CN)_2^+$. HPLC also shows that the slurry at the end of synthesis contains ≥70% *trans*-Cr(2,3,2-tet)$(CN)_2^+$. This result shows that the cyanide substitution occurs with efficient cis ---> trans isomerization Similar behavior was also observed in the synthesis of the analogous [Cr(cyclam)$(CN)_2$]$ClO_4$ where only *trans*-Cr(cyclam)$(CN)_2^+$ was isolated whether the starting material is *cis*- or *trans*-Cr(cyclam)$Cl_2^+$.

The trans product was filtered off. The filtrate contained predominantly *cis*-Cr(2,3,2-tet)$(CN)_2^+$ together with minor amounts of Cr(2,3,2-tet)(Cl)$(CN)^+$ and *trans*-Cr(2,3,2-tet)$(CN)_2^+$, as described below.

Fig. 3.2.7 shows the chromatographic peak development in the synthesis. With the depletion of A (12.2 min) during the reaction, peaks N (2.5 min), S (3.0 min) and two small peaks, E (5.8 min) and F (6.1 min) were gradually developed (line four of Table 3.2.2). The peaks for DMSO solvent, *trans*-Cr(2,3,2-tet)$(CN)_2^+$(S) and *cis*-Cr(2,3,2-tet)$Cl_2^+$ (A) were confirmed with authentic samples. A study of the reaction between *cis*-Cr(2,3,2-tet)$Cl_2^+$ and DMSO eliminates the possibility that peaks E and F were due to solvent coordination. One criterion (section 4.2) commonly used for assignment of chromatographic peaks in this method is that the cis isomer elutes before trans isomer of a given cationic species at this working pH (=3). Since this reaction is expected to be the substitution of $Cl^-$ in *cis*-Cr(2,3,2-tet)$Cl_2^+$ by $CN^-$ ligand, it is believed that the peak N, elutes just prior to *trans*-Cr(2,3,2-tet)$(CN)_2^+$ is *cis*-Cr(2,3,2-tet)$(CN)_2^+$. Also the comparison of retention times for *trans*-Cr(2,3,2-tet)$(CN)_2^+$ (3.0 min) and *cis*-Cr(2,3,2-tet)$Cl_2^+$ (12.2 min) implies that the species

corresponding to retention times 5.8 and 6.1, E and F, are cis and trans isomers of Cr(2,3,2-tet)(Cl)(CN)+.

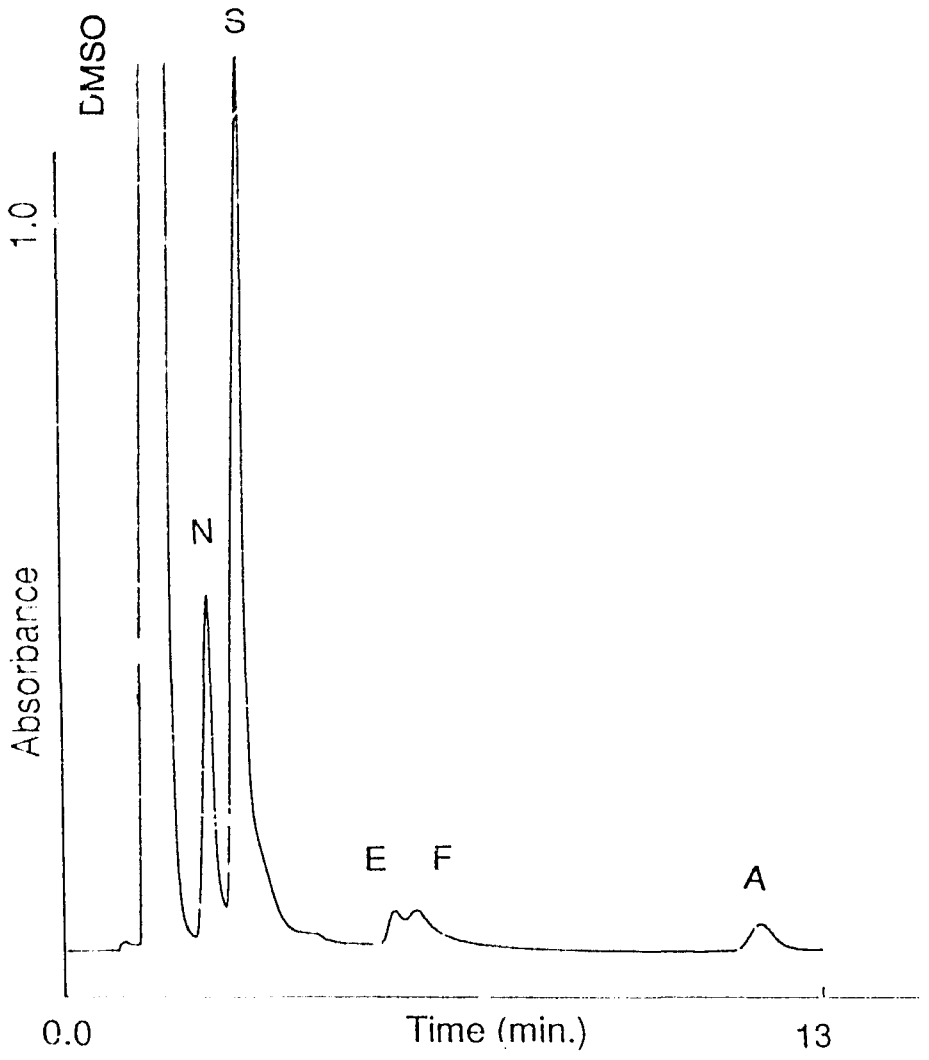


**Fig. 3.2.7** HPLC chromatograms of the solution at the synthesis and characterization of *cis*-$Cr(2,3,2\text{-tet})(CN)_2^+$.

**Key :** N = *cis*-$Cr(2,3,2\text{-tet})(CN)_2^+$ , S = *trans*-$Cr(2,3,2\text{-tet})(CN)_2^+$, A = *cis*-$Cr(2,3,2\text{-tet})Cl_2^+$, E and F = *cis*- and *trans*-$Cr(tn)_2(CN)Cl^+$.

**Conditions** : eluents; 25 mM hexanesulfonate and 25 mM triethylamine in 5% methanol at pH 3.0; Flow rate 2 mL $min^{-1}$; Detection wavelength 220 nm.

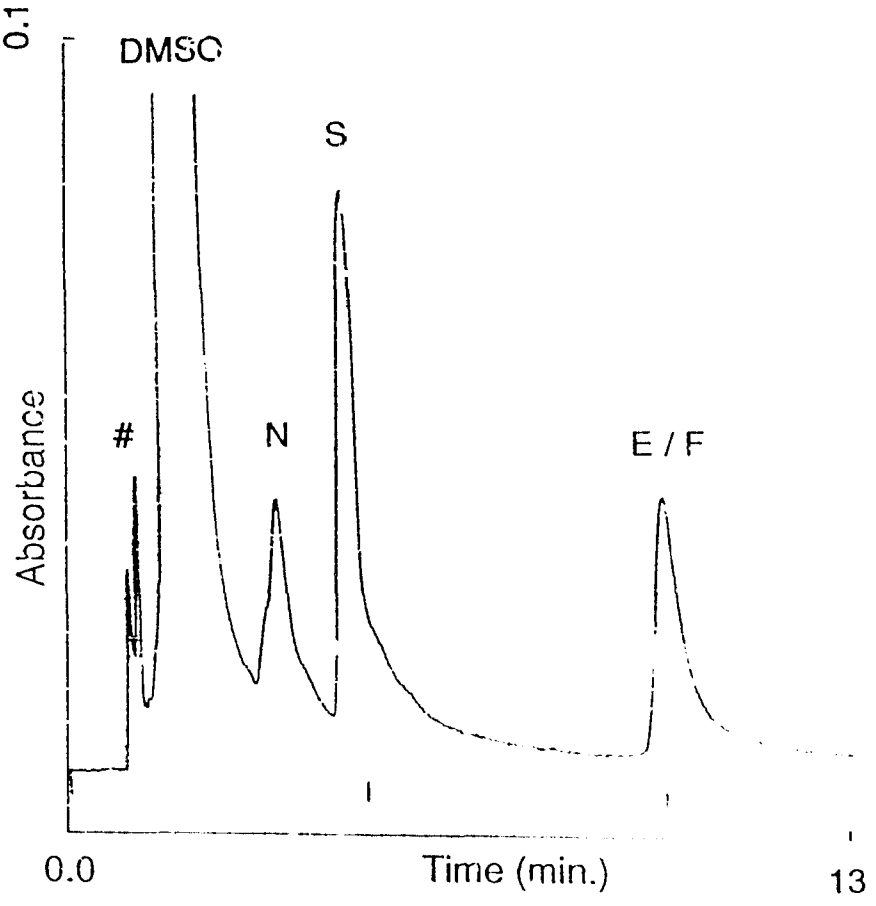


**Fig. 3.2.8** HPLC chromatograms of the synthesis and characterization of *cis*-$Cr(2,3,2\text{-tet})(CN)_2^+$, under 12.5 mM triethylamine.

**Key :** Same as for Fig. 3.2.7 except # = anion or artifact peaks

**Conditions** : eluents; 25 mM hexanesulfonate and 12.5 mM triethylamine in water at pH 3.0; Flow rate 2 mL $min^{-1}$; Detection wavelength 220 nm.

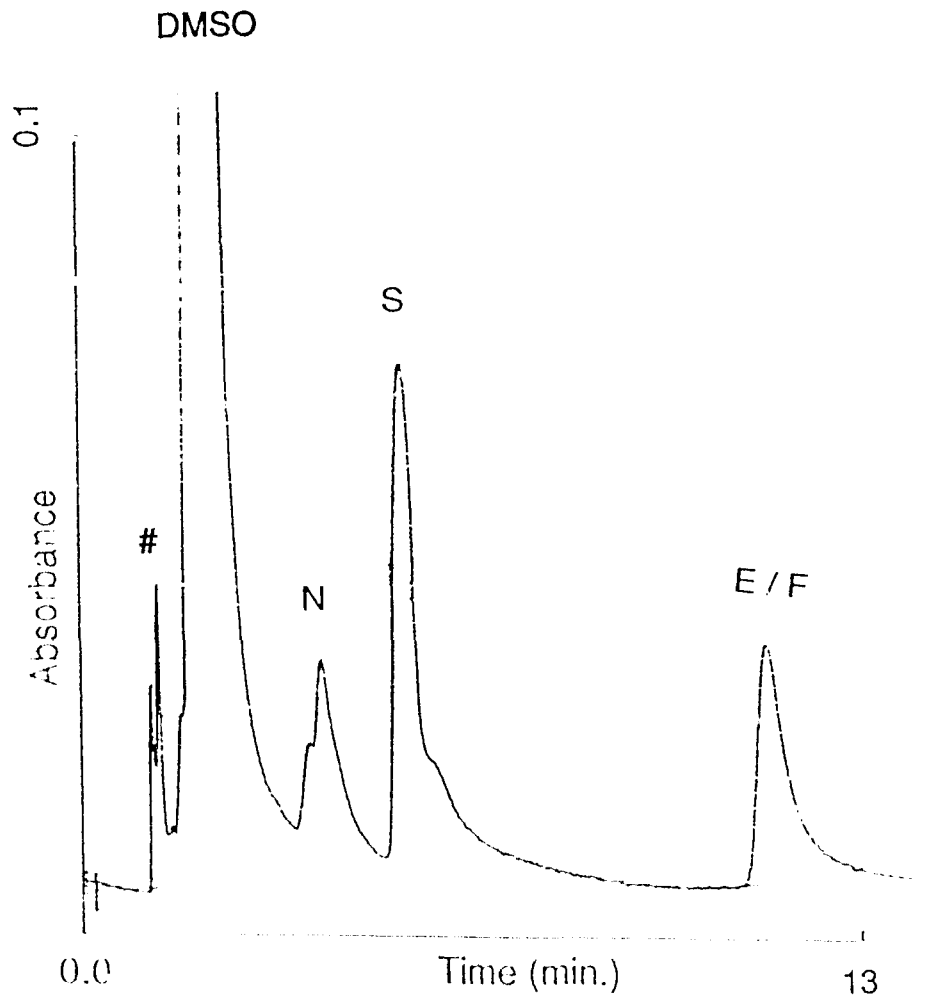


**Fig. 3.2.9** HPLC chromatograms of the synthesis and characterization of *cis*-$Cr(2,3,2\text{-tet})(CN)_2^+$, under 10 mM triethylamine.

**Key :** Same as for Fig. 3.2.7 except # = anion or artifact peaks

**Conditions** : Same as for Fig. 3.2.8, except for triethylamine concentration.

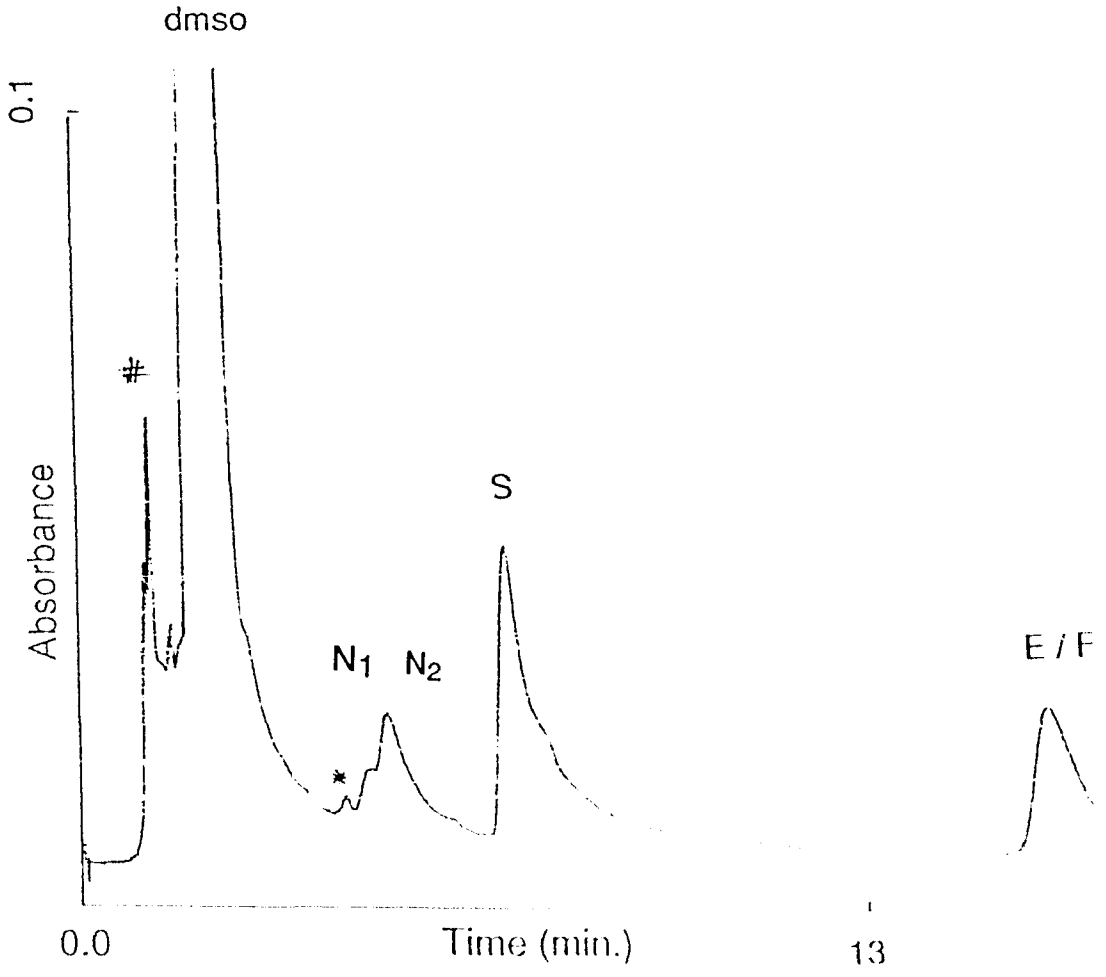


**Fig. 3.2.10** HPLC chromatograms of the synthesis and characterization of *cis*-Cr(2,3,2-tet)$(CN)_2^+$, under 5 mM triethylamine.

**Key :** Same as for Fig. 3 2.8, peaks $N_1$ and $N_2$ are component peaks of N (see section 3.2.2), * = unidentified small peak.

**Conditions** : Same as for Fig. 3.2.9.

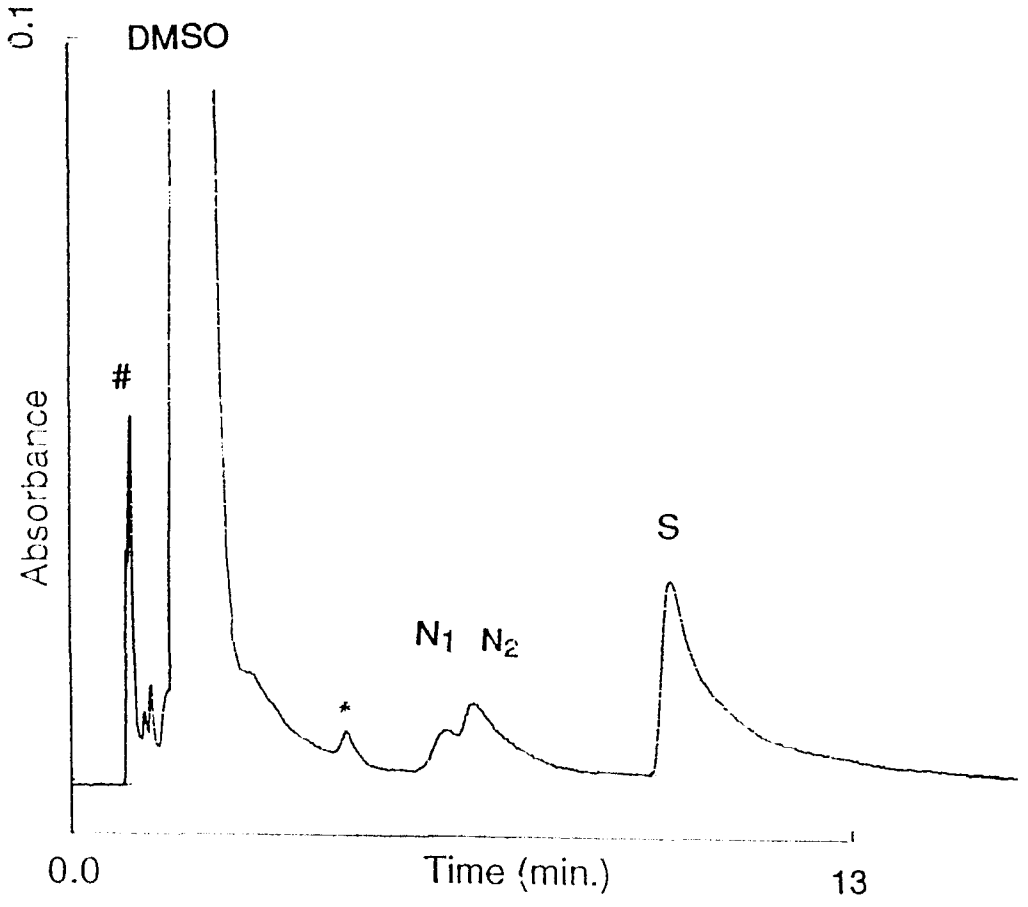


**Fig. 3.2.11** HPLC chromatograms of the synthesis and characterization of *cis*-Cr(2,3,2-tet)$(CN)_2^+$, under 2 mM triethylamine.

**Key :** Same as for Fig. 3.2.10.

**Conditions** : Same as for Fig. 3.2.9.

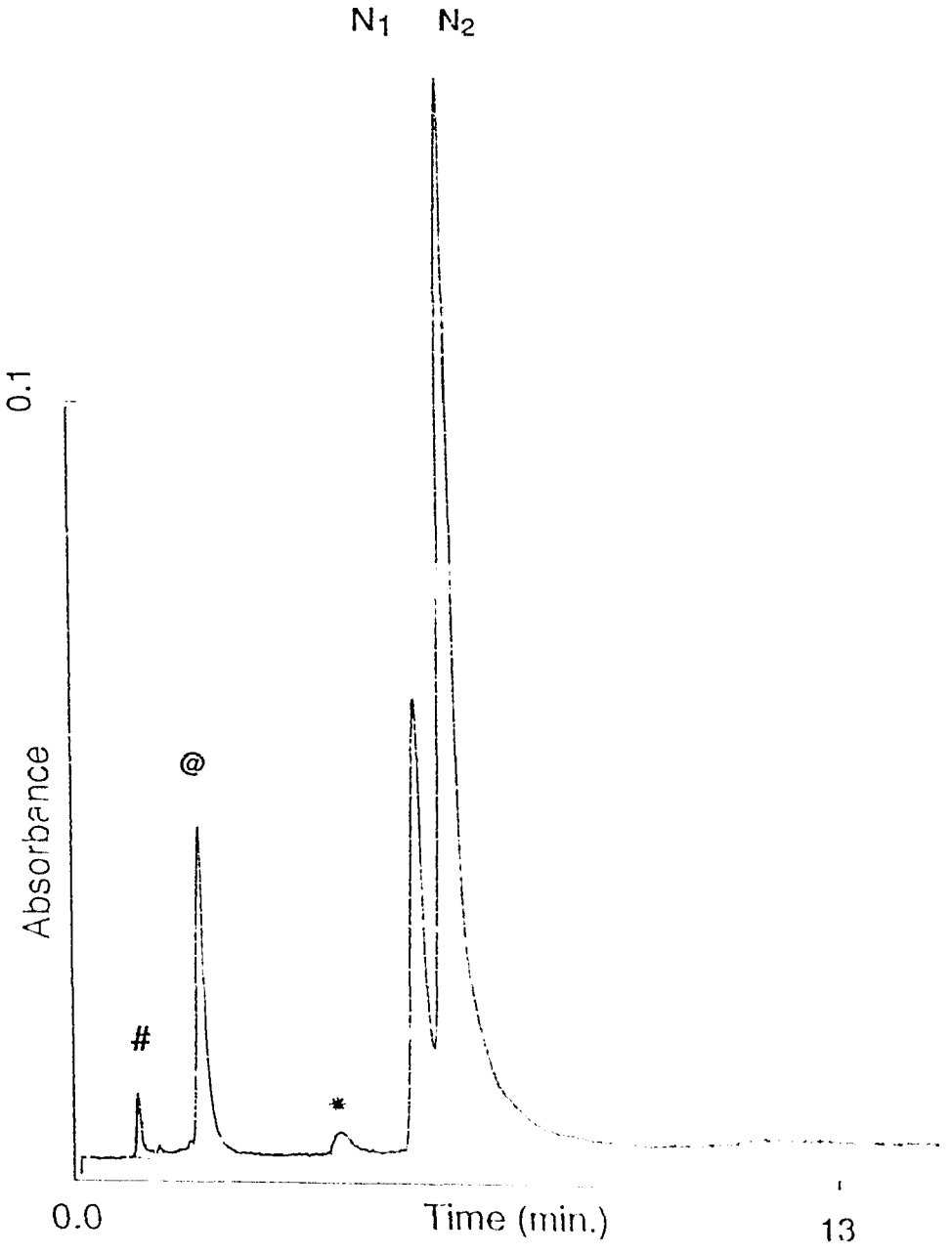


**Fig. 3.2.12** HPLC chromatograms of the isolated *cis*-Cr(2,3,2-tet)$(CN)_2^+$ in solution

**Key :** Same as for Fig. 3.2.10, @ DMSO (contaminant).

**Conditions** : Same as for Fig. 3.2.11

**Table 3.2.2** HPLC retention times of various complexes in the characterization of *cis*-Cr(2,3,2-tet)$(CN)_2^+$, and photolysis of *trans*-Cr(2,3,2-tet)$(CN)_2^+$ under different eluent conditions. [c] This work.

| Eluent composition | | Retention time (min) | | | | | | |
|---|---|---|---|---|---|---|---|---|
| %$CH_3OH$[a] | IIA[b] | N | S | P | T | A | E | F |
| 0 | BSA[c] | | 3.0 | 3.7 | 11.0 | | | |
| 0[e] | BSA[d] | | 3.3 | 4.2 | 14.3 | | | |
| 0 | HSA | | 3.5 | 15.0 | | | | |
| 5 | HSA | 2.5 | 3.0 | 10.9 | 40 | 12.2 | 5.8 | 6.1 |
| 20 | HSA | | 2.3 | 6.4 | 15.6 | | | |
| 30 | HSA | | 1.9 | 4.2 | 5.2 | | | |
| 40 | HSA | | 1.8 | 2.9 | 4.5 | | | |

**Peaks assignment** (see section 3.2): N = *cis*-Cr(2,3,2-tet)$(CN)_2^+$, S = *trans*-Cr(2,3,2-tet)$(CN)_2^+$ , T = *trans*-Cr(2,3,2-tet)$(H_2O)(CN)^{2+}$ , P = *trans*-Cr(2,3,2-tetH)$(H_2O)(CN)_2^{2+}$ , A = *cis*-Cr(2,3,2-tet)$Cl_2^+$, e and F = *cis*- and *trans*-Cr(2,3,2-tet)$(CN)Cl^+$

**Key:** [a] 90 % methanol, [b] IIA = ion interaction agent, [c] BSA = butanesulfonic acid (Na salt), [d]HSA = hexanesulfonic acid (Na salt).

**Conditions:** eluents; 25 mM IIA (BSA or HSA), 25 mM ([e] except in second row where 12.5 mM) triethylamine in methanol / water at pH 3.0; flow rate 2 mL / min. Detection wavelength = 220 nm.

**Table 3.2.3** Variation of HPLC retention times upon decreasing the triethylamine (TEA) concentration in eluents, in the characterization of *cis*- and *trans*-$Cr(2,3,2\text{-tet})(CN)_2^+$.

| x mM TEA | Retention time (min) | | |
|---|---|---|---|
| x | $N_1$, $N_2$ | S | E/F |
| 25 | 2.6, 2.7 | 3.4 | 7.3 |
| 12.5 | 3.6, 3.8 | 4.6 | 10.3 |
| 10 | 3.9, 4.1 | 5.3 | 11.6 |
| 5 | 4.5, 5.0 | 7.0 | 16.4 |
| 3 | 5.8, 6.2 | 9.0 | 21 |
| 2 | 6.5, 7.1 | 10.6 | 25 |
| 0 | 11.9, 13.3 | 22 | -- |

**Peaks Assignment:** Same as for Table 3.2.2 except $N_1$, $N_2$ = components of peak N (see section 3.2.2).

**Conditions:** Same as for Table 3.2.2 except HSA in water was always used.

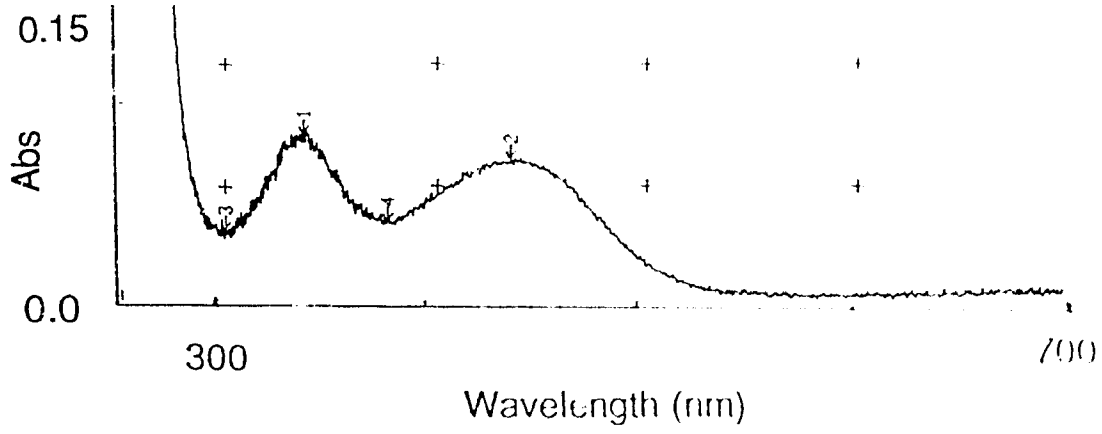


**Fig. 3.2.13** UV/Vis spectrum of *cis*-$Cr(2,3,2\text{-tet})(CN)_2^+$ isolated in aqueous solutions.

In order to further investigate the assignment of peak N, chromatograms were run under different conditions that increase the retention times. This was achieved by decreasing the methanol and competing ion (triethylamine hydrochloride) contents in eluents. There was no significant effect on increasing the concentration of the ion interaction agent (sodium hexanesulfonate). Such chromatograms are shown in Figures 3.2.8 to 3.2.11 and the appropriate retention times are listed in Tables 3.2.2 and 3.2.3. It can be seen that the peak N splits into two peaks ($N_1$ and $N_2$) while S stays as a single peak upon increasing the retention times. This is consistent with our assignment of peaks N and S because the cis isomer has two configurations ($\alpha$ and $\beta$ forms) depending on the relative position of the coordinated primary amine ends of the 2,3,2-tet ligand[101] whereas there are no such configurations for the trans isomer.

Under the chromatographic conditions used in Fig 3.2.11, where $N_1$ and $N_2$ elute at 6.5 and 7.1 min respectively, negatively charged species like $Cr(tn)(CN)_4^-$ and $Cr(CN)_6^{3-}$ * were unretained (1 min) in the column while the neutral species $Cr(tacn)(NCS)_3$ # has a very low retention time (2 min). This shows that the peak N is unlikely to be a neutral or negatively charged species.

In order to obtain further evidence for the above peak assignment and to isolate the material corresponding to peak N, Ion Exchange (IE) Chromatography was employed (section 2.1.8). The IE column fractions were analyzed by HPLC under the conditions used for Fig. 3.2.7. It shows that the order of elution through the IE column is S, N and E/F respectively. Since the

---

* Sample available in our laboratory.
# Synthesized using a new synthetic route by the author (unpublished work).

elution order of two isomers with same charge through an IE column is always trans before cis, this result is also consistent with our peak assignment that N is *cis*-Cr(2,3,2-tet)$(CN)_2^+$.

Due the significant overlap of N [*cis*-Cr(2,3,2-tet)$(CN)_2^+$] and E/F [Cr(2,3,2-tet)(Cl)$(CN)^+$] bands in the IE column, only a small portion of the material N could be isolated in solution. Injection of a sample of this solution N to HPLC under the condition used for Fig. 3.2.11, shows (Fig. 3.2.12) the presence of $N_1$ and $N_2$ components. The UV/Vis spectrum of this solution (Fig. 3.2.13) shows LF bands at 337 and 435 nm, similar to the spectrum of *trans*-Cr(2,3,2-tet)$(CN)_2^+$. As described in section 3.1.1b, it is expected that spectra of *cis*- and *trans*-Cr(2,3,2-tet)$(CN)_2^+$ are similar to each other except for their molar absorptivities. The measured molar absorptivity of this solution is 71 ± 5 at 435 nm, based on Cr analysis in solution. Comparison of this value with cis and trans isomers of $Cr(en)_2(CN)_2^+$ shows that the material N has the higher molar absorptivity value expected for *cis*-Cr(2,3,2-tet)$(CN)_2^+$.

The chromatographic results together with UV/Vis spectra support that the identity of the compound (N) obtained in solution is *cis*-Cr(2,3,2-tet)$(CN)_2^+$.

### 3.2.3 Thermal stability of *trans*-[Cr(2,3,2-tet)$(CN)_2$]$ClO_4$

Cyano complexes usually undergo efficient acid catalyzed cyanide aquation reactions (section 1.12). Therefore the thermal stability of this complex (~7 x $10^{-3}$ M) was studied in various acidic (and basic) solutions by UV/Vis spectroscopy and HPLC.

The UV/Vis spectrum of the complex remains unchanged in 1 x $10^{-3}$ M $HClO_4$ acid at 28°C for at least 3 hours. The pseudo first order rate constant for any thermal reaction at this pH (=3) can be estimated to be $< 1 \times 10^{-5}$ $s^{-1}$ at

28°C using uncertainties in measurable changes in chromatographic peak areas.

In 3 x $10^{-2}$ M $HClO_4$ acid also the UV/Vis spectrum remains unchanged for about an hour at 28°C. On prolonged standing, however, the spectrum shifts slowly towards the red. HPLC shows a slow decay and growth of peaks S and T respectively (Table 3.2.2). Under these conditions no other observable peaks were developed. The pseudo first order rate constant of the thermal reaction, measured by HPLC, at this pH is ≤1.2 x $10^{-2}$ $s^{-1}$ at 28°C. It is well established[15] that Cr(III) dicyanospecies undergo acid catalyzed cyanide loss in aqueous media stereoretentively to produce cyanoaquo species. Therefore the above thermal product, T, can be assigned as *trans*-$Cr(2,3,2\text{-tet})(H_2O)(CN)^{2+}$ (Reaction 3.2.1).

$$t\text{-}Cr(2,3,2\text{-tet})(CN)_2^{+} + H_3O^{+} \text{------>} t\text{-}Cr(2,3,2\text{-tet})(H_2O)(CN)^{2+} + HCN \qquad (3.2.1)$$

Treating the above solution with a few drops of 3 M $HClO_4$ to make the $H_3O^+$ concentration about 0.5 M rapidly decreases the peak S and greatly enhances T. Heating of this solution at 70°C for 15 min completly decomposes S and decreases the area of T developing 3 peaks at retention times longer than T. These additional peaks are likely to be corresponding to species with greater than 2+ overall charge but no detailed investigation was done to identify them.

The compound was very stable in base showing no UV/Vis spectral changes upon standing of the complex in 0.1 M NaOH for 2 h at 28°C. The pseudo first order rate constant for any thermal reaction at this pH (= 13) can be estimated to be ≤ 1 x $10^{-5}$ $s^{-1}$ at 28°C based on uncertainties in measurable changes in chromatographic peak areas.

The above results show that the compound can be considered thermally stable under the pH values at which photochemical experiments were carried out.

### 3.2.4 Photolysis of *trans*-[Cr(2,3,2-tet)$(CN)_2$]$ClO_4$

The exposure of the compound to 436 nm radiation shows a visual change in colour and a red shift in the UV/Vis spectrum. Fig. 3.2.14 shows the spectral changes upon photolysis against the thermal blank (the difference spectra) and the reagent blank. Photolysis maintained good isobestic points at 300, 345, 395 and 445 nm up to a higher extent (> 50%) of conversion (measured by both pH stat method and HPLC). it implies that the reaction produces a constant product mixture. The difference spectra also shows that 436 nm wavelength lies in a minimum region where photoproducts have smaller molar absorptivity than the starting complex. Therefore 436 nm is a good wavelength for photochemical studies since the complications due to secondary photolysis would be at a minimum.

The quantum yield of proton uptake at 436nm as measured by proton uptake at pH 3.0 was $\Phi_T = 0.09 \pm 0.01$ (5 runs) at 15°C for <10% conversion. This will include both amine and cyanide loss modes. Proton uptake plots for low (<10%) and high extents (>25% ) of conversion show that they are linear in the former case and curved in the latter case. The curvature of proton uptake can be attributed to quenching or photochemistry by photoproducts[68]. (Details of this phenomenon will be discussed in section 4.2.) This indicates that the quenching of photoreaction by photoproducts becomes significant at higher extents of photolysis.

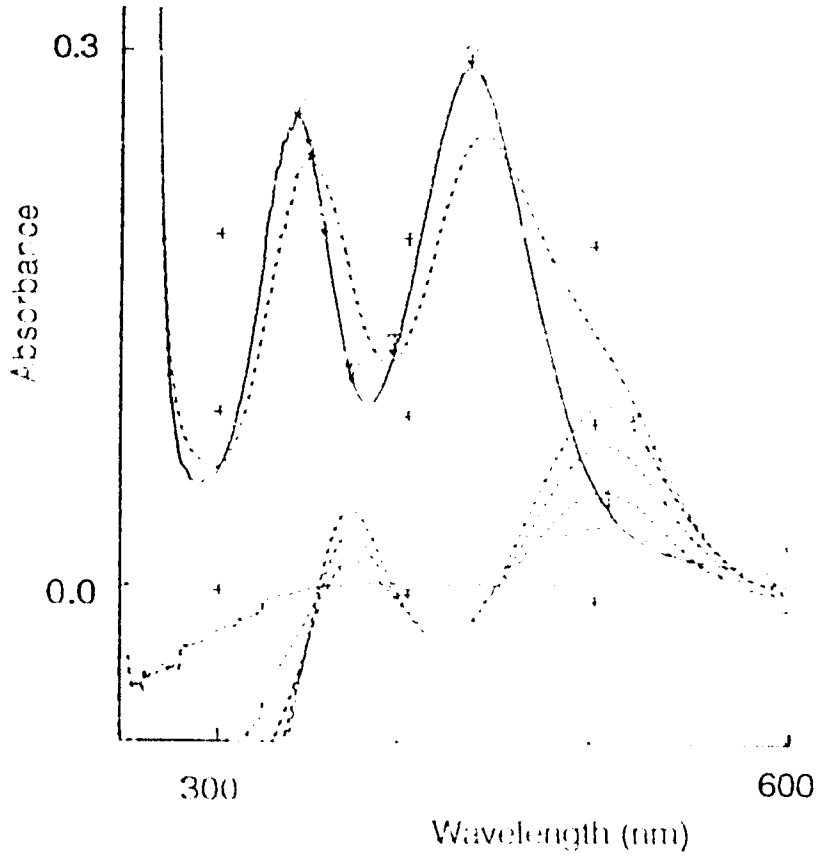


**Fig. 3.2.14** UV/Vis spectral changes upon photolysis of *trans*-Cr(2,3,2-tet)$(CN)_2^+$ in 3 x $10^{-2}$ M $HClO_4$ at 10°C.

Upper curves; Spectra against reagent blanks, before (——) and after (----) photolysis. Lower curves; Spectra againt the thermal blank (difference spectra) on exposure to 8 x $10^{-8}$ einsteins $s^{-1}$ light at 436 nm for 10, 20, 30, and 40 min.

The quantum yield of $CN^-$ photoaquation, $\Phi_{CN^-}$, was $\leq 0.02$ based on the detection limit of the cyanide electrode used. Therefore the major photoproduct is not due to cyanide loss.

The photoproducts were investigated using HPLC. Under all eluent conditions, with varied retention times over a wide range, only one photoproduct was observed. Typical chromatograms are shown in Figures 3.2.15 and 3.2.16 and the appropriate retention times are listed in Table 3.2.2. During photolysis the peak area of the starting complex (S) linearly decreases while the photoproduct peak (P) linearly increases. The relative variation of absolute peak areas suggests that at the detection wavelength of 226 nm the molar absorptivity of P is (1.5 ± 0.1) times that of S assuming all product peak areas are being observed.

During isolation of the photoproduct (see section 3.2.5a) using IE chromatography, the band was collected in several fractions. All these fractions had the same UV/Vis spectra (see later, Fig. 3.2.17) and gave the same single peak in HPLC. This result provides further evidence confirming that there was only one photoproduct.

The small peak T (*trans*-Cr(2,3,2-tet)$(H_2O)(CN)^{2+}$), <1% of S, seen in chromatograms is present in the sample as an impurity. If *cis*-Cr(2,3,2-tet)$(H_2O)(CN)^{2+}$ is present as a product, it is expected to elute just before T at any given eluent condition. The retention time of the observed photoproduct (P) does not correspond to this position but it is intermediate to those for 1+ (S) and 2+ (T) ions (Table 3.2.2). This is typical for a complex with a 2+ charge, but with one dangling protonated amine ligand, indicating the product is Cr(2,3,2-tetH)$(H_2O)(CN)_2^{2+}$. At the position for small peak M present in the sample as an impurity, a minor photoproduct was detected at higher extents of photolysis.

This M has the expected retention time for *cis*-Cr(2,3,2-tet)($H_2O$)$(CN)^{2+}$ but it is less than 1% of P.

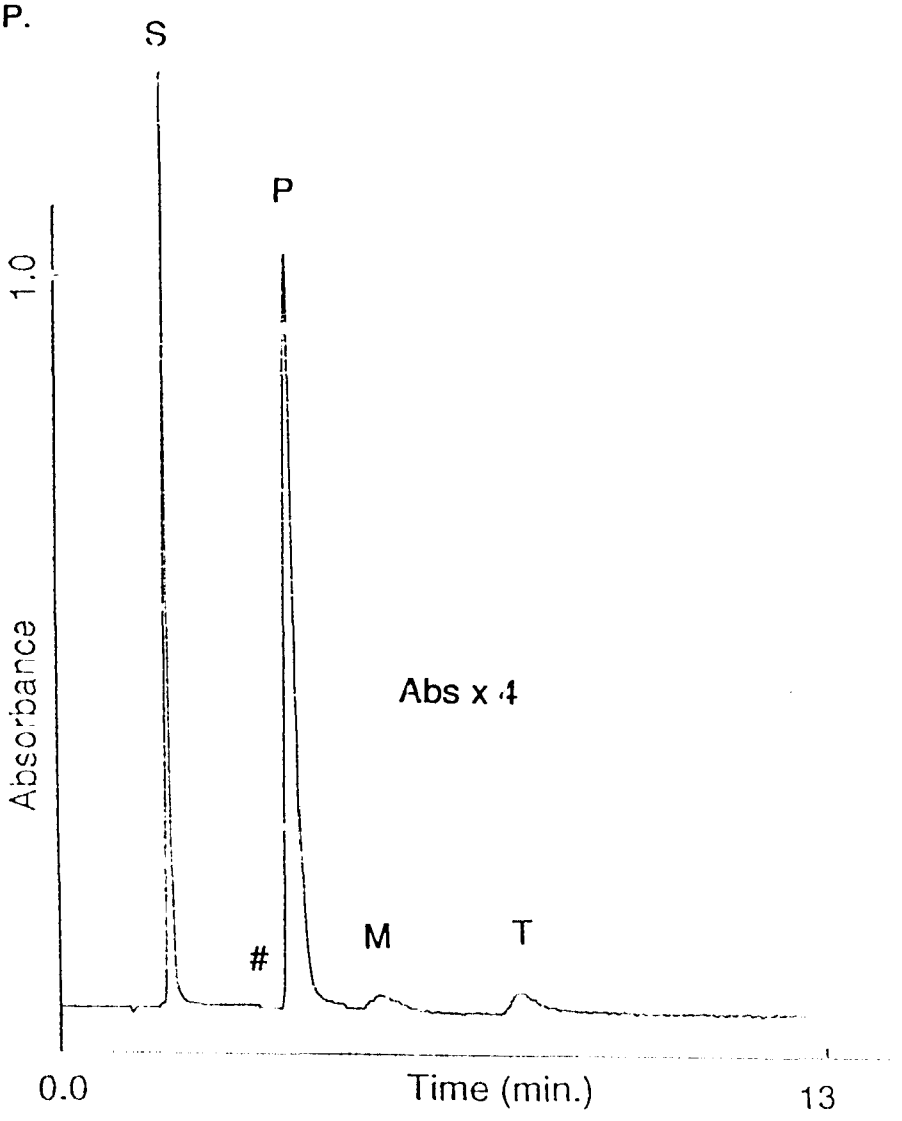


**Fig. 3.2.15** HPLC chromatograms showing peak development on the photolysis of *trans*-Cr(2,3,2-tet)$(CN)_2^+$.

**Key** : S = *trans*-Cr(2,3,2-tet)$(CN)_2^+$, P = photoproduct ("Cr(? 3,2-tetH)($H_2O(CN)_2^{2+}$"), T = *trans*-Cr(2,3,2-tet)($H_2O$)$(CN)^{2+}$, M = Impurity peak coinsided with a minor photoproduct (see section 3.2.4), # = scale change.

**Conditions** : eluents; 25 mM hexanesulfonate and 25 mM triethylamine in 30% methanol at pH 3.0; Flow rate 2 mL $min^{-1}$; Detection wavelength 226 nm.

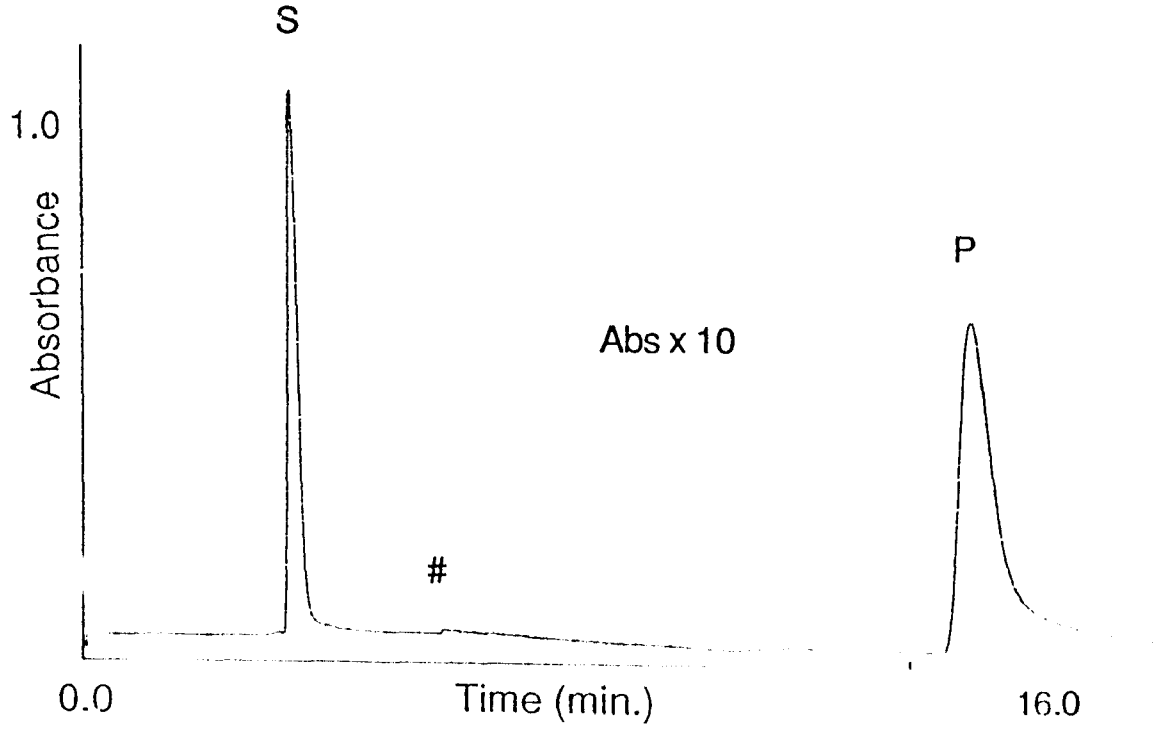


**Fig. 3.2.16** HPLC chromatograms showing peak development on the photolysis of *trans*-Cr(2,3,2-tet)$(CN)_2^+$ under different eluent conditions.

**Key :** Same as for Fig. 3.2.15

**Conditions** : Same as for Fig. 3.2.15 except % methanol = 0 (100% water).

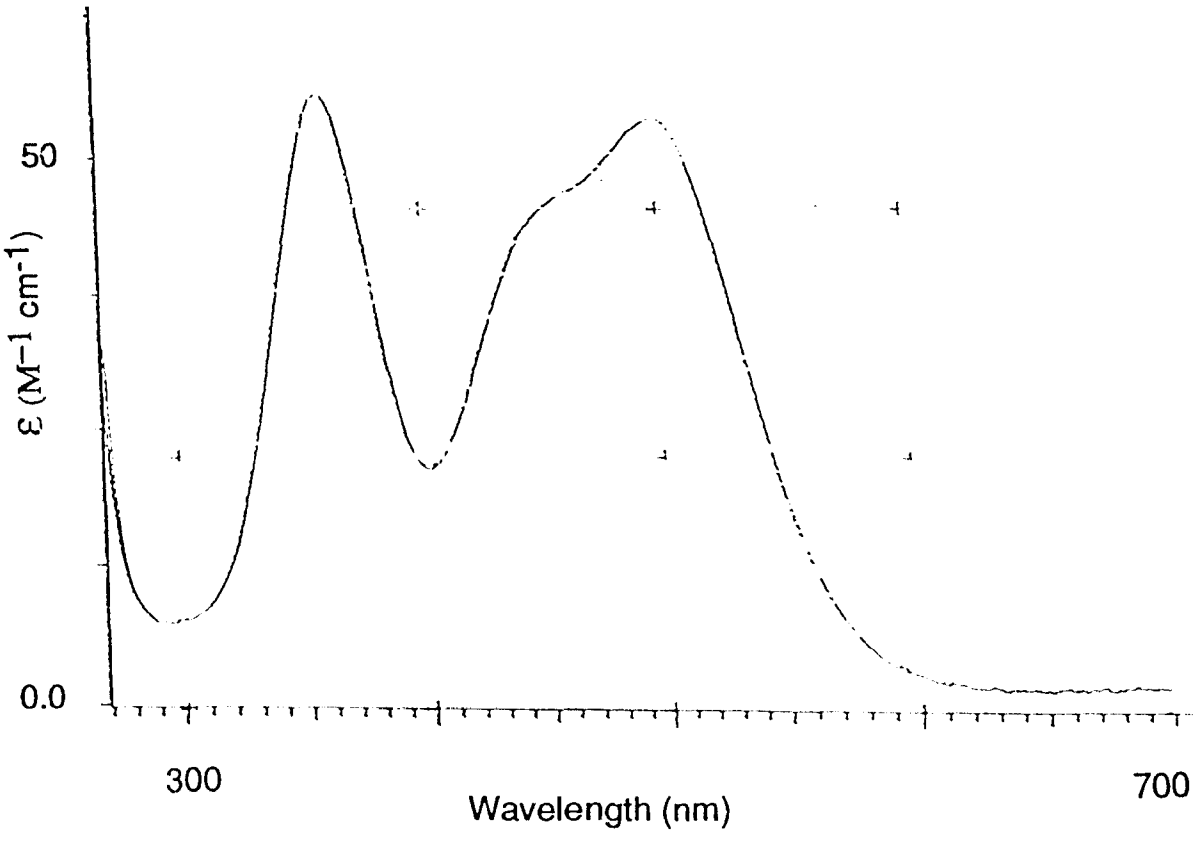


**Fig. 3.2.17** UV/Vis spectrum of the isolated photoproduct of *trans*-Cr(2,3,2-tet)$(CN)_2^+$ in room temperature aqueous solution.

It was also observed that on photolysis starting at a solution pH of 3, the pH increases upon photolysis whereas no pH change was observed if the photolysis was carried out at pH 6. Since there was no $CN^-$ loss, this behaviour is also consistent with the fact that the photoproduct is Cr(2,3,2-tetH)$(H_2O)(CN)_2^{2+}$ (equations 3.2 to 3.4) since the estimated $pK_a$ values (section 2.4.9) for coordinated $H_2O$ and 2,3,2-tetH ligands to a Cr(III) center are ~4.5 and ~10.5 respectively.

$$Cr(2,3,2\text{-tet})(CN)_2^+ \text{ ---- pH 3 ----> } Cr(2,3,2\text{-tetH})(H_2O)(CN)_2^{2+}, \quad \Delta H^+ = 1 \quad (3.2.2)$$

$$\text{---- pH 6 ----> } Cr(2,3,2\text{-tetH})(OH)(CN)_2^+, \quad \Delta H^+ = 0 \quad (3.2.3)$$

$$\text{---- pH 12 ---> } Cr(2,3,2\text{-tet})(OH)(CN)_2, \quad \Delta H^+ = -1 \quad (3.2.4)$$

Thus the absence of a $CN^-$ loss mode, the relative retention times of HPLC peaks and relative variation in pH upon photolysis show that the photoproduct is Cr(2,3,2-tetH)$(H_2O)(CN)_2^{2+}$.

### 3.2.5 Isomeric Identity of the Photoproduct

It is crucial to establish the isomeric identity of the photoproduct at least so far as to whether two CN are cis or trans to each other (see section 3.3). The following approaches were used to solve this problem.

(a) UV/Vis spectrum :

The photoproduct was isolated in solution as follows. A 3 ml solution of $1.2 \times 10^{-2}$ M complex in $1 \times 10^{-3}$ M $HClO_4$ was photolyzed at 10°C up to 20% conversion (pH-stat method). This solution was loaded on to a 4 cm (in water) cation exchange column (SP-Sephadex C-25) thermostated at ~2°C and eluted with cold $NaClO_4$ in $1 \times 10^{-3}$ M $HClO_4$. The yellow band containing *trans*-

$Cr(2,3,2\text{-tet})(CN)_2^+$ was completely eluted with 30 ml 0.1 M $NaClO_4$. Then pale purple fractions (10 ml each) of the photoproduct were collected with 30 ml of 0.2 M $NaClO_4$. The pH of this solution was 3. The UV/Vis spectrum of this isolated photoproduct (Fig. 3.2.17) was then obtained using a 10 cm spectrophotometer cell. The molar absorptivity at 500 nm (the lowest energy band maxima) was 57 $M^{-1}$ $cm^{-1}$ based on chromium analysis in solution. The spectrum shows a red shift in peak maxima upon adjusting pH to ~ 9 that is reversible on reacidification to ~pH 3, showing that the photoproduct has at least one coordinated water molecule.

The UV/Vis spectrum of the photoproduct was obtained by another method without isolating the photoproduct. Spectra were recorded on a computer disk before and after 20% photolysis (pH-stat method) in 1 x $10^{-3}$ M $HClO_4$ . Then by subtracting the former spectrum from the latter (section 2.4.1), the photoproduct spectrum (Fig. 3.2.18) was obtained.

Both methods gave similar spectra for the photoproduct. The peak maxima are shifted to the red compared to the starting complex. The lowest energy ligand field band of the spectrum was analysed on the basis of ligand field theory. The three components of this band ($^4B_2$ <--- $^4A_2$) correspond to 45° rotation of charge in the three orthogonal planes containing the ligands. It can be expected that there would be larger splitting in the lowest energy LF band in the isomer with trans cyanides over the cis isomer. This is because the average ligand fields in the three planes differ more for the trans than for the cis isomer. A quantitative estimation of the position of each component of this band was done as follows.

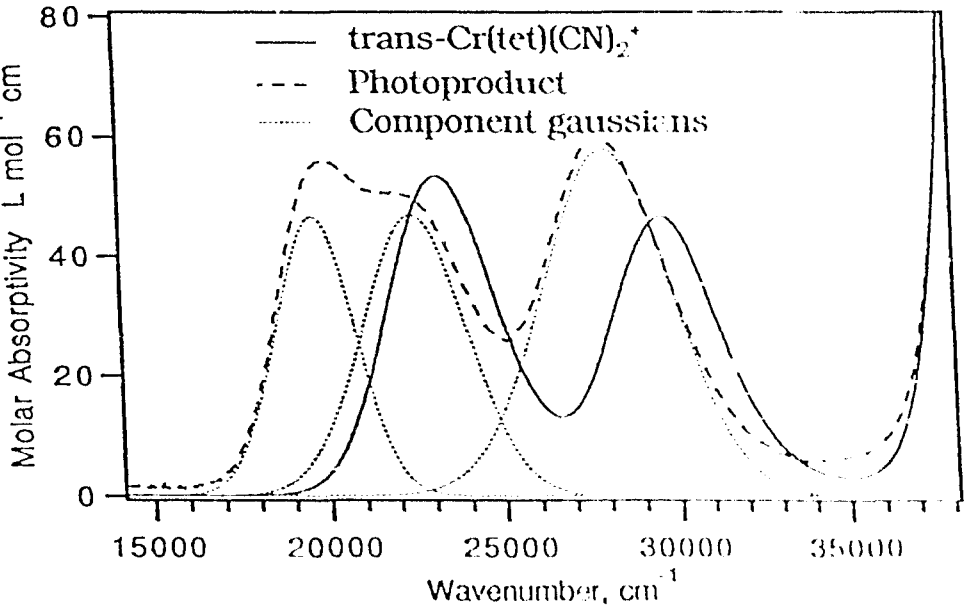


**Fig. 3.2.18** UV/Vis spectra of *trans*-Cr(2,3,2-tet)$(CN)_2^+$, the calculated spectrum of the photoproduct and gaussian components.

**Table 3.2.4** Calculated peak maxima of components of $^4T_{2g}$ band of $CrN_3(H_2O)(CN)_2^+$. (See section 3.2.5a)

| *trans*-[a] | | *cis*-[a] | |
|---|---|---|---|
| Ligands | Calculated $\lambda_{max}$ (nm) | Ligand | Calculated $\lambda_{max}$ (nm) |
| 2 CN, 2 N, -- | 415 | 2 CN, N, W | 435 |
| 2 CN, N, W | 435 | CN, 3 N, -- | 440 |
| --, 3 N, W | 490 | CN, 2 N, W | 460 |

[a] refers to the relationship between $CN^-$ ligands. $N_3 = (NH_3)_3$ = 2,3,2-tetH$^+$; W = $H_2O$. Gaussian analysis of the experimental spectrum shows bands at 444 and 508 nm.

Using 10Dq values for cyanide, amine (assumed to have 10Dq equal to $NH_3$) and water as 2.66, 2.16 and 1.73 $\mu m^{-1}$ respectively, the calculation of average ligand field strengths for each component estimates the wavelengths of maxima at 490, 435 and 415 for the trans and 460, 440 and 435 for the cis isomer respectively (Table 3.2.4). This shows that the separation between bands is 75 nm in the case of trans whereas it is only 25 nm in cis isomer. The lowest energy band in the experimental spectrum (plotted on a wavenumber scale) was resolved into two gaussians with maxima at 508 and 444 nm (Fig. 3.2.18). The observed large (64 nm) separation between the two gaussian maxima and the presence of a long wavelength peak (508 nm) both imply that the photoproduct is the isomer with trans cyanides.

(b) Stereochemistry of the recoordination of photoproduct:

We have observed that the photoproduct undergoes thermal recoordination of the dangling ethylenediamine arm (see below) and therefore we took the advantage of this behavior to establish the isomeric identity.

While the photoproduct (P) can be considered stable in pH 3 acid ($k_1 \leq 8 \times 10^{-5}$ $s^{-1}$ at 12°C), HPLC analysis shows that upon standing in neutral or basic media P depletes gradually developing a peak with the correct retention time for the starting complex (S) under the same eluent condition. Mixing this thermal product with an authentic sample of S and running chromatograms under very different conditions (Figures 3.2.15 and 3.2.16, Table 3.2.2) confirms that the thermal product of P, indeed has the same retention time as S. On standing, a photolysed solution at pH 11 shows a gradual change in UV/Vis spectrum towards the blue approaching the spectrum of $Cr(2,3,2\text{-tet})(CN)_2^+$ and

maintaining good isobestic points at 361, 418, 455 and 619 nm (Fig. 3.2.19). The UV/Vis spectrum of the final thermal product (Fig. 3.2.20) from the isolated P is similar to that of *trans*-Cr(2,3,2-tet)$(CN)_2^+$, including the molar absorptivity ($\varepsilon_{432}$ of the recoordinated product = 50 ± 5 $M^{-1}$ $cm^{-1}$). Also the spectrum in aqueous medium is independent of the pH confirming that the thermally recoordinated product has no coordinated water molecules. These results consistently indicate that the photoproduct (P) undergoes thermal recoordination to produce *trans*-Cr(2,3,2-tet)$(CN)_2^+$. A similar recoordination process that produces $Cr(en)_3^{3+}$ was previously reported for $Cr(en)_2(enH)(H_2O)^{4+}$.[113] Chromatograms under eluent conditions where *cis*- and *trans*-Cr(2,3,2-tet)$(CN)_2^+$ peaks are nicely separated (Fig. 3.2.11 and 3.2.12) show that the recoordination of P produces *trans*-Cr(2,3,2-tet)$(CN)_2^+$ exclusively, without producing any *cis*-Cr(2,3,2-tet)$(CN)_2^+$. Assuming that the recoordination process is stereoretentive, this demonstrates that the photoproduct has trans cyanides.

The rate constant of recoordination (measured by HPLC) at 25°C in 0.2 M $NaClO_4$ is dependent on the pH (Table 3.2.5). Even though data was measured only at three pH values, it suggests that the rate of recoordination is fastest at pH 6 and much slower at higher or lower pH values. When the estimated $pK_a$ values (section 2.4.9) of coordinated $H_2O$ (~4.5) and 2,3,2-tetH (~10.5) are taken into account, it suggests that the active species for recoordination is Cr(2,3,2-tetH)$(OH)(CN)_2^+$. Therefore the recooordination process can be represented by the reaction 3.2.5.

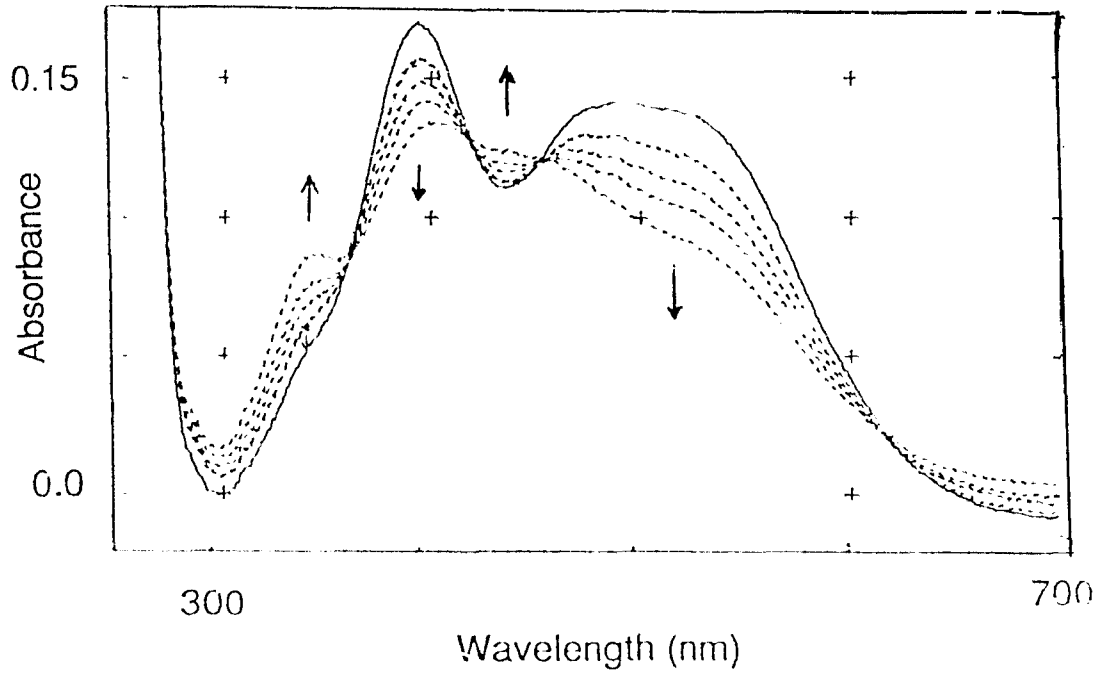


**Fig. 3.2.19** UV/Vis spectral changes upon the recoordination of the photoproduct in 1 x $10^{-3}$ M NaOH at 28°C.

Standing times; dark line = 5 min, dotted lines = 60, 90, 120 and 150 min.

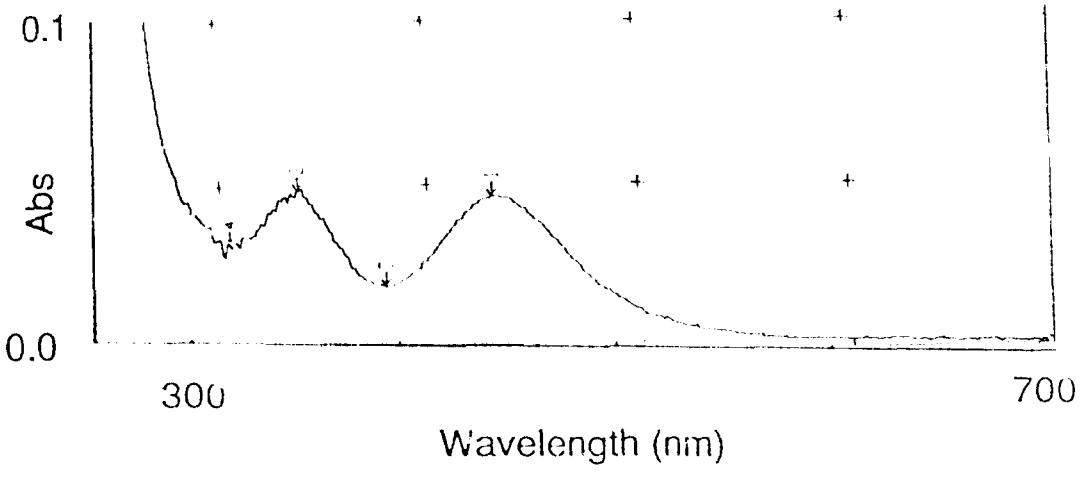


**Fig. 3.2.20** UV/Vis spectrum of the final product obtained by allowing the isolated photoproduct of *trans*-Cr(2,3,2-tet)$(CN)_2^+$ to stand in pH 6 aqueous solutions for 50 min. at 28°C.

**Table 3.2.5** pH dependence of the pseudo-first-order rate constants and half-lives for the recoordination of $Cr(2,3,2\text{-tet})(H_2O)(CN)_2^{2+}$.

| pH | k ($s^{-1}$) | $t_{1/2}$ |
|---|---|---|
| 3 | $\leq 6 \times 10^{-6}$ | $\geq$ 32 h |
| 6 | $1.5 \times 10^{-3}$ | 8 min |
| 9 | $4 \times 10^{-4}$ | 29 min |

$Cr(2,3,2\text{-tet\_H})(H_2O)(CN)_2^{2+}$

$\rightleftharpoons$ $pK_a \sim 4.5$

$Cr(2,3,2\text{-tet\_H})(OH)(CN)_2^{+} \longrightarrow$ *trans*- $Cr(2,3,2\text{-tet})(CN)_2^{+}$ (3.2.5)

$\rightleftharpoons$ $pK_a \sim 10.5$

$Cr(2,3,2\text{-tet})(OH)(CN)_2$

(c) Attempts to obtain the crystal structure:

Considerable effort was made to obtain a crystal of the photoproduct isolated using IE chromatography (section 3.2.5a) and therefore present in aqueous 0.2 M $NaClO_4$ solution. These attempts involved the use of anions like $ClO_4^-$, $SO_4^{2-}$, $Ni(CN)_4^{2-}$ and fractional crystallization of the isolated photoproduct. These attempts, however, were not successful. This is probably due to very high solubility and efficient recoordination of the photoproduct, and difficulty of isolation in high concentrations, free from electrolytes.

### 3.2.6 Emission Properties of *trans*-[Cr(2,3,2-tet)(CN)$_2$]ClO$_4$.

The compound emits at room temperature in acidic aqueous solution and in DMSO with a peak maximum at 705 nm. The relative intensity was approximately the same in both solvents. This wavelength is similar to the emission maxima of analogous compounds (Table 1.11.1).

The lifetime of emission ($\tau$) is 30 ± 1 μs in acidic aqueous solution at 20°C. Many other Cr(III) cyanoam(m)ine complexes show relatively long emission lifetimes (Table 1.11.1). The temperature dependence of life-time shows that a plot of ln $\tau$ vs 1/T is linear in the temperature range 10 - 40°C (Fig. 3.2.21) and the activation energy of emission is 38 ± 1 kJ mol$^{-1}$.

A Stern-Volmer plot of $1/\tau$ vs [OH$^-$] shows that the emission is linearly quenched by OH$^-$ (Fig. 3.2.22). The collisional quenching rate constant ($k_q$) of emission is 4 x 10$^8$ M$^{-1}$s$^{-1}$ at 20°C. Thus OH$^-$ ions efficiently quench the emission of *trans*-Cr(2,3,2-tet)(CN)$_2^+$ as they do for many other Cr(III) cyanoam(m)ine complexes.

### 3.2.7 Percentage Reaction via the Doublet State

One way of measuring the fraction of photoreaction that goes via the doublet excited state is to measure the quenchable portion of the reaction with a suitable quencher. A direct method, on the other hand, of measuring this is the use of the conductivity change associated with the photoreaction using flash photolysis experiments. We employed the latter method for this system.

The photolysis of the complex takes up a proton in acidic aqueous media (reaction 3.2.6).

$$t\text{-Cr(2,3,2-tet)(CN)}_2^+ + H_3O^+ \xrightarrow{h\upsilon} t\text{-Cr(2,3,2-tetH)(H}_2\text{O)(CN)}_2^{2+} \qquad (3.2.6)$$

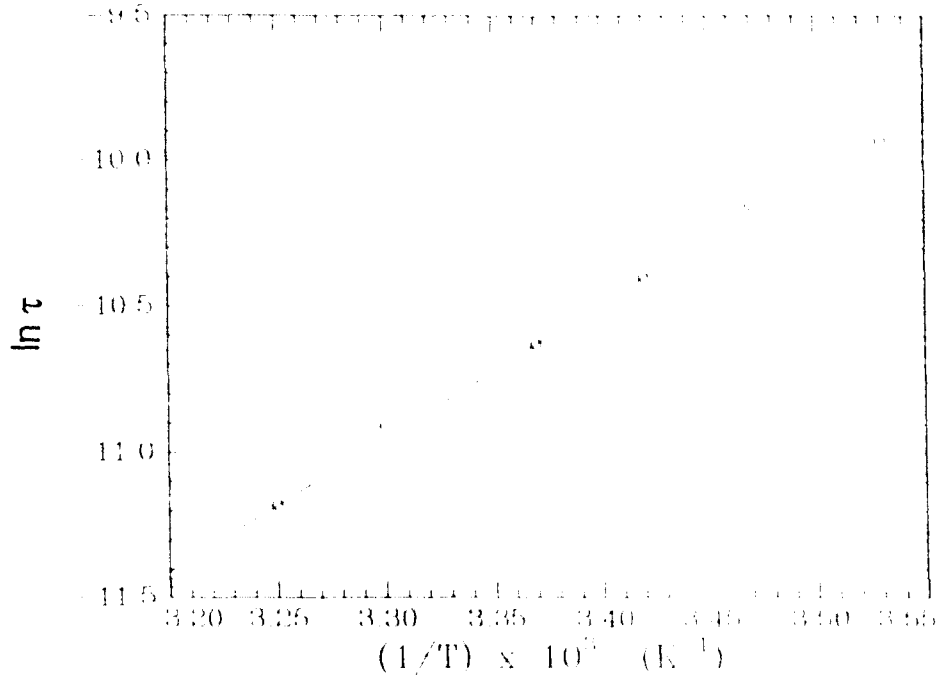


**Fig. 3.2.21** Temperature dependence of the emission life-time of *trans*-$[Cr(2,3,2\text{-tet})(CN)_2](ClO_4)$ in aqueous solutions

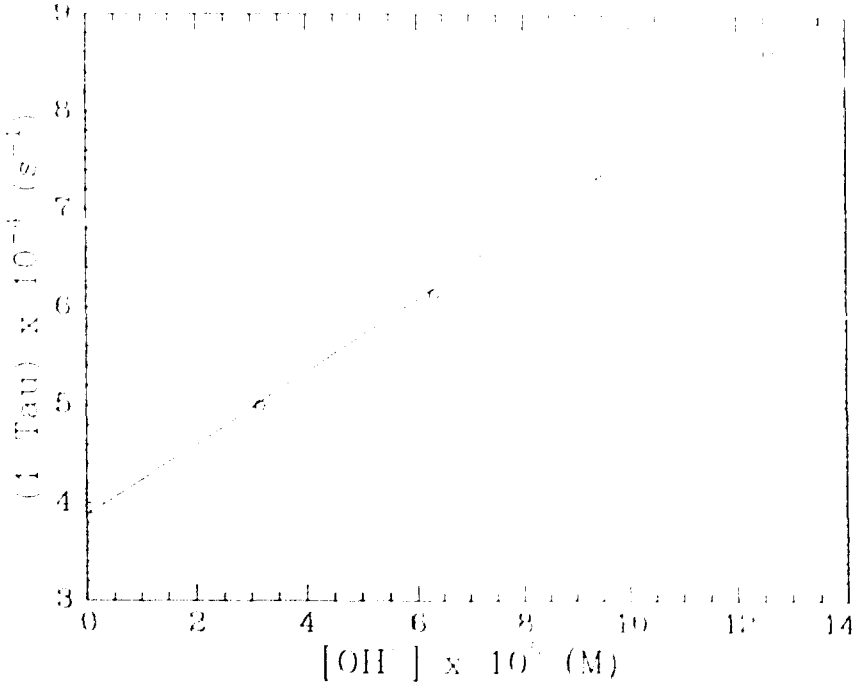


**Fig. 3.2.22** Stern-Volmer plot for quenching of the emission life-time of *trans*-$[Cr(2,3,2\text{-tet})(CN)_2](ClO_4)$ by $OH^-$ in aqueous solutions at 20°C.

The ionic conductivity of the starting complex and the photoproduct are expected to be approximately the same whereas that of $H_3O^+$ is much higher. Therefore under the experimental conditions used (section 2.4.1 i) the drop in conductivity associated with the reaction is sensitive and measurable in the time scale (ns to μs) of the photoreaction.

A typical conductivity decay curve is shown in Fig. 3.2.23. The signal intensity was linear with the laser power (Fig. 3.2.24). Test experiments with absorbance matched solutions of $K_2Cr_2O_7$ in same solvent ($1 \times 10^{-3}$ M $HClO_4$) shows that the baseline does not change with the flashing of the laser (Fig. 3.2.25). If a concentrated solution (0.8 M) of $K_2Cr_2O_7$ is used, a slight change in baseline indicating an increase in conductivity was observed. This effect can be attributed to heating of the solution by the nonradiative decay of the light energy absorbed by $K_2Cr_2O_7$ solution.

The lifetime of the excited state which leads to the reaction measured by analysing the conductivity decay curve is 26 ± 1 μs at 21°C. At the same temperature, the lifetime of the doublet emission decay is 28 ± 1 μs. That they are in agreement within the experimental uncertainty, shows that the measured reaction indeed goes 100% via the doublet state. This is because the decay curve extrapolates to the baseline at t = 0 indicating the complete photoreaction occurs with the doublet lifetime and there is no component ("fast") which occurs during the laser flash. Fig. 3.2.26 shows, for illustration, the type of curve obtained for $Cr(NH_3)_6^{3+}$. It clearly shows the two component product formation.

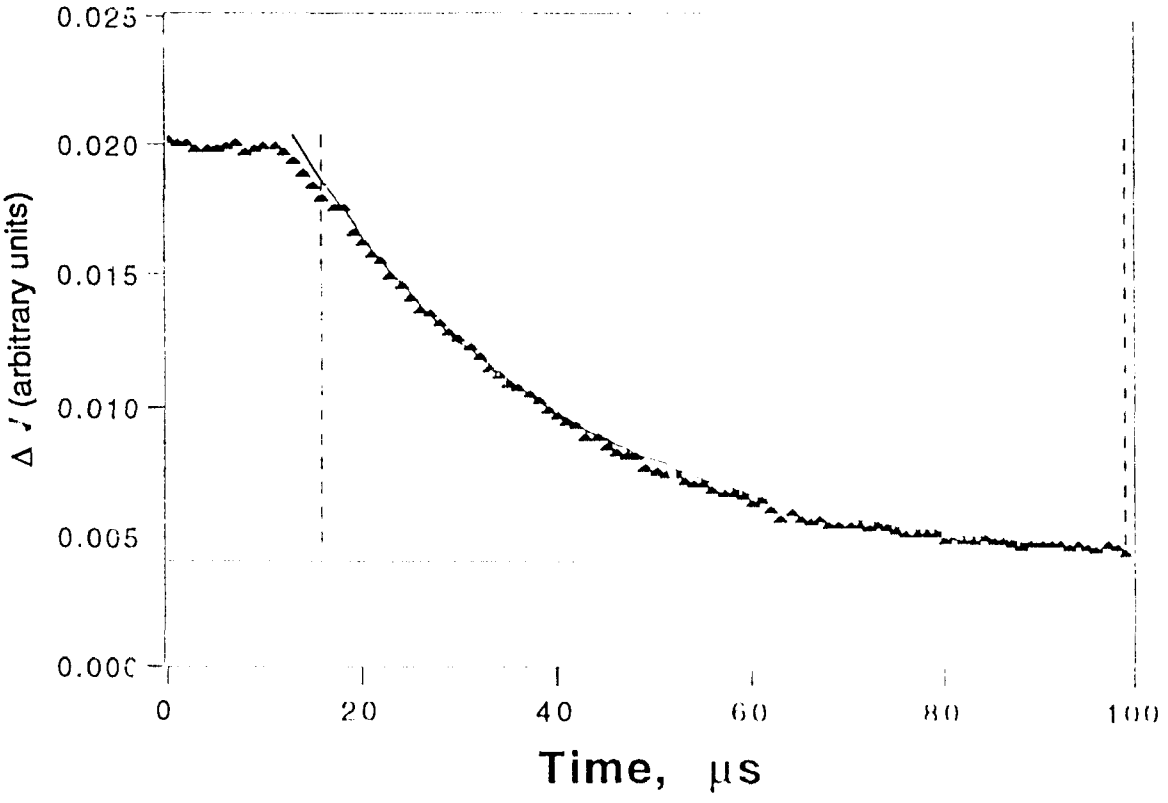


**Fig. 3.2.23** Conductivity decay during the photoaquation of *trans*-Cr(2,3,2-tet)$(CN)_2^+$ in 1 x $10^{-3}$ M $HClO_4$.

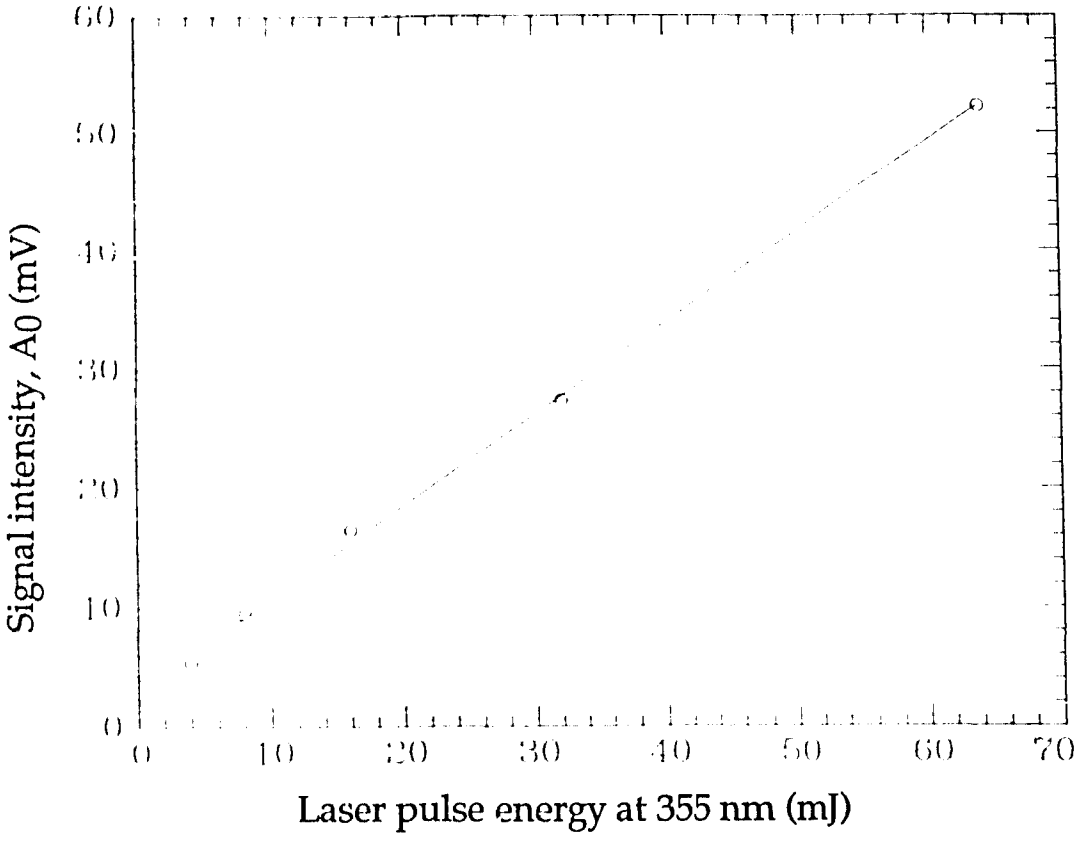


**Fig. 3.2.24** Nd-Yag laser pulse energy dependence of the signal intensity of conductivity decay curves shown in Fig. 3.2.23.

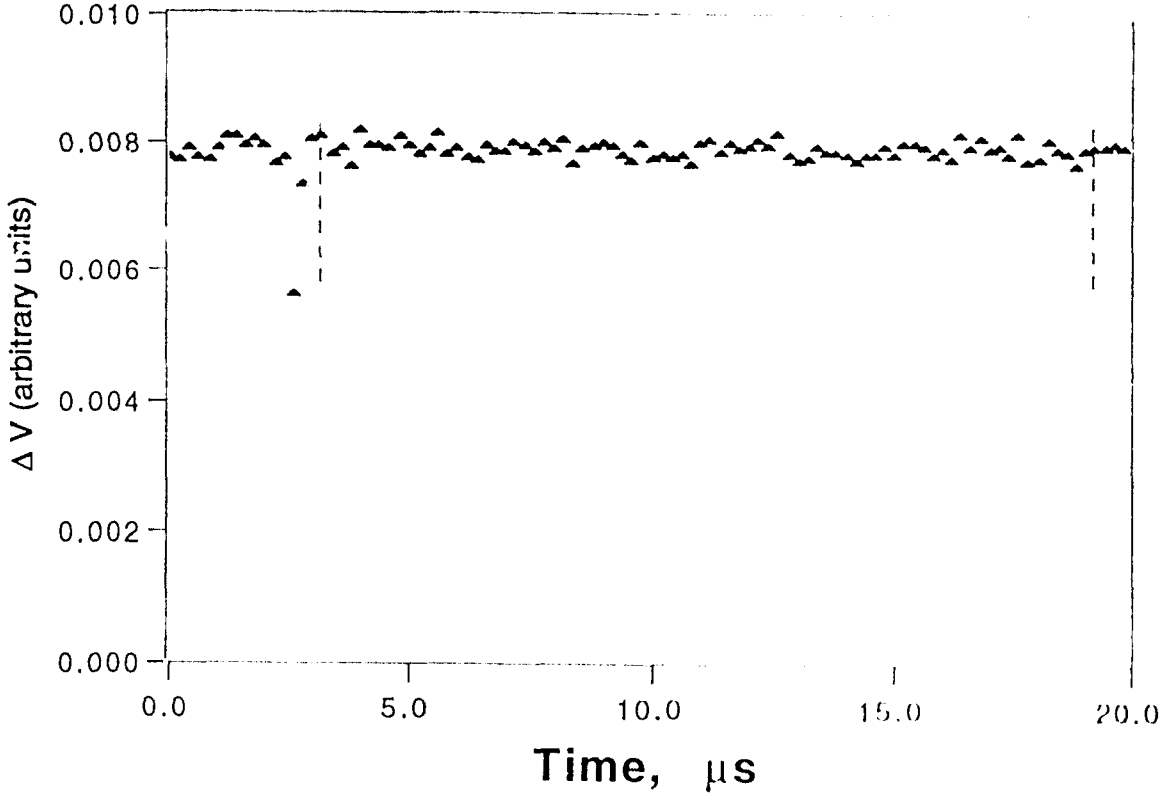


**Fig. 3.2.25** Conductivity changes on irradiation of a $K_2Cr_2O_7$ in 1 x $10^{-3}$ M $HClO_4$ with same absorbance and irradiarion conditions as the conductivity experiment shown in Fig. 3.2.23.

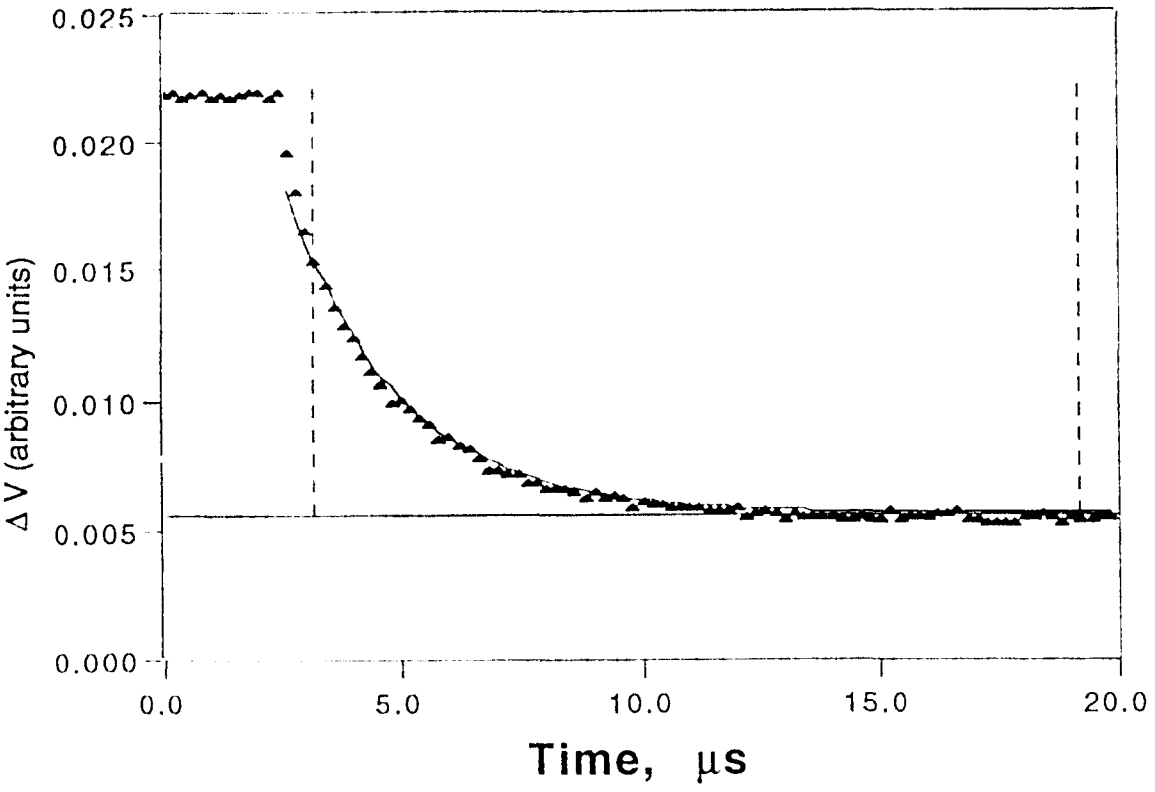


**Fig. 3.2.26** Conductivity decay during the photoaquation of $Cr(NH_3)_6^{3+}$ in 1 x $10^{-3}$ M $HClO_4$.

## 3.3 Discussion

### 3.3.1 Thermal Reactions

The acid catalyzed thermal aquation of the title complex ($\leq 1.2 \times 10^{-2}$ $s^{-1}$ at 28°C) is slower than the analogous *trans*-$Cr(NH_3)_4(CN)_2^+$ ($1.2 \times 10^{-2}$ $s^{-1}$ at 25°C)[75], as observed by comparing the pseudo first order rate constants in $3 \times 10^{-2}$ M acid. Although a detailed investigation of the rate constants or their pH dependence was not done, the compound was found to be stable under the time scales (< 1 h) and conditions at which photolysis (pH ~3) or $CN^-$ determination (pH ~12) experiments are usually carried out. Therefore, for these experiments, no correction was required for the thermal aquation of the compound.

Although the photoproduct is also stable in pH = 3 acid solution, it undergoes rapid recoordination at higher pH values (section 3.2.5 b). Interestingly the rate is fastest when the photoproduct takes the Cr(2,3,2-tetH)(OH)$(CN)_2^+$ form (~ pH 6). By considering the $pK_a$ values of Cr-(2,3,2-tetH) and Cr-($H_2O$) groups, we have represented the recoordination process in equation 3.2.5. At low pH values (< 3), the one ended amine arm is protonated, and therefore inert to substitution, and coordinated water is unable to take up this proton. Therefore the recoordination is inhibited at low pH values. At high pH values (> 11), on the other hand, the amine end is deprotonated but now the displacement of $OH^-$ by amine is difficult since $OH^-$ is a poor leaving group. Therefore it is reasonable to expect slow rates for recoordination. At intermediate pH values (~6) the proton on the amine arm apparently facilitates the displacement of coordinated $OH^-$. The process simultaneously removes the proton on amine and coordinated $OH^-$, forming a

stable water molecule and producing the starting complex. The process can be schematically represented as in Fig. 3.3.1. Even though a detailed investigation of this pH dependence of recoordination is beyond the scope of the present work, to our knowledge this is an interesting new phenomenon.

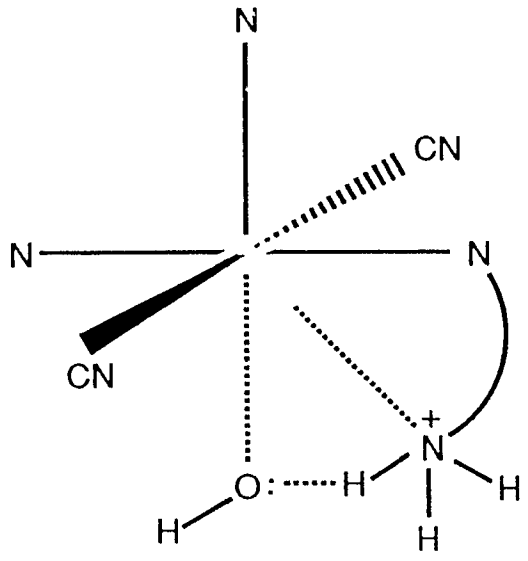


**Fig. 3.3.1** A mechanistic representation of the thermal recoordination of *trans*-Cr(2,3,2-tetH)(OH)$(CN)_2^+$.

### 3.3.2 Stereochemistry of Equatorial Ligand Loss

Stereochemical change accompanying axial ligand loss from Cr(III) complexes is well established both experimentally and theoretically, and it has been shown to be a requirement of the reaction. For equatorial ligand loss, however, the situation is less clear and fewer results are available (section 3.1.1). Vanquickenborne and Ceulemans have theorized that in equatorial ligand loss from complexes of the type $CrL_4X_2$ , a trigonal bipyramid intermediate in its excited state is formed which can undergo branching to its ground state to uncertain extents. Therefore, the reaction loses stereospecificity.[114] Experimentally, the photostereochemistry of equatorial ligand loss was established only in a comparative study of $Cr(NH_3)_5F^{2+}$ and *trans*-$Cr(en)_2(NH_3)F^{2+}$.[115] Here, assuming the axial mode is 100% stereomobile and $\Phi_{axial}/\Phi_{equatorial}$ ratio is comparable for the two compounds, it was shown that 19% of the photoreaction of $Cr(NH_3)_5F^{2+}$ was equatorial $NH_3$ loss, and for this mode at least 80% of the reaction occured with stereochemical change. This result provides evidence that equatorial ligand loss from $^4E$ state is stereomobile, similar to axial ligand loss from the same state.

*trans*-$CrN_4(CN)_2^+$ type complexes allow us to explore the stereochemistry of equatorial ligand loss from the $^4B_2$ state. The photoproducts of *trans*-$Cr(NH_3)_4(CN)_2^+$ however, cannot establish whether stereochemical change is complete even though Zinato et el.'s interpretation was "equatorial photoaquation is partially stereoretentive and partially stereomobile."[117]

These facts raise the question whether stereochemical change is a requirement for equatorial ligand loss, similar to the axial ligand loss. Our results clearly show that it is not.

### 3.3.3 Excited State Processes

Assuming the photoreactive state of *trans*-Cr(2,3,2-tet)$(CN)_2^+$ is the lowest energy quartet state and the ligand field strength of each coordinated nitrogen of 2,3,2-tet is equivalent to that for $NH_3$, Vanquickenborne and Ceulemans (VC) theory (section 1.5.2 and Table 1.5.1) indicates that the $^4E/^4B_2$ energy gap is 0.25 $\mu m^{-1}$ with the $^4B_2$ state being lower in energy. $I^*$(M-L) values for the $^4B_2$ state for Cr-CN and Cr-N are 0.9 and 1.9 $\mu m^{-1}$ respectively and for the higher energy $^4E$ state are 1.3 and 1.1 $\mu m^{-1}$ respectively. Therefore the weakest bond is the Cr-N bond in the $^4B_2$ state; consistent with the experimentally observed amine loss. Whether the process is stereoretentive or stereomobile, the reaction from the $^4B_2$ state should leave the axial cyanides unchanged. Consistent with this, our experiments established that the cyanide ligands in the photoproduct have the trans geometry.

It is a possibility that the higher energy quartet excited state may also act as a primary reactive state in violation of Kasha's rule. It was therefore necessary to consider the possibility that the observed reaction was from the higher lying $^4E$ state. Even in this state, $I^*$(Cr-N) is the smallest, though the difference from $I^*$(Cr-CN) is now smaller. No detectable cyanide was photoreleased. Stereochemical change is allowed for amine loss from the $^4E$ plane of excitation, an archetypal axial process, and it should occur with *trans* entry to produce *cis*-Cr(2,3,2-tet)$(H_2O)(CN)^{2+}$. Since the product has *trans* cyanides, we can conclude that the photoproduct is not due to the involvement of the higher lying $^4E$ state. Therefore the photoreaction arises from the $^4B_2$ state and is confined to the equatorial plane.

VC theory calculations cannot distinguish which of the four coordinated nitrogens of 2,3,2-tet is actually leaving. Our expectation is that only the primary

amine ends can be photolyzed (section 3.1.2). Since each of the secondary amine centers are linked to adjacent nitrogens with a short carbon chain, it is unlikely for these centers to aquate.

It is, however, necessary to eliminate this possibility. If the reaction is the loss of one of the secondary amine centers, it is very unlikely that the process could be stereoretentive due to the steric strain enforced by the ligand on the incoming water molecule. The secondary amine substitution, however, can occur with stereochemical change, producing a product with a nine membered ring (Fig 3.3.2). Our results on thermal recoordination eliminate this possibility, however.

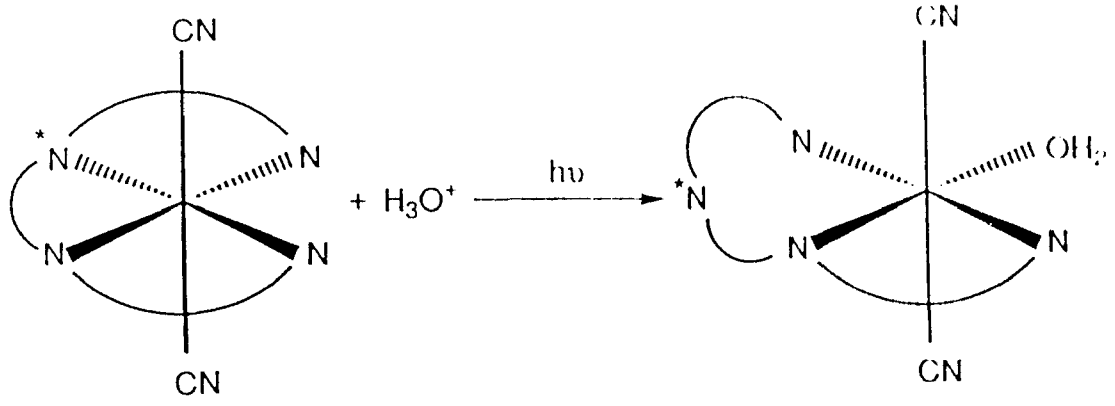


**Fig. 3.3.2** A possible photoaquation process of *trans*-Cr(2,3,2-tet)$(CN)_2^+$ if one of the secondary amines of the 2,3,2-tet ligand is released.

To satisfy our observation that the photoproduct thermally produces the starting complex in neutral or basic media, the reverse reaction corresponding to Fig. 3.3.2 has to take place. It would have to involve the recoordination of a central amine ligand with stereochemical change during coordination. Such a thermal process is highly improbable. On the other hand if the terminal primary amine is lost photochemically, the reverse reaction is just stereoretentive recoordination of the free end of the amine. Such recoordination is thermally allowed and examples showing parallel processes have been reported. Therefore our results show that the photoreaction of the title compound involves the loss of a terminal primary amine end. We have already argued (section 3.1.2) that the terminal amine loss cannot occur with stereochemical change. Therefore, we conclude that the photoreaction is stereoretentive.

The above discussion assumes that the photoreactive state of the title compound is the $^4B_2$ state. The reaction is stereoretentive, however, and goes 100% via the doublet state, in contrast to analogous cyanoammine and am(m)ine compounds for which the fraction is only about 75% (Table 3.3.1). Therefore the possibility of direct doublet excited state reaction cannot be ignored for this molecule.

Other complexes which show 100% reaction via the doublet are *cis*-$Cr(cyclam)(NH_3)_2^{3+}$,[49] $Cr(bipy)_3^{3+}$,[9, 116] $Cr(phen)_3^{3+}$,[9] *trans*-$Cr(en)_2F_2^+$,[82] *trans*-$Cr(en)_2(NH_3)F^{2+}$ [117] and $Cr(NH_3)_5F^{2+}$.[117] For the first four complexes, stereochemistry of photoproducts is not unambiguously established. In *trans*-$Cr(en)_2(NH_3)F^{2+}$, more than 65% of the reaction is axial ammonia loss and this mode shows complete stereochemical change. For $Cr(NH_3)_5F^{2+}$ it has been

**Table 3.3.1** The percentage "slow" components of the photoaquation of some Cr(III) am(m)ine and acidoammine complexes, determined by conductivity method.

| Complex | % slow component | Ref. |
|---|---|---|
| $Cr(NH_3)_6^{3+}$ | 74 ± 4 | 82 |
| $Cr(en)_3^{3+}$ | 67 ± 7 | 82 |
| $Cr(tn)_3^{3+}$ | 78 | 82 |
| *cis*-$Cr(cyclam)(NH_3)_2^{3+}$ | 100 | 49 |
| $Cr(NH_3)_5(CN)^{2+}$ | 74 ± 4 | 82 |
| $Cr(NH_3)_4(CN)(NCS)^{+}$ | 77 ± 3 | 58 |
| $Cr(NH_3)_5(NCS)^{2+}$ | 77 ± 3 | 82 |
| $Cr(2,3,2\text{-tet})(CN)_2^{+}$ | 100 | This work |

established[115] (section 3.3.2) that >96% of the overall reaction is stereomobile and of this 15% corresponds to equatorial ligand loss. Thus quartet reactivity has been shown for a Cr(III) complex with some equatorial ligand loss from the $^4E$ state. It could have been a more useful comparison if such measurements were done for species that show 100% reaction via the doublet and photoreaction is predominantly equatorial ligand loss from the $^4B_2$ state. Unfortunately, such data are not available so far.

The observation of stereochemical change confirms that the quartet has been the reactive state (section 1.8). Therefore, the above results on *trans*-$Cr(en)_2(NH_3)F^{2+}$ and $Cr(NH_3)_5F^{2+}$ confirm that the photoreactive state is the quartet for the title molecule even though the reaction occurs 100% via the doublet. Therefore, by analogy, the photoreactive state of the title molecule is also most probably the quartet state.

About 30% of the photoreaction of the analogous compound[52] *trans*-$Cr(NH_3)_4(CN)_2^+$ produces *cis*-$Cr(NH_3)_4(H_2O)(CN)_2^+$ that has been attributed to reaction from the $^4E$ state. The facts that the title molecule does not show this component and its reaction goes 100% via the doublet state suggest that in these molecules the doublet pathway does not reach the $^4E$ state and the observed $^4E$ state reaction for *trans*-$Cr(NH_3)_4(CN)_2^+$ is due to the prompt reaction.

The above idea is consistent with the results reported for *trans*-$Cr(en)_2(NCS)F^{+}$,[118] in which the quantum yield of the prompt reaction was wavelength dependent and this wavelength effect for the unquenched reaction was very small. But the above idea is apparently inconsistent with the results for *trans*-$Cr(NH_3)_4(CN)(NCS)^{+}$,[58] which showed 75% of the reaction via the doublet and three reaction modes namely $NH_3$, $CN^-$ and $NCS^-$ losses. The first

mode can be attributed to the low lying $^4B_2$ reaction and the later two modes to the $^4E$ state reaction. All these three modes were quenched in parallel with $Cr(C_2O_4)_3^{3-}$ maintaining the same product ratio by the routes. Therefore it was proposed that both the slow and fast components of the reaction initiate from a common precursor ($^4E/^4B_2$) quartet state(s). The $^4E/^4B_2$ energy gap for *trans*-$Cr(NH_3)_4(CN)(NCS)^+$ is very small (0.03 $\mu m^{-1}$) and thermal population is feasible. For *trans*-$CrN_4(CN)_2^+$ and *trans*-$CrN_4(NCS)F^+$ the gaps are high (0.25 and 0.23 $\mu m^{-1}$ respectively). Therefore, the comparison of the later complexes with *trans*-$Cr(NH_3)_4(CN)(NCS)^+$ may not be truly valid.

The emission lifetime and apparent activation energy values of *trans*-$Cr(2,3,2\text{-tet})(CN)_2^+$ are roughly close to the analogous complexes (Table 1.11.1). Therefore emission properties are parallel with the complexes showing normal stereochemical change.

Most of the known Cr(III) photochemistry occurs via reactions out of the lowest quartet excited state and the doublet participates, probably only as a reservoir of excitation energy (section 1.8). All the experimental results of this compound are consistent with the $^4B_2$ state reaction. Therefore we believe the reactive state of the title compound is the lowest energy quartet ($^4B_2$). The observed unexpected photochemistry can be explained by using Vanquickenborne and Ceulemans's approaches, as follows (section 3.3.4).

### 3.3.4 Possible Explanations for the Stereoretentive Nature of the Photoreaction

Fig. 3.3.3, comparable with Fig 1.6.3, gives an orbital description of VC theory of photostereochemistry (section 1.6.2) to $Cr(2,3,2\text{-tet})(CN)_2^+$ where the reaction is confined to the 2,3,2-tet plane. The square pyramidal intermediate

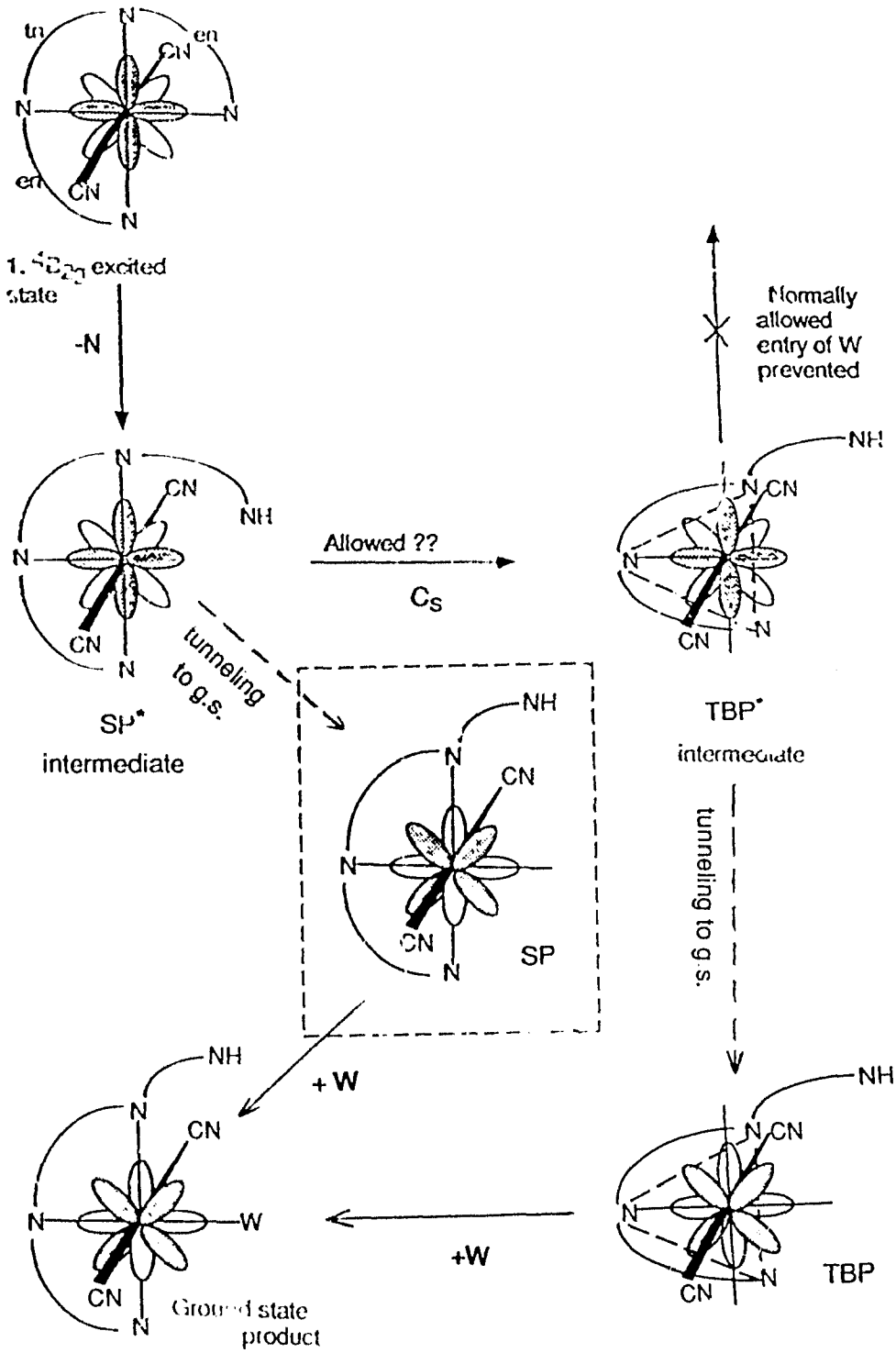


**Fig. 3.3.3** A schematic representation of the application of Vanquickenborne and Ceulemans theory to the photoaquation of *trans*-$Cr(2,3,2\text{-tet})(CN)_2^+$.

**Key:** W = $H_2O$, g.s. = ground state

formed has one primary amine and two secondary amines (one of which also contains a dangling arm). Upon collapsing of the SP to TBP intermediate, the only symmetry element maintained is the plane of ligand motion ($C_s$). Therefore, according to "Rule 2" the TBP is reached in its excited state (similar to $^4B_2$ of Fig. 1.6.2). Further isomerization of this intermediate following a trans attack is hindered by the linking carbon chains of the ligand. Hence, this TBP cannot lead to the *cis*-Cr(2,3,2-tetH)$(H_2O)(CN)_2^{2+}$ product.

The $C_s$ path is characterized by avoided crossing to the ground state and therefore it is possible for the excited TBP to tunnel through this avoided crossing to form the ground state TBP (similar to $^4A_1$ of Fig 1.6.2). This ground state allows the entry of the incoming ligand cis to the leaving ligand to produce *trans*-Cr(2,3,2-tetH)$(H_2O)(CN)_2^{2+}$ product.

The tunneling to the ground state from excited TBP is not an efficient process. This is consistent with the fact that $\Phi_N$ of this compound is much smaller compared to the analogous compounds; ~15% of *trans*-$Cr(en)_2(CN)_2^{+}$,[53] and ~35% of *trans*-$Cr(NH_3)_4(CN)_2^{+}$,[52]

It is also important to consider what steric strains these en, tn type chains would impose on the SP* ---> TBP* isomerization. The bite angle (N-Cr-N angle) enforced by a coordinated en ligand on Cr(III) center is ~83° whereas that by tn is 90°.[53] Therefore, it is expected that SP* species would have similar bite angles. The appropriate angles in a TBP structure are 120°. Can this 2,3,2-tet ligand be sufficiently stretched to increase the bite angle to 120°? Inspection of a molecular model shows that the tn ring with the chair conformation may allow such a stretch, but not the en ring. Therefore it is a likelihood that steric strain of the ligand would not allow complete SP* ---> TBP* isomerization. It leaves the possibility that SP* intermediate itself may lower its

energy by tunneling directly to its ground state, as shown in the insert box of the Fig. 3.3.3. This ground state SP intermediate can then undergo the allowed stereoretentive substitution to produce *trans*-$Cr(2,3,2\text{-tetH})(H_2O)(CN)_2^{2+}$ product.

It is also clear that the 2,3,2-tet ligand would allow some flexibility to stretch from SP, even though it may not be enough to form a stable TBP structure. It seems imperative that the tunneling to the ground state take place at some intermediate geometry between $SP^*$ ---> $TBP^*$ isomerization and the appropriate intermediate can then form the experimentally observed stereoretentive trans photoproduct.

The observed photoreaction can alternatively be explained using the Jahn-Teller approach to photostereochemistry (section 1.6.3). The entering species of this particular molecule is an excited SP species with two cyanides, one primary amine and one secondary amine in basal positions, and a secondary amine in apical position (Fig. 3.3.3). An SP intermediate can usually rearrange to two other forms of SP species via a TBP structure while maintaining the axial ligands unchanged (Fig. 1.6.4). In this case two cyanide ligands occupy the axial positions of the TBP (Fig.3.3.3). Due to the linkage of equatorial amine centers by carbon chains, such isomerization to other SP species is not possible in this molecule. Therefore the population of the SP ground states of the other side of the surface intersection point through transverse tunneling is impossible, independent of the position of the surface intersection point.

The exact position of the surface intersection point is uncertain anyway since a Jahn-Teller treatment has not been done for this molecule. It is, however, reasonable to assume this point will be close to the centrosymmetric

situation of a $CrL_5$ type fragment. This is because the three equatorial ligands are primary and secondary amines which are relatively close in ligand field strength compared to the introduction of a hetero-ligand. Therefore the displacement of the intersection point is much smaller than shown in Figures 1.6.6 and 1.6.7, that are constructed for $CrN_4F^{2+}$ and $CrN_3F_2^+$ species.

The $SP^*$ entering species of the molecule will start decaying and isomerizing towards the TBP intermediate. Due to the rigidity of the linking chains the nuclear momentum along the required ligand motions would be decreased preventing stereochemical change and probably facilitating lateral tunneling to populate the ground state of its own SP intermediate. This will undergo solvent substitution to produce the stereoretentive *trans*-Cr(2,3,2-tetH)$(H_2O)(CN)_2^{2+}$ product. Thus the observed stereoretentive reaction can be accommodated in Jahn-Teller approach of photostereochemistry. It implies that the regular stereochemical change expected for analogous compounds is altered by the title molecule due to the presence of 2,3,2-tet ligand which retards the nuclear motion. Since the process now takes place via an inefficient pathway, the quantum yield of this compound is expected to be lower than analogous compounds, consistent with the experiment.

Thus by extending either VC theory of photostereochemistry or Jahn-Teller approach, the observed photoreaction can be explained. Both explanations assign this unexpected reactivity to the presence of the 2,3,2-tet ligand which has primary and secondary amine coordination centers and linkages with short length carbon chains. Therefore one would expect similar stereoretentive reactions, though inefficient, for other compounds which hinder photoreaction due the presence of polydentate or macrocyclic ligands.

*Trans*- Cr(cyclam)$Cl_2^+$ shows some stereoretentive reaction to produce *trans*-Cr(cyclam)$(H_2O)Cl^{2+}$, but with a very small quantum yield, $\Phi_{Cl^-} = 3.3 \times 10^{-4}$ (Table 1.13.1). Earlier this result was incorporated[6] to a residual, inefficient pathway parallel to that of Co(III). This so called "inefficient pathway" may have the same type of mechanism proposed for *trans*-Cr(2,3,2-tet)$(CN)_2^+$. The proton uptake quantum yield of *trans*-Cr(cyclam)$(NH_3)_2^{3+}$ was $\leq 1 \times 10^{-4}$ (Table 1.13.1). These very low quantum yield values of cyclam complexes compared to their 2,3,2-tet analogs can be attributed to the rigidity of cyclam which does not permit sufficient structural distortion to promote the stereoretentive reaction.

# CHAPTER FOUR

## Wavelength Dependence of Prompt Photoreaction in Cr(III) Complexes. Is Photoaquation of $Cr(tn)_3^{3+}$ Competitive with Vibrational Relaxation?

## 4.1 Introduction

$Cr(tn)_3^{3+}$ undergoes photoaquation ($\Phi$ = 0.15) producing two geometric isomers, *cis*- and *trans*-$Cr(tn)_2(tnH)(H_2O)^{4+}$ (eq. 4.1.1).[63, 108]

$$Cr(tn)_3^{3+} + 2H_3O^+ \xrightarrow{h\upsilon} c\text{-}Cr(tn)_2(tnH)(H_20)^{4+} + t\text{-}Cr(tn)_2(tnH)(H_20)^{4+} \quad (4.1.1)$$

The product composition is 40 and 60% of *cis* and *trans* isomers respectively. It was shown by flash photolysis experiments with conductivity detection (section 3.2.7) that the slow and prompt components for this reaction are 22 and 78 % respectively.[82] Quenching methods have independently produced similar results.

Kirk and Ibrahim[97] recently investigated the product isomer composition on irradiation into the quartet state in the presence of hydroxide which quenches the doublet reaction pathway leaving the prompt reaction. Moreover, they examined the product distribution of the unquenched reaction (without a quencher) upon excitation to doublet and quartet states. They expressed the product isomer composition in terms of percentage *cis* isomer and represented their findings, as in Fig. 4.1.1. The key findings were as follows.

(a) The percentage *cis* isomer due to the prompt reaction (62% ± 2%), is higher than due to the unquenched reaction (40 ± 3%) on irradiation to the doublet or the usual excitation region of the quartet.

(b) The prompt reaction shows an increase in percentage *cis* isomer as the irradiation wavelength moves along the tail (465 - 514 nm) of the lowest energy quartet state ("red edge effect").

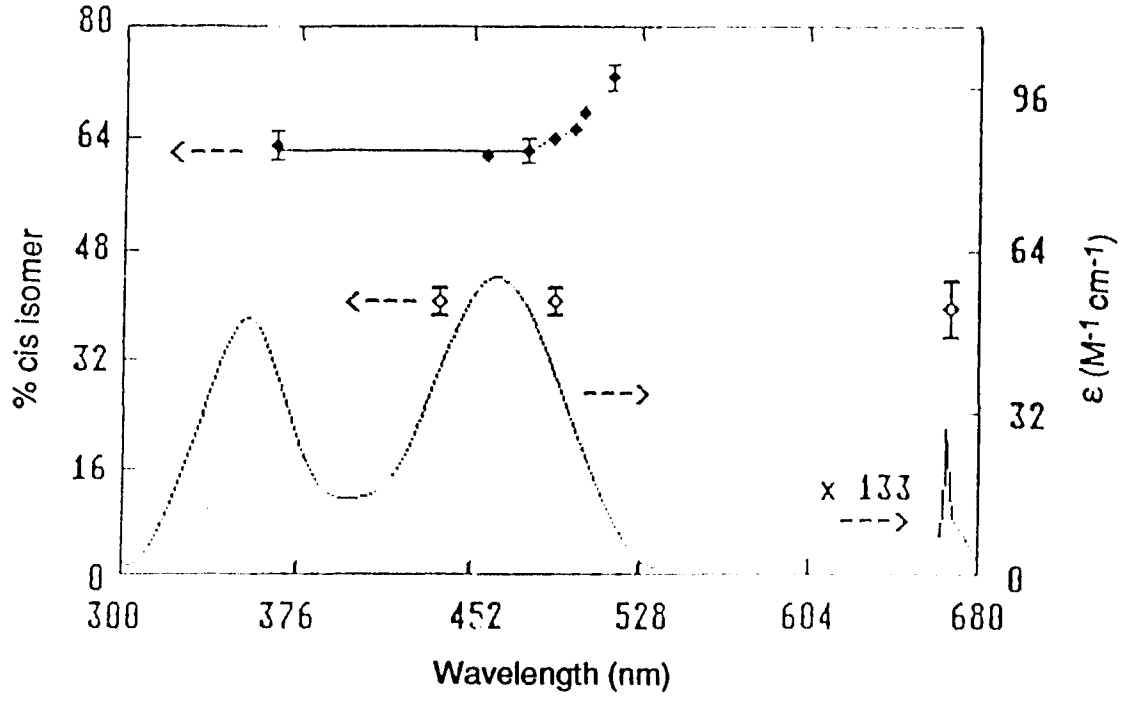


**Fig. 4.1.1** UV/Vis spectrum and percentage cis photoproduct of $Cr(tn)_3^{3+}$.

**Key :** Arrows indicate that the spectral data are referenced to the right axis; product percentage to the left. open diamonds = irradiation into the quartet and doublet states without quencher; filled diamonds = irradiation into the quartet state with the doublet fully hydroxide quenched.

Their interpretations for the above observations are given in the following two expressions.

(a) "The difference arises because of the specific vibrational excitation of the Frank-Condon quartet state."

(b) "photochemical reaction arising from the quartet state must be competitive with vibrational relaxation and therefore occurs in a time of a few picoseconds or faster."

An early study of wavelength dependence of unquenchable photoracemization yield in $Cr(phen)_3^{3+}$ was also interpreted as the competition of the reaction with vibrational and/or solvent relaxation.[119] Wavelength dependent quenching in *trans*-$Cr(en)_2F(NCS)^+$, on the other hand, was interpreted in terms of reaction via two quartet states.[120]

All these experimental results are important in the context of previous reports[58, 120b] of wavelength independence of product yield. Theoretically also, it has pointed out that a photoprocess might exhibit non-equilibrium dynamics (section 1.13.3).

The objective of the present work is the further investigation of Kirk & Ibrahim's findings. Therefore it was considered necessary to study the wavelength dependence of product ratio(s) of,

(a) molecules other than $Cr(tn)_3^{3+}$, probably showing more than one reaction mode, on $OH^-$ quenching of the doublet state

(b) $Cr(tn)_3^{3+}$ using quenchers alternative to $OH^-$

In order to examine the above factors, we have taken the following approaches.

(a) *trans*-$Cr(tn)_2(CN)_2^+$ was chosen as a suitable substitute molecule for $Cr(tn)_3^{3+}$. While we were attempting to use this molecule for wavelength dependence studies, we observed the interesting new phenomenon of quenching of the photoreaction by its own photoproducts. The work turned out to be significant of its own merit and therefore is presented separately in section 4.2, together with the factors pertaining to wavelength dependence study.

(b) $Cr(tn)(CN)_4^-$ was chosen as a suitable quencher alternative to $OH^-$. It turned out that the molecule is a good quencher, in general, for energy transfer quenching studies of transition metal complexes. Therefore, its quenching properties are presented separately in section 4.3. The wavelength dependence study of $Cr(tn)_3^{3+}$ using this quencher is presented in section 4.4.

## 4.2 Thermo- and Photoaquation of *trans*-$[Cr(tn)_2(CN)_2]ClO_4$. Quenching of Photochemistry by Photoproducts

### 4.2.1 Introductory Comments

Cr(III) cyanoam(m)ine complexes usually undergo efficient photosubstitution reactions and have long-lived doublet excited states which emit from room temperature aqueous solutions (section 1.11). These properties offer a favorable circumstance for the study of photophysical behavior of the excited states under photochemical conditions.

In several instances it has been observed that 1,3-diaminopropane (tn) complexes may behave differently from the analogous ammine and diaminoethane (en) complexes.[63, 121] Specifically, tn seems to be a much

poorer leaving ligand than other comparable amines with similar LF strengths, a feature which promotes preferential loss of the other ligands in the molecule. Therefore we can expect the title compound to show a larger extent of cyanide photoaquation than *trans*-$Cr(NH_3)_4(CN)_2^+$ and *trans*-$Cr(en)_2(CN)_2^+$ which do not show any measurable cyanide yield.

The title compound would therefore be a suitable and interesting candidate molecule for wavelength dependence studies of product stereochemistry similar to that done for $Cr(tn)_3^{3+}$ (section 4.1). It might also offer the additional feature of two roughly equal reaction modes with potential for wavelength and temperature dependence of their ratio.

### 4.2.2 Results

4.2.2.1 Characterization and thermal aquation

The compound was fully characterized by the following methods. Thermal properties of the compound are included in (d) below.

(a) Elemental Analysis

Analytical data were, % found (calculated) : C 27.4 (27.3), H 5.6 (5.7), N 23.6 (23.9), Cr 14.2 (14.8). The experimental results are in good agreement with the values calculated for $[Cr(tn)_2(CN)_2]ClO_4$.

(b) UV/Vis Spectroscopy

The UV/Vis spectrum of the compound shows two LF bands at 441 and 344 nm (Fig. 4.2.1). As shown in table 3.2.2, the wavelengths of the peak maxima and their absorptivity ratio are close to the analogous *trans*-$[Cr(NH_3)_4(CN)_2]ClO_4$[74] for which the ratio is distinguishable for *cis* and *trans* isomers, 1.3 and 1.0 respectively (Table 3.2.1). It supports the *trans* geometry

for our product. The comparison of the peak maxima and absorptivity ratio with en or 2,3,2-tet analogs is not reasonable because these ligands enforce some angular distortion at Cr in contrast to ammonia or tn ligands. It is also notable that the molar absorptivities for our compound are higher than for the tetrammine, as is usual for chelate compounds.

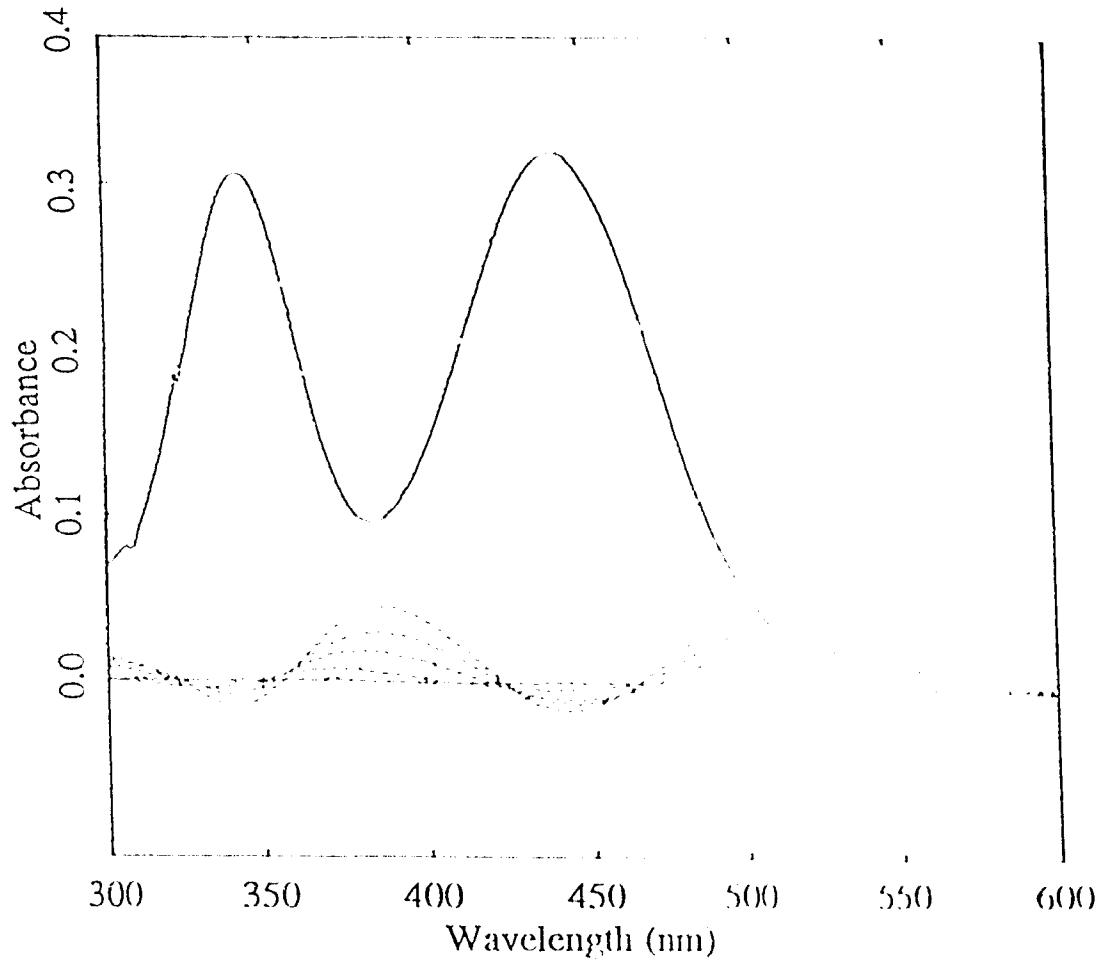


**Fig. 4.2.1** UV/Vis absorption spectrum and photolysis difference spectrum for *trans*-$[Cr(tn)_2(CN)_2]ClO_4$ . Conditions for difference spectrum: 6.0 x $10^{-3}$ M complex in 1 x $10^{-3}$ M $HClO_4$ . Dotted lines correspond to room temperature exposure to 50 mW of 458 nm radiation for 0, 2, 5, 7 and 10 minutes.

(c) IR Spectroscopy

In the infra-red spectrum, a band occurs near 2130 $cm^{-1}$ which can be attributed to the CN stretch. This band is very weak as might be expected for Cr(III) dicyanoam(m)ine complexes and therefore it cannot be used as a proof of geometry or isomeric purity.

In past work, it has been found[122] that an IR criterion to distinguish cis and trans isomers of the analogous bis en complexes is the band pattern between 395 to 550 $cm^{-1}$. All cis complexes show a pattern of at least four bands in this region whereas the trans complexes usually show only three strong bands, although anion effects can increase this number.[123] Our complex has three strong bands at 410, 455 and 510 $cm^{-1}$, consistent with trans geometry.

(d) Thermal Aquation

Cr(III) cyano complexes undergo stereoretentive acid catalyzed aquation in acidic aqueous medium (section 1.12). Here the reaction can be expected to occur in two distinct steps as was shown for *trans*-$Cr(NH_3)_4(CN)_2^+$.

$$Cr(tn)_2(CN)_2^+ + H_3O^+ \text{-----> } Cr(tn)_2(H_2O)(CN)^{2+} + HCN \qquad (4.2.1)$$

$$Cr(tn)_2(H_2O)(CN)^{2+} + H_3O^+ \text{-----> } Cr(tn)_2(H_2O)_2^{3+} + HCN \qquad (4.2.2)$$

UV/Vis spectrophotometric monitoring of 6 x $10^{-3}$ M, room temperature solutions of *trans*-$[Cr(tn)_2(CN)_2]ClO_4$ at various concentrations of $HClO_4$ demonstrated cyanide aquation whose rate increased with acid concentration. At 3 x $10^{-3}$ M $HClO_4$, aquation occurred with three isosbestic points to give a stable product after 100 min (Fig. 4.2.2). Comparison of our data to that reported for the *cis*- and *trans*-$Cr(NH_3)_4(CN)_2^+$ (see Table 4.2.1), shows that the

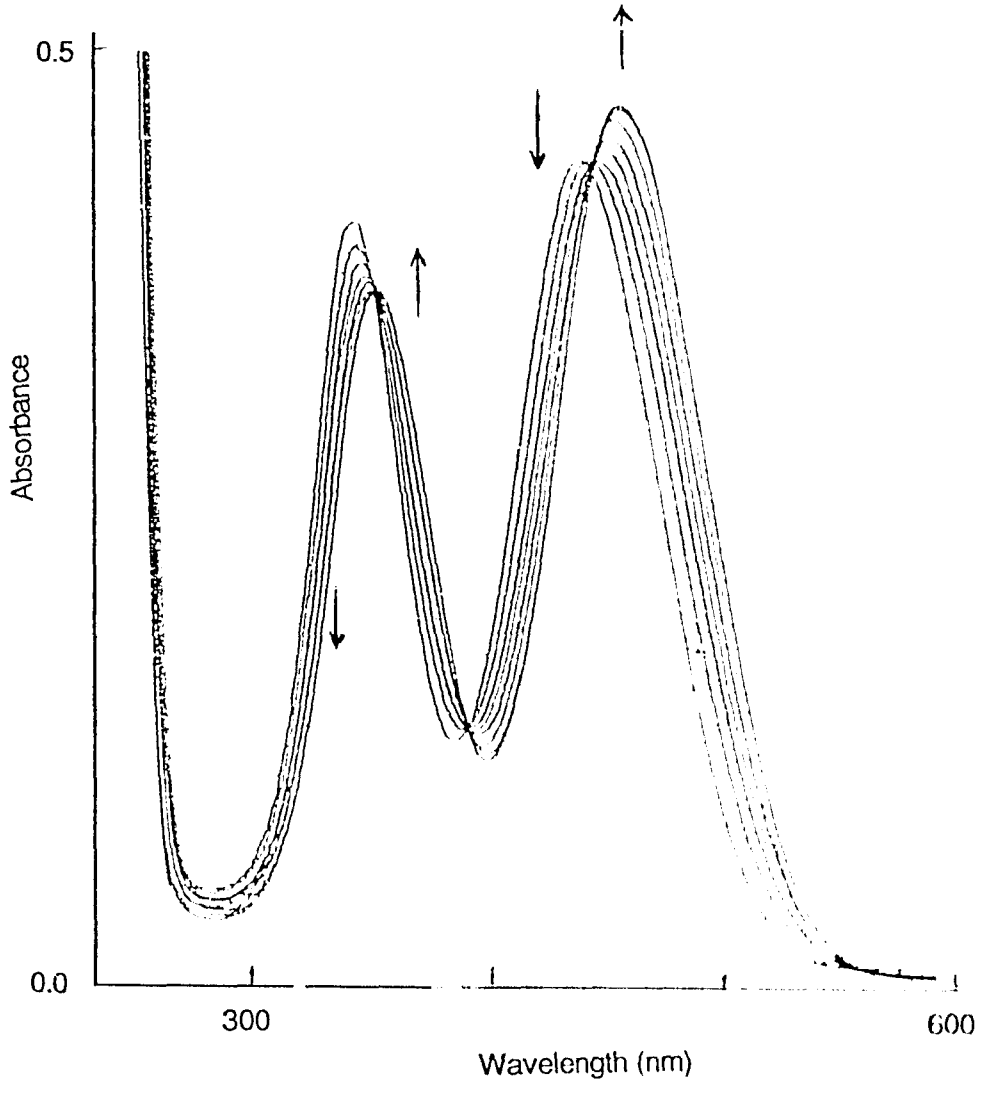


**Fig. 4.2.2** UV/Vis spectral changes during the themal aquation of the first cyanide ligand of *trans*-$[Cr(tn)_2(CN)_2]ClO_4$. (see equation 4.2.1.)
The curves correspond to the standing of the 6 x $10^{-3}$ M complex in 3 x $10^{-2}$ M $HClO_4$ for 0, 15, 30, 45, 60, 90, and 135 min.

**Table 4.2.1** Spectral data for thermal acid catalysed reaction of *trans*-$Cr(tn)_2(CN)_2^+$

| | Reaction 1 | | | | | Reaction 2 | | | | | | Ref. |
|---|---|---|---|---|---|---|---|---|---|---|---|---|
| Starting complex | Isosbestics | | | Product spectra | | Isosbestics | | | Product spectra | | | |
| | λ, nm (ε, relative) | | | | | λ, nm (ε, relative) | | | | | | |
| *t*-$Cr(tn)_2(CN)_2^+$ | 356 | 393 | 450 | 356 | 462 | 361 | 417 | 508 | 366 | 452 | 520 | b |
| | (1.0) | (0.4) | (1.2) | (1.0) | (1.3) | (2.0) | (1.0) | (1.3) | (1.5) | (1.0) | (0.72)[a] | |
| *t*-$Cr(NH_3)_4(CN)_2^+$ | 357 | 387 | 449 | 354 | 468 | 361 | 412 | 511 | 368 | 476 | 510 | 77 |
| | (1.0) | (0.4) | (1.3) | (1.0) | (1.5) | (2.6) | (1.0) | (1.8) | (1.4) | (1.0) | (0.92)[a] | |
| *c*-$Cr(NH_3)_4(CN)_2^+$ | no isosbestics | | | 355 | 468 | 367 | 405 | 479 | 366 | 495 | | 77 |
| | | | | (1.0) | (1.06) | (2.7) | (1.0) | (3.3) | (0.75) | (1.0) | | |

a) Spectral data match closely those for authentic[100] trans-$Cr(tn)_2(H_2O)_2^{3+}$; namely 368(1.5), 452(1.0), 520(0.68) whereas *cis*-$Cr(tn)_2(H_2O)_2^{3+}$ has 366(0.89), 490(1.0). The 520 nm value is for a shoulder.

b) This work

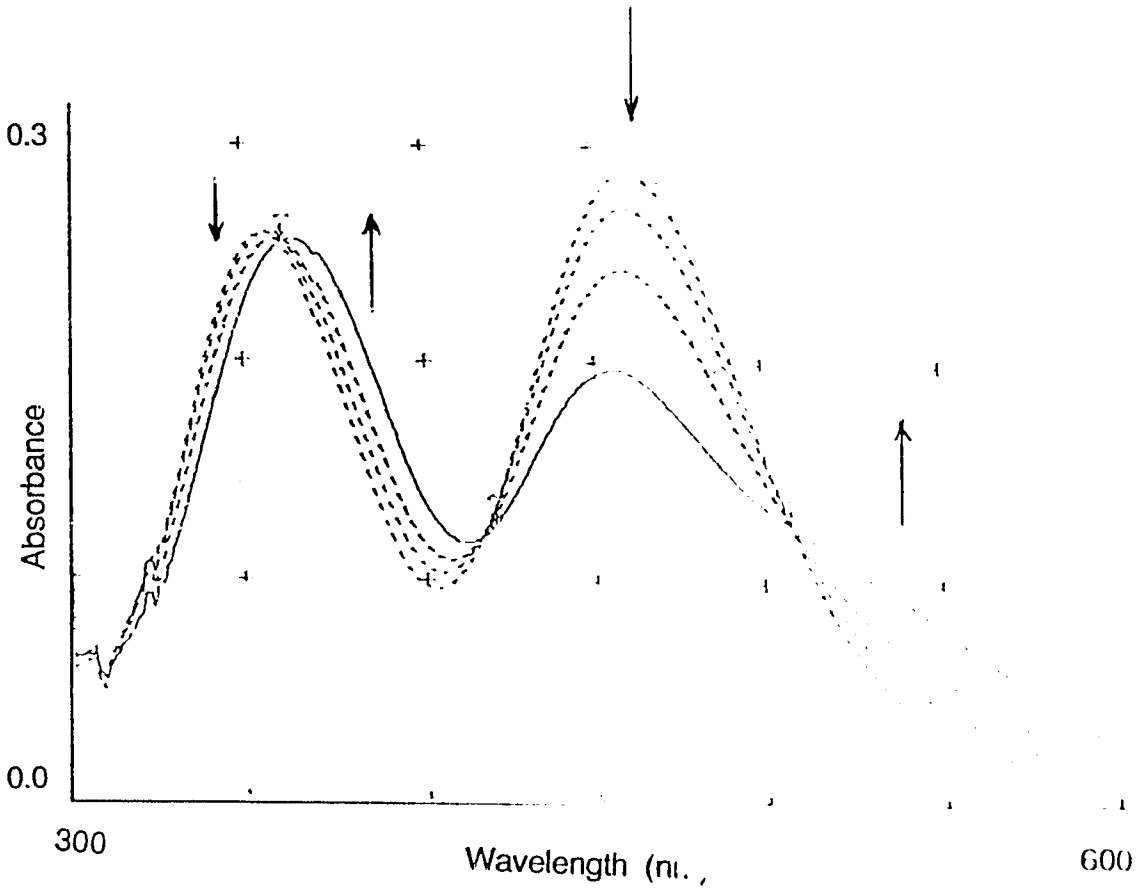


**Fig. 4.2.3** UV/Vis spectral changes during the thermal aquation of the second cyanide ligand of *trans*-$[Cr(tn)_2(CN)_2]ClO_4$. (see equation 4.2.2.) The curves correspond to the standing of the 6 x $10^{-3}$ M complex in 2.0 M $HClO_4$ for 0, 15, 55, and 160 min.

reaction corresponds to loss of the first cyanide to form *trans*-$Cr(tn)_2(H_2O)(CN)^{2+}$, reaction 4.2.1. The same reaction occurs immediately in 0.3 M $HClO_4$, and the monocyanoaquo product is again stable for at least 12 hours. A point of interest is the greater stability of the mono-aquo product up to 1 M acid, while at this acid concentration, the tetrammine analog readily aquates right through to the diaquo product.

At 2 M $HClO_4$, however, the *trans*-$Cr(tn)_2(H_2O)(CN)^{2+}$ formed reacts further. This reaction also shows three isobestic points (Fig. 4.2.3) which parallel those for formation of *trans*-$Cr(NH_3)_4(H_2O)_2^{3+}$ from *trans*-$Cr(NH_3)_4(H_2O)(CN)^{2+}$ (see Table 4.2.1). After 8 hours a stable compound remains whose spectrum matches reasonably well with that[100] for *trans*-$Cr(tn)_2(H_2O)_2^{3+}$.

The isosbestic behavior and the product spectra are consistent not only with this pathway but also with the trans configuration for all these species. Therefore, our results of UV/Vis spectrophotometric analysis established that the aquation reaction proceeds as expected in two separable steps (equations 4.2.1 and 4.2.2) and the title compound has the *trans* geometry. A small amount of *cis* impurity present in the sample, however, could not be detected by this method.

The first aquation step of *trans*-$Cr(NH_3)_4(CN)_2^{+}$ has been shown[75] to have a strongly non-linear hydrogen ion dependence arising from participation of protonated and un-protonated forms (section 1.12). We did not investigate this aspect. The measured pseudo first order rate constant for the first step (eq. 4.2.1) at 15°C in 5 x $10^{-4}$ M $HClO_4$/0.050 M $KClO_4$ was 1 x $10^{-5}$ $s^{-1}$ (pH-stat method). The rate constant for the second step of the reaction was not

measured although our results show that it is much smaller than for the first step.

(e) HPLC analysis of thermal products

Reversed phase HPLC allowed us to separate authentic samples[100] of *cis*- and *trans*-$Cr(tn)_2(H_2O)_2^{3+}$ ions into baseline resolved peaks (Fig. 4.2.4). The cis isomer elutes before the trans with retention times of 6.5 and 7.3 minutes respectively. The product obtained from the second step of aquation in 2 M $HClO_4$ was injected under these chromatographic conditions. The major peak had a retention time of 7.3 minutes, confirming that the final thermal product is *trans*-$Cr(tn)_2(H_2O)_2^{3+}$. The chromatogram also showed a small peak for the cis isomer at 6.5 minutes, less than 5% of the major peak.

This cis product could have arisen from a small amount of isomerization before or during the aquation process. Cr(III) thermal reactions are known to be stereo-retentive, however, so it may be revealing some cis impurity in our starting material. This leads us to a 95% lower limit on the isomeric purity of the *trans*-$[Cr(tn)_2(CN)_2]ClO_4$.

4.2.2.2 Emission Properties

At room temperature in aerated solution, the complex shows an intense, structured emission with a maximum at 703 nm (Fig 4.2.5). For $Cr(NH_3)_4(CN)_2^+$, the emission band positions were 701 and 700 nm for cis and trans isomers respectively (Table 1.11.1), in close agreement with the title complex. The emission maximum for $Cr(tn)_2(CN)_2^+$ in DMSO was at 705 nm.

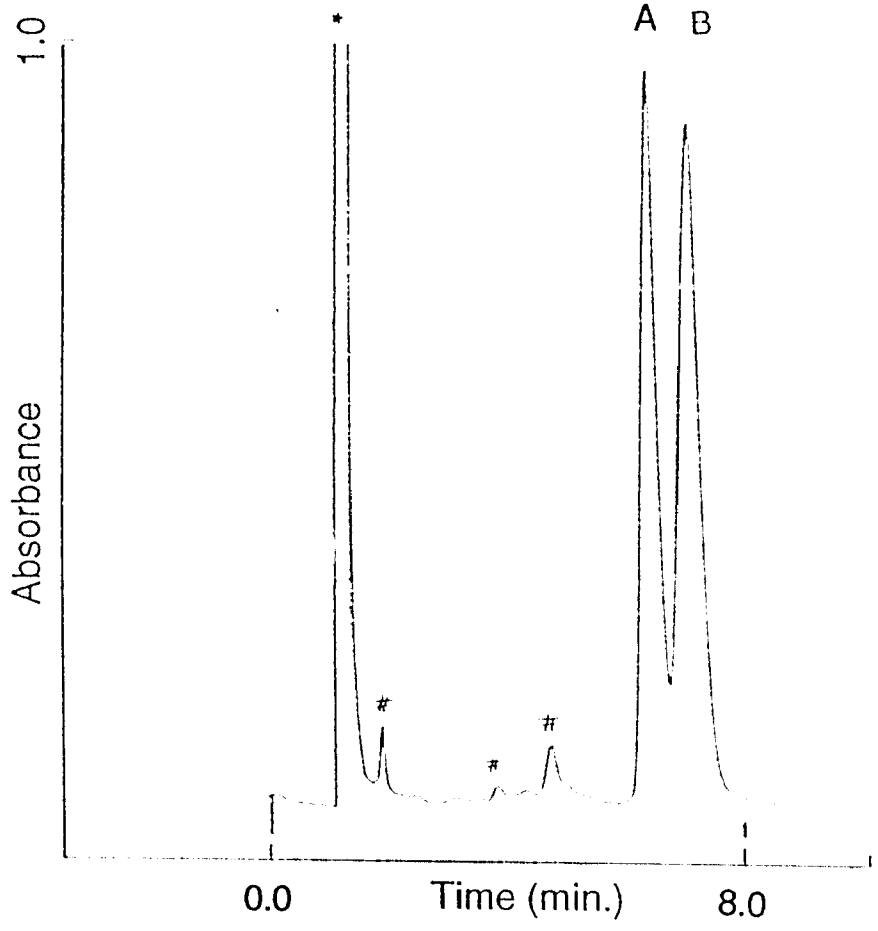


**Fig. 4.2.4** HPLC analysis of the authentic sample mixture of *cis*- and *trans*-$Cr(tn)_2(H_2O)_2^{3+}$.

**Key :** A = *cis*-$Cr(tn)_2(H_2O)_2^{3+}$, B = *trans*-$Cr(tn)_2(H_2O)_2^{3+}$, # = impurity peaks, * = anion peak

**Conditions** : eluents; 25 mM sodium butanesulfonate and 25 mM triethylamine in 10% methanol at pH 2; Flow rate 2 mL $min^{-1}$; Detection wavelength 240 nm.

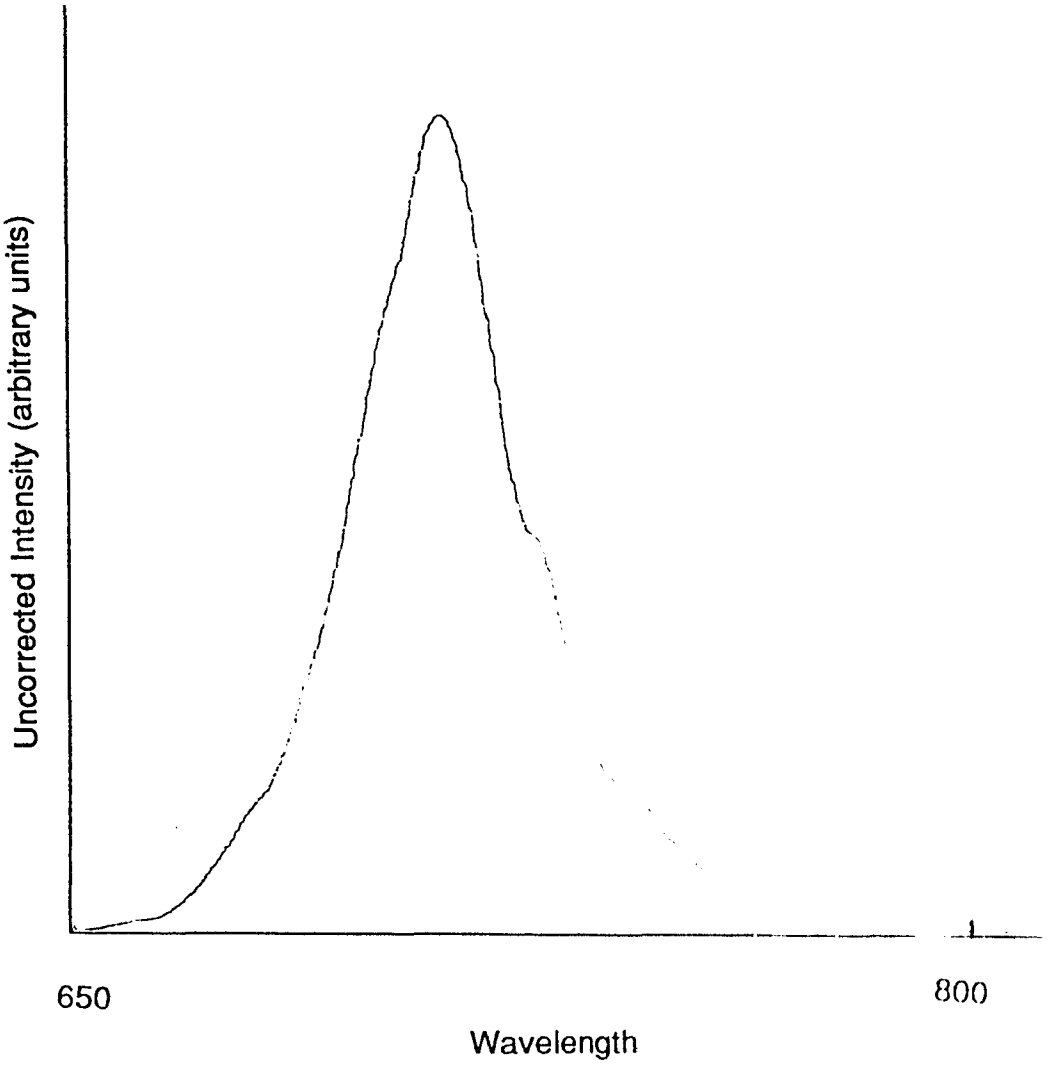


**Fig. 4.2.5** Emission spectrum of *trans*-$[Cr(tn)_2(CN)_2]ClO_4$ at room temperature.

**Conditions :** 6 x $10^{-3}$ M complex in water, irradiation wavelength = 440 nm

The emission lifetime of the complex appeared to be decreasing slowly with time upon standing in an aqueous solution at 20°C. This effect will be considered in detail in section 4.2.3. The initial lifetime was, therefore, obtained by extrapolation of solution lifetimes versus time data to zero time, 185 ± 15 μs at 20°C in aerated aqueous solution.

The doublet excited state was efficiently quenched by hydroxide ion giving a linear Stern-Volmer plot with a $K_{SV}$ value of 9 x $10^5$ $M^{-1}$. It corresponds to a collisional quenching rate constant of 5 x $10^9$ $M^{-1}$ $s^{-1}$, approaching diffusion controlled.

4.2.2.3 Photolysis Studies

Photolysis of the title compound in acidic aqueous medium (1 x $10^{-3}$ M $HClO_4$) leads to aquation of cyanide and of one end of the tn ligand, shown by proton uptake and cyanide measurements in solution.

For all photolysis runs for this compound, the pH-stat method gave proton uptake versus time plots with downward curvature (Fig. 4.2.6a), a phenomenon we have never observed with other complexes, e. g. $Cr((cyclam)(en)^{3+}$ which gave linear plots (Fig. 4.2.6b).

The curvature of the proton uptake versus time plots for this complex was present in all of fifteen photolysis runs to between 3 and 12% conversion at 10 - 15°C. For a subset of four runs where samples absorbing ~0.6 were photolysed to 5% conversion at 436 nm, the slope of the plot at the end of photolysis was 71 ± 3% of the initial slope.

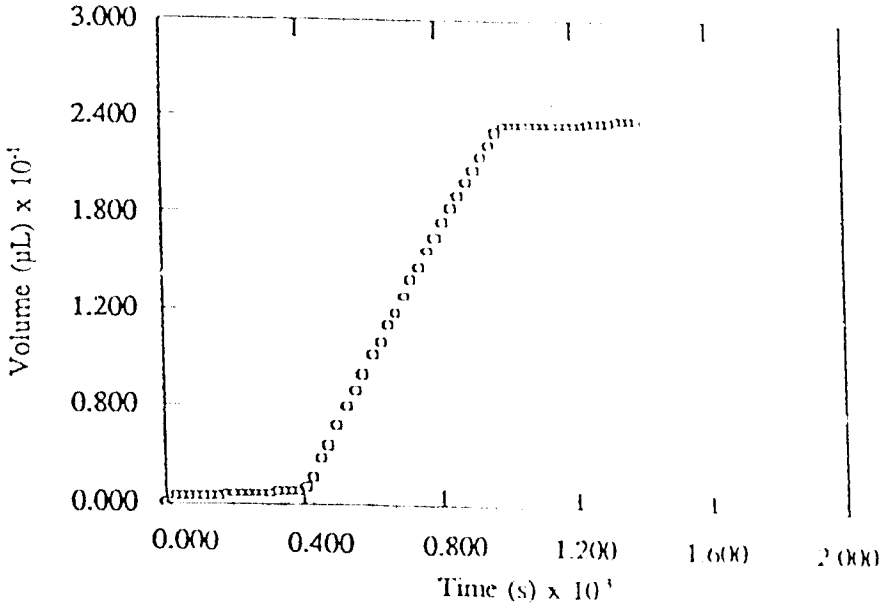


(a)

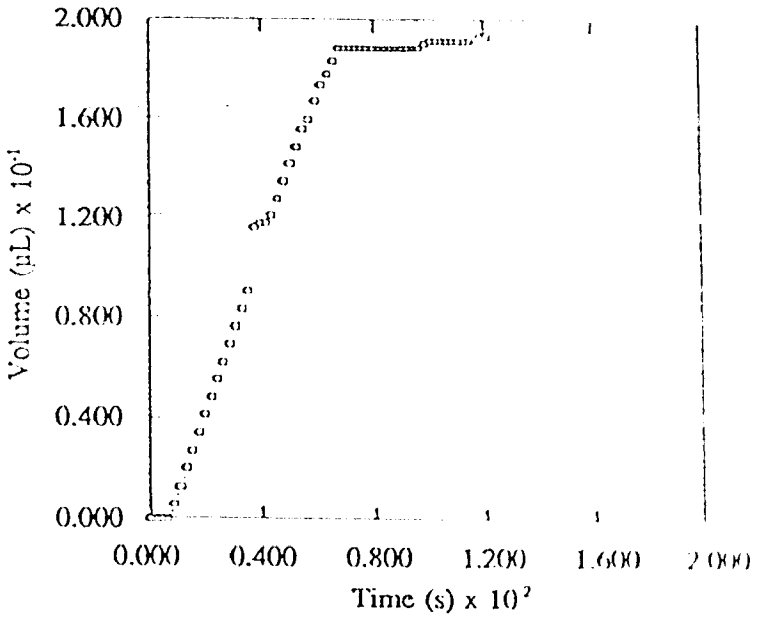


(b)

method with 0.0730 M $HClO_4$ titrant of (a) *trans*-$[Cr(tn)_2(CN)_2]ClO_4$ and (b) $[Cr(cyclam)(en)](ClO_4)_3$. The latter plot also illustrates the non-fatal loss of tracking that can occur when mixing or electrode response is momentarily inadequate.

This decrease in the photochemical rate with extent of photolysis could have three possible causes;

(a) decreasing absorption by the complex upon photolysis.

(b) absorption of light by photoproducts, the inner filter effect

(c) quenching of the doublet excited state of the starting complex by its photoproducts.

The first of these is inconsistent with the low extent of photolysis. The second is excluded by our selection of 365, 458 and 436 nm as the photolysis wavelengths. These are close to minima in the photolysis difference spectrum (see Fig. 4.2.1) where photoproducts absorb less strongly than the starting complex.

To investigate (c), the room temperature doublet emission lifetime in the solution was measured immediately before ($136 \pm 5$ μs) and after ($84 \pm 3$ μs) photolysis to 5% conversion. Note that the emission lifetime of the thermal blank was also decreased to $119 \pm 4$ μs. The decreases in lifetime show that the doublet excited state of *trans*-$Cr(tn)_2(CN)_2^+$ is quenched by the thermal and photoproducts.

This emission quenching effect can be compared semiquantitatively with the photochemical results by using the above lifetime values if we know the distribution of the photoreaction into slow and fast components. By measuring the conductivity change associated with the photoreaction, as done for *trans*-$Cr(2,3,2\text{-tet})(CN)_2^+$ (section 3.2.7), the slow component of the reaction was established to be $57 \pm 8$ % of the reaction[#]. Assuming the quenching process is

[#] (1) Conductivity experiment was done by Dr. A. D. Kirk. (2) The uncertainty of the result is higher than usual since the τ of the sample used was only $87 \pm 3$ μs and needed correction.

dynamic in nature, the estimated@ photochemical rate at the end of photolysis is then 81 ± 14 % of the initial value. This calculated value is in agreement with the experimentally measured slope variation within the experimental uncertainty. This result supports the claim that the observed curvature arises because of quenching of the doublet state of the complex by its own thermal and photoproducts. If we assume that all products quench equally efficiently, the estimated* collisional quenching rate constant was $2 \times 10^7$ $M^{-1}$ $s^{-1}$.

Total quantum yield values $\Phi_T$ were evaluated from the initial slopes of the rate plots (Fig. 4.2.6) with correction for the thermal reaction as follows. The experimental proton uptake curve was fitted to a quadratic equation in time and the initial slope(at t=0) obtained as the coefficient of the first order term. The rate of thermal proton uptake was either estimated by linear regression on sections of the proton uptake plot before and after the photolysis or was calculated using the known thermal rate constant. This rate was then subtracted from the initial slope to get the total corrected initial proton uptake rate.

The direct cyanide measurement gives only an apparent quantum yield ($\Phi_{CN^-,a}$) since it is not corrected for quenching effect. Due to high uncertanities in determining the cyanide quantum yield, it was not possible to measure the time dependence of the rate. We have therefore assumed the two photoreaction modes are quenched to the same extent[58], and have calculated

---

@ Rate(t) / Rate(0) = (0.43 + 0.57 x 84 / 185) / (0.43 + 0.57 x 136 / 185) = 0.81

* Proton uptake was 17.7 µL of 0.0730 M perchloric acid. Total thermal and photoproduct = 1.29 µmol in 3.1 mL solution, i.e. $4.2 \times 10^{-4}$M. By substituting this quencher concentration and lifetime data in Stern-Volmer equation, $k_q = 1.6 \times 10^7$ $M^{-1}$ $s^{-1}$.

the initial cyanide quantum yield ($\Phi_{CN^-}$) by using simple proportion to the apparent total quantum yield ($\Phi_{T,a}$) as in equation 4.2.3.

$$\Phi_{CN^-} = \Phi_{CN^-,a} \times (\Phi_T / \Phi_{T,a}) \quad (4.2.3)$$

The quantum yield of tn mode can then be calculated by equation 4.2.4.

$$\Phi_{tn} = \Phi_T - \Phi_{CN^-} \quad (4.2.4)$$

The quantum yields are tabulated in Table 4.2.2. It shows that the cyanide mode is, 42 ± 5 % at 436 nm and 31 ± 5 % at 458 nm, of the total yield. By taking the average value, we can say that the cyanide photoaquation mode is about 37 ± 6 % of the total yield, and may show some wavelength dependence in such a way that the cyanide mode is increased at shorter wavelengths of excitation.

**Table 4.2.2** Quantum yields for photolysis of *trans*-$[Cr(tn)_2(CN)_2]ClO_4$

| λ(nm) | $\phi_T$ | $\phi_{CN^-}$ | $\phi_{tn}$ |
|---|---|---|---|
| 458 | 0.075 ± 0.004 | 0.023 ± 0.004 | 0.052 ± 0.004 |
| 436 | 0.083 ± 0.004 | 0.035 ± 0.004 | 0.048 ± 0.005 |
| 365 | 0.118 ± 0.002 | ---- | ---- |

In acidic aqueous solution at 15 °C. The means and standard deviations are for sets of three runs throughout.

4.2.2.4 Chromatographic Analysis of Photoproducts

The original objective of this work (section 4.1) required a precise, rapid and convenient technique for the analysis of photoproducts. Conventional ion exchange chromatography was tried using several resins but it failed to separate all photoproducts. Also it was complicated by resin catalyzed decomposition of the complexes and the total time for a chromatogram was very long (~2 hours).

We therefore optimized the reversed phase HPLC technique for this analysis. A sample chromatogram showing the products of a single photolysis is shown in Fig. 4.2.7 in which all primary thermo- and photoproducts were resolved in less than 7 minutes.

In Cr(III) photoaquation, the product geometry can usually be predicted by the rule involving trans attack of the entering ligand in the plane of excitation (section 1.6). Thus *trans*-$Cr(tn)_2(CN)_2^+$ could photoaquate to *cis*- and *trans*-$Cr(tn)(tnH)(H_2O)(CN)_2^{2+}$, where cis and trans are used here to denote the relationship of the cyanide ligands, and to *cis*-$Cr(tn)_2(H_2O)(CN)^{2+}$. The unavoidable thermal reaction will give *trans*-$Cr(tn)_2(H_2O)(CN)^{2+}$.

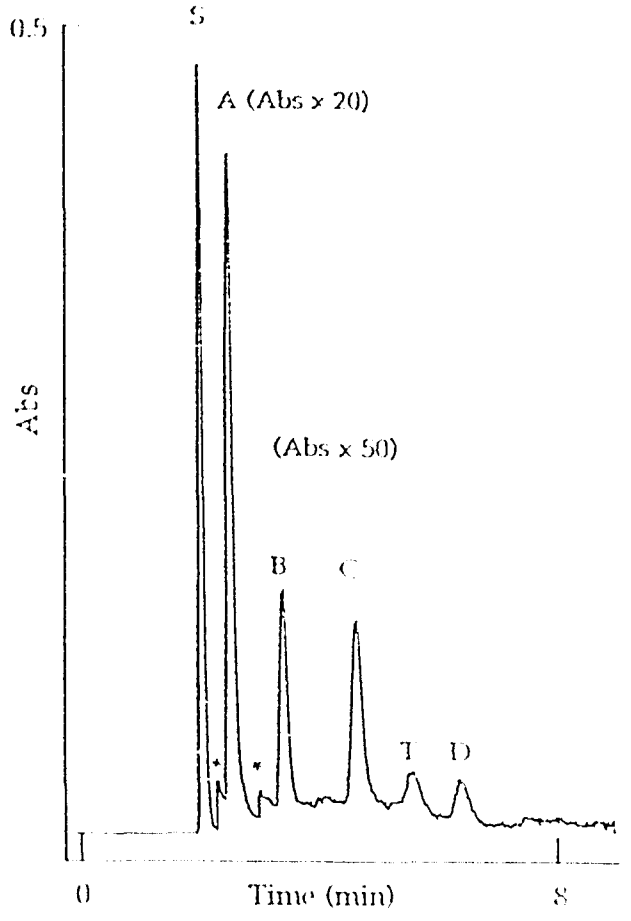


**Fig. 4.2.7** HPLC analysis of thermal and photoproducts of *trans*-$[Cr(tn)_2(CN)_2]ClO_4$ .

**Key :** A = *trans*-$Cr(tn)(tnH)(H_2O)(CN)_2^{2+}$, B = *cis*-$Cr(tn)(tnH)(H_2O)(CN)_2^{2+}$, C = *cis*-$Cr(tn)_2(H_2O)(CN)^{2+}$, S = *trans*-$Cr(tn)_2(CN)_2^{+}$ (starting complex), T = *trans*-$Cr(tn)_2(H_2O)(CN)^{2+}$ (thermal product), D = a secondary photoproduct, * = scale changes.

**Conditions** : eluents; 25 mM sodium butanesulfonate and 12.5 mM triethylamine in water at pH 3.0; Flow rate 2 mL $min^{-1}$; Detection wavelength 240 nm.

Experience with the chromatographic behavior of similar complexes suggests the following guidelines to aid in peak identification:

(a) Cations elute in order of increasing charge, and unit charge difference creates a bigger separation than is seen between isomers.

(b) In the case of tn aquation, one end of the ligand remains coordinated and, at our pH, the free end protonates, resulting in a unit charge increase for the product. This "dangling" plus charge does not contribute fully to the charge seen by the chromatographic process, however. Here such species should elute with retention times between the 1+ (starting material) and 2+ (cyanide loss) ions.

(c) For most geometric isomers of Cr(III) aquo-complexes, the cis elutes before the trans at eluent pH's around 3, an order that can be reversed[63] in a higher pH range.

(d) Substitution of am(m)ine ligands by aquo ligands in otherwise similar complexes causes more rapid elution.

The peak corresponding to the starting complex, S, was easily identified by injection of the pure complex. When the complex was allowed to stand in an acidic medium, a peak developed at T showing this to be the elution time of *trans*-$Cr(tn)_2(H_2O)(CN)^{2+}$ ion. The peak C which elutes just before this was therefore assigned to the expected cis isomer, (c above).

The tn loss species should elute before C & T, and in the sequence cis before trans, suggesting the assignment A = *cis*-$Cr(tn)(tnH)(H_2O)(CN)_2^{2+}$ and B = *trans*-$Cr(tn)(tnH)(H_2O)(CN)_2^{2+}$; note that the geometric relationship of the tnH and $H_2O$ ligands in these compounds is not known.

To obtain more definitive evidence for the peak assignments, the thermal reactions of the photoproducts were studied. Generally aquation of monoacido complexes is slower than corresponding diacidos and it has been found that, in contrast to the usual sequence, *trans*-$Cr(NH_3)_4(CN)_2^+$ aquates faster than its cis isomer (section 1.12).

A photolysed sample was acidified to make it about 1 M in $HClO_4$ and the reaction was followed chromatographically for over one hour. Peaks S, A, B and C decreased gradually, enhancing T greatly, and generating new peaks at longer retention times than shown on Fig. 4.2.7. The times for disappearance of A, B and C were quite distinct, about 15, 50 and 80 minutes respectively. These results indicate that A = *trans*-$Cr(tn)(tnH)(H_2O)(CN)_2^{2+}$, B = *cis*-$Cr(tn)(tnH)(H_2O)(CN)_2^{2+}$ and C = *cis*-$Cr(tn)_2(H_2O)(CN)^{2+}$ . We consider the rate data for A and B more definitive than the conflicting sequence suggested by guideline (c) and adopt this last assignment in the following discussion.

Chromatography allows semi-quantitative analysis of photoproducts. For 488 and 458 nm photolysis the integrated relative peak areas, A : B : C, are (7.4 ± 0.5) : 1.0 : (0.92 ± 0.13) and (4.7 ± 0.6) : 1.0 : (1.22 ± 0.05) (in four runs each). Therefore C / (A + B) ratios are 0.11 and 0.21 respectively, consistent with the proportional increase in cyanide loss at shorter wavelength shown by the quantum yield data in section 4.2.2.3.

A and B have the same set of coordinating atoms and differ only in geometry. Since the detection wavelength is in the charge transfer region, these two products are likely to have very similar molar absorptivities so that the peak areas give close to true A : B ratio. Product C has a different set of coordinating atoms, however, so the proportion of cyanide reaction mode cannot be estimated reliably chromatographically. Indeed, our results indicate

that the product C has a lower molar absorptivity than the other products. For instance, at 458 nm photolysis the peak areas indicate that 17 ± 2 % of the reaction is cyanide, compared with 31 ± 5% by direct cyanide measurement. Consistent with this, we observe that the total peak area was less than the peak area decrease of starting material, S, and this deficit increased toward shorter irradiation wavelengths where more C is produced.

### 4.2.3 Discussion

4.2.3a Quenching of Photochemistry by Photoproducts

An interesting result is that the photoproducts efficiently quench the photoreaction. We believe this is the first such observation in the photochemistry of inorganic systems, although the effect of thermal products was previously indicated.[120c] For this quenching effect, the long lifetime of the doublet state obviously is important. It may also be assisted by the presence of cyanide ligands that favor efficient energy transfer[125] and low charges on the reactant and photoproduct molecules. In other systems there is often a greater Coulomb barrier to bimolecular quenching of reactant by product.

The estimated quenching rate constant is only $10^7$ $M^{-1}$ $s^{-1}$ which is almost three orders of magnitude down from our measured value for $OH^-$ and considerably less than expectation for a diffusion controlled ($k_q$ = ~$10^{10}$ $M^{-1}$ $s^{-1}$) process. This suggests the potential for such quenching in reactants having shorter excited state lifetimes if higher $k_q$ values are involved. In the study of the photochemistry of *trans*-Cr(2,3,2-tet)$(CN)_2^+$ we found that the proton uptake versus time plots were linear at low extents of photolysis whereas they show a downward curvature at high extents of photolysis. It indicates that the efficiency of quenching by its photoproducts has been smaller than that for

*trans*-$Cr(tn)_2(CN)_2^+$. In these two similar complexes, the major differences are that *trans*-$Cr(2,3,2\text{-tet})_2(CN)_2^+$ does not show any cyanide loss and its emission lifetime is about 15% of *trans*-$Cr(tn)_2(CN)_2^+$. Assuming the efficiency of quenching is not affected by the nature of photoproducts, this comparison indicates that the long emission lifetime is the most important factor in quenching of the photoreaction by its photoproducts.

4.2.3b Photoaquation of Cyanide

There is clearly a significant cyanide reaction mode in this molecule whereas the analogous compounds with ammine,[52] en[53] and 2,3,2-tet (section 3.2.4) do not show any detectable cyanide mode. Also this mode increases on increasing the excitation wavelength to shorter wavelength, both by direct and chromatographic measurements. This reaction mode is not predicted by the VC theory (section 1.5.2) and in the following we will argue that it represents a further example of the competitive ligand loss phenomenon reported for complexes with tn as the bidentate ligand.

VC theory calculations, assuming tn = $2NH_3$, show the $^4E/^4B_2$ energy gap in this molecule is 0.25 $\mu m^{-1}$ with the $^4B_2$ state the lower in energy (Table 1.5.1). Predictions for this lowest excited state are exclusive loss of equatorial tn (calculated excited state bond strengths: tn = 0.9; CN = 1.9 $\mu m^{-1}$), which should give[6, 124] the sole product with trans cyanides (A). There should be no cyanide loss from this state and its predicted reactivity accounts for the major product observed.

The cyanide mode and product B can be accounted for if one allows the possibility of reaction also from the higher lying $^4E$ state. This should again lose tn to give B, having cis cyanides, but now the calculated excited state bond

strengths are much closer (tn =1.1; CN = 1.3 $\mu m^{-1}$) and the poor leaving ability of tn can assist in the loss of the cyanides present[63, 121] on both possible planes of labilization.

The calculated $^4E$ / $^4B_2$ spacing argues against thermal population of $^4E$ from $^4B_2$, although this could be altered by strong interactions with the nucleophilic solvent.[6] For this molecule, which shows ~43% prompt reaction, the more likely situation is direct population by branching from the Franck-Condon state, with rapid, irreversible relaxation and reaction of the generated $^4E$ precursor, in violation of Kasha's rule. Such a model is more consistent with the observed decrease in the tn mode and increase in cyanide as the irradiation wavelength moves towards the higher energy quartet component. The nature and pathway of the reaction via the doublet is unclear.

The study shows that *trans*-$Cr(tn)_2(CN)_2^+$ is another example of a complex in which tn serves to promote photoaquation of a ligand that does not normally leave. The molecule shows interesting wavelength dependence, and offers the potential for study of quartet and doublet reaction modes, their temperature dependence, etc.

4.2.3c Wavelength Dependence study of *trans*-$Cr(tn)_2(CN)_2^+$

Such a study requires precise measurement of the small changes in product yields or product stereochemistry with wavelength and necessitates precise product analysis. Unfortunately, the precise work required is hampered by the non-linearity of the time course of photolysis, the need to assume that both modes are quenched to the same extent and also the large thermal corrections to the cyanide mode. Therefore, this system was considered

unsuitable for the kind of wavelength dependence study that prompted our initial investigation.

## 4.3 Photochemistry and Photophysics of $Na[Cr(tn)(CN)_4]$. A New Quencher for Energy Transfer Quenching Studies

### 4.3.1 Introductory Comments

Hydroxide ion is widely used as a quencher in photochemistry and photophysics of transition metal complexes in aqueous solutions. This is probably because it usually satisfies most of the criteria (section 4.4.3) of a good quencher. For instance the collisional quenching rate constant of the quenching of doublet decay of $Cr(tn)_3^{3+}$ by $OH^-$ approaches diffusion controll and is $6 \times 10^{10}$ $M^{-1}$ $S^{-1}$ at 25°C, showing the high efficiency of $OH^-$ as a quencher.

The use of hydroxide, sometimes, suffers problems. In one instance, hydroxide was shown to lead to reactive quenching.[120d] Also use of $OH^-$ makes it mandatory to maintain a high pH value which is unsuitable in many instances, due to deprotonation of ligands or instability of complexes. For instance $Cr(NH_3)_4(H_2O)(CN)^{2+}$ deprotonates coordinated water generating a non-emitting hydroxo species.[58] $Cr(NH_3)_4(CN)F^{2+}$ brings about cloudiness, due to fast thermal decomposition.[58]

The commonly used alternative quenchers to $OH^-$ are transition metal complexes like $Cr(CN)_6^{3-}$ or $Cr(C_2O_4)_3^{3-}$. The problems associated with these quenchers are several; precipitation with cationic (particularly with 3+) complexes, significant absorption of visible light by the quencher at desired wavelengths, and insufficient solubility in some solvents. All these problems

would interfere our major objective of this work; finding an alternative quencher for wavelength dependence studies of the photoaquation of $Cr(tn)_3^{3+}$.

$Cr(tn)(CN)_4^-$ can be expected to be a suitable quencher, due to the following reasons.

(a) Cyanide is a $\pi$ accepting ligand (section 1.3). Therefore, metal electron delocalization to four cyanide ligands should give rise to a low lying doublet energy level which is capable of being an energy acceptor to promote energy transfer quenching.

(b) Relatively low charge (-1) on the complex could minimize precipitation with a highly charged species, like $Cr(tn)_3^{3+}$.

(c) The expected UV/Vis spectrum indicates that the compound would not significantly absorb light at longer (>460 nm) wavelengths. Therefore the red edge region (465 - 514 nm) of $Cr(tn)_3^{3+}$ would be accessible with this quencher.

(d) $CN^-$ is also considered as a "Conducting ligand"[125] which would enhance the efficiency of quenching.

Therefore we synthesized the new molecule $Na[Cr(tn)(CN)_4]$. The characterization, and some photochemical, photophysical and quenching properties of $Cr(tn)(CN)_4^-$, specially those relevant to wavelength dependence study of $Cr(tn)_3^{3+}$, were studied.

## 4.3.2 Results

### 4.3.2.1 Characterization

(a) UV/Vis Spectroscopy

The compound shows two LF bands with peak maxima at 408 and 329 nm in acidic aqueous solutions (Fig. 4.3.1 and Table 3.2.1). The wavelength of the LF peak maxima of $Cr(tn)(CN)_4^-$ should be between the peak maxima of $Cr(tn)_2(CN)_2^+$ and $Cr(CN)_6^{3-}$. The value can be estimated by averaging the energy of the band maxima of the latter two complexes. The peak maxima estimated for $Cr(tn)(CN)_4^-$ (Table 3.2.1) are in good agreement with the expected values. Theis type of estimate successfully predicts the peak maxima of a series of Cr(III) cyano am(m)ine complexes.

(b) Emission Spectroscopy

The title compound does not emit in aqueous solutions, but it emits in DMSO and DMF with lifetimes of 4 and 17 μs respectively at 20°C . The observed peak maxima of the emission spectra are at 748 and 747 nm in DMSO and DMF respectively. Again the estimated wavelength of the emission maxima using the energy values for $Cr(tn)_2(CN)_2^+$ and $Cr(CN)_6^{3-}$ is in excellent agreement with the observed value (Table 1.11.1).

(c) IR Spectroscopy

The compound shows a sharp but weak peak at 2160 $cm^{-1}$, which can be attributed to a cyanide stretching band of cyanide coordinated to a Cr(III) center. A similar peak was also observed for $Cr(NH_3)_5(CN)^+$ at 2140 $cm^{-1}$.

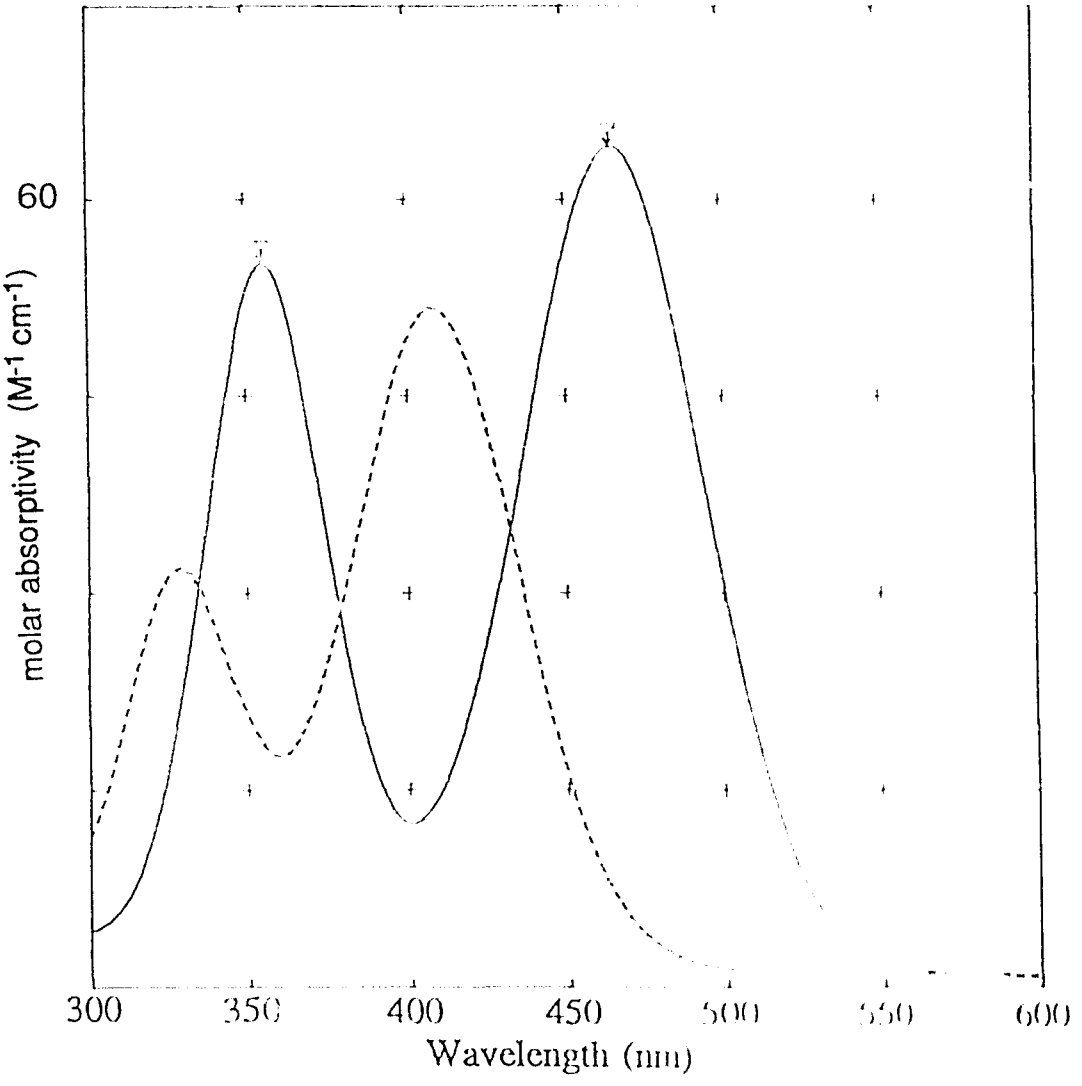


**Fig. 4.3.1** UV/Vis absorption spectra of $Na[Cr(tn)(CN)_4]$ (-----) and $[Cr(tn)_3]Cl_3$ (——) in room temperature acidic aqueous solutions.

4.3.2.2 Photostability

The quantum yield of photolysis at 406 nm measured by proton uptake was 0.040 ± 0.006 at 21°C in $HClO_4$ (pH = 3) and 0.10 M $KClO_4$. No attempts were made to identify photoproducts, but it is reasonable to believe that the reaction is photoaquation of one end of the tn ligand (see section 4.3.3).

The quantum yield of photoaquation of $Cr(CN)_6^{3-}$ is 0.09.[126] Therefore, $Cr(tn)(CN)_4^-$ is more photo-stable than the previously used common transition metal quencher, $Cr(CN)_6^{3-}$. With respect to photostability, however, $Cr(C_2O_4)_3^{3-}$ is a better quencher than $Cr(tn)(CN)_4^-$ since photochemistry of $Cr(C_2O_4)_3^{3-}$ consists racemization only,[127] with a quantum yield of 0.09.

4.3.2.3 Thermal Stability

The pseudo first-order rate constant, measured by the pH-stat method, for thermal aquation was $4 \times 10^{-5}$ $s^{-1}$ at 20°C in $1 \times 10^{-2}$ M $HClO_4$ and 0.1 M $KClO_4$. It corresponds to a half life of ~5 hours, at pH 2. No attempts were made to identify the thermal products, but it is believed that the reaction would be acid catalyzed cyanide aquation (section 1.12).

Photochemical experiments are usually carried out at pH 3 aqueous solutions, where the rate of the aquation reaction of $Cr(tn)(CN)_4^-$ should be even slower than the value measured at pH 2. Therefore, no interference due to the thermal reaction of $Cr(tn)(CN)_4^-$ is expected during the time scale of a photochemical experiment.

4.3.2.4 Quenching Efficiency

A Stern-Volmer plot of reciprocal lifetime of $Cr(tn)_3^{3+}$ against $Cr(tn)(CN)_4^-$ concentration is linear with a slope (= $k_q$) of $3 \times 10^8$ $M^{-1}$ $s^{-1}$ at 20°C in acidic ($1 \times 10^{-3}$ M $HClO_4$) aqueous solutions. Typical $k_q$ values for

quenching of the emission of a transition metal complex by another transition metal complex[3] lie between 1 x $10^5$ to 1 x $10^9$ $M^{-1}$ $S^{-1}$, and our value is among the highest reported. For instance, $Cr(C_2O_4)_3^{3-}$ was successfully used for quenching studies of *trans*-$Cr(NH_3)_4(CN)(NCS)^+$, for which $k_q$ = 3 x $10^8$ $M^{-1}$ $s^{-1}$, at 20°C. Therefore $Cr(tn)(CN)_4^-$ can be considered as an efficient quencher.

4.3.2.5 Solubility Properties

Using the Stern-Volmer equation the calculated $Cr(tn)(CN)_4^-$ concentration for quenching of 90% of the emission of $Cr(tn)_3^{3+}$ was 1.3 x $10^{-2}$ M (3.3 mg $mL^{-1}$) and that for 99% was 4.7 x $10^{-2}$ M (12 mg $mL^{-1}$). Tests showed the solubility of $Cr(tn)(CN)_4^-$ in acidic aqueous solution, in the presence of $Cr(tn)_3^{3+}$, is good enough for quenching of the emission of the latter complex.

$Cr(tn)(CN)_4^-$ is also readily soluble (section 2.1 5) in DMSO and DMF. Therefore, this complex can also be used for quenching studies in non-aqueous solvents.

4.3.2.6 Light absorption by quencher

The UV/Visible spectrum of the title compound is shown in Fig. 4.3.1. One of the apparent disadvantages of the title compound as a quencher is that it absorbs a fair amount of light up to about 460 nm of the visible region. While the molar absorptivities of peak maxima at 329 and 408 are 35 and 55 $M^{-1}$ $cm^{-1}$ respectively, the value at 460 nm is 8 $M^{-1}$ $cm^{-1}$. Since the light absorption at longer wavelengths is minimal, $Cr(tn)(CN)_4^-$ will be a good quencher for experimental excitation wavelengths longer than 460 nm.

The first LF band maxima of $Cr(tn)_3^{3+}$ is at 464 nm and along its red edge, the light absorption by $Cr(tn)(CN)_4^-$ is negligible, especially at the two major Argon Ion Laser wavelengths of 488 and 514 nm. Therefore, the title compound is a good quencher for the intended wavelength dependence study along the red edge of $Cr(tn)_3^{3+}$.

### 4.3.3 Discussion

An ideal quencher for photochemical and photophysical studies in the condensed phase should have the following properties:

(a) thermostability

(b) photostability

(c) high efficiency of quenching (high value of $k_q$)

(d) high solubility

(e) freedom from interference with the complex of study or its products

(f) freedom from analytical interferences

(g) freedom from absorption of light by the quencher at the wavelength(s) of excitation.

The criteria (a) - (f) are expected to be satisfactory for quenching of the excited states of many other transition metal complexes by $Cr(tn)(CN)_4^-$. The above criterion (g) is, however, perfect only for wavelengths longer than 460 nm. There are many complexes in which the visible spectrum extends well over 460 nm. For such complexes, $Na[Cr(tn)(CN)_4]$ satisfies all the criteria listed above. Therefore, we consider that $Na[Cr(tn)(CN)_4]$ is a good quencher, in general, for quenching of photochemistry and photophysics of transition metal complexes.

For wavelength dependence study along the red-edge of $Cr(tn)_3^{3+}$ with $Cr(tn)(CN)_4^-$, data supporting the criteria (e) and (f) are given in section 4.4. Therefore, $Na[Cr(tn)(CN)_4]$ fulfills all these criteria and we were able to use this quencher successfully for our wavelength dependence study (section 4.4).

VC theory calculations (section 1.5.2) for $Cr(tn)(CN)_4^-$ show that the $^4B_2$ state is lower in energy ($^4E/^4B$ gap = 12.6 $\mu m^{-1}$) and the bond strengths of this excited state are: $I^*(Cr\text{-}N) = 0.90$ (assuming tn = 2 $NH_3$), $I^*(Cr - CN_{eq}) = 1.1$ and $I^*(Cr - CN_{ax}) = 1.8\ \mu m^{-1}$. Therefore the theory predicts the loss of one end of the tn as the major mode. (It is notable that Adamson's Rules predict the loss of CN, *trans* to tn, instead.) But, tn is a poor leaving ligand and therefore a lower quantum yield is expected, consistent with the observed $\Phi = 0.04$.

The mechanism of the quenching of an excited state process of a transition metal complex by another transition metal complex is usually believed to be "electronic energy transfer" in nature, even though experimental proofs have been provided only on a few occasions.[13] The direct test for confirming this mechanism, is observing the emission of the quencher. It was not possible to examine this aspect for quenching of $Cr(tn)_3^{3+}$ by $Cr(tn)(CN)_4^-$ in aqueous solutions, since the quencher does not emit in water. However, in an independent experiment, where $Cr(tn)_2(CN)_2^+$ and $Cr(tn)(CN)_4^-$ were present in 1:1 ratio in DMSO, upon excitation of $Cr(tn)_2(CN)_2^+$ at a wavelength where the absorbance by $Cr(tn)(CN)_4^-$ was negligible (460 nm), the emission of $Cr(tn)(CN)_4^-$ was observed together with the residual emission of $Cr(tn)_2(CN)_2^+$ # (Fig. 4.3.2). Therefore, at least in one instance, we have shown

---

# Unpublished work by the author.

that the mechanism of quenching by $Cr(tn)(CN)_4^-$ involves electronic energy transfer.

## 4.4 Wavelength Dependence Studies of $Cr(tn)_3^{3+}$ with $Na[Cr(tn)(CN)_4]$ Quencher

### 4.4.1 HPLC Analysis of $Cr(tn)_3^{3+}$ photolysis

In order to carry out the wavelength dependence study of the photoproduct distribution of $Cr(tn)_3^{3+}$, it is necessary to have a good analytical method to determine the product ratio. The technique adopted[63, 97] for this purpose was RP-HPLC. Baseline resolved peaks were not obtained for the photoproducts. Therefore, the chromatograms were improved before pursuing further work.

A sample chromatogram under the present conditions is shown in Fig. 4.4.1. In that, the starting complex, $Cr(tn)_3^{3+}$ (S) and two major photoproducts; *cis* and *trans*-$Cr(tn)_2(tnH)(H_2O)^{4+}$ (D & E respectively) are well resolved. These peaks were identified by the known thermal and photochemical properties of $Cr(tn)_3^{3+}$, as it was previously done.[63] The peak area ratio (D/E) was reproducible with high precision (uncertainty ≤1%), even under low extent (~3%) of photolysis (see Fig. 4.4.2). This high sensitivity was presumably due to our selection of 228 nm detection wavelength (changed from previously used value of 240 nm). This is because at shorter wavelengths molar absorptivities are expected to be higher. Also in the

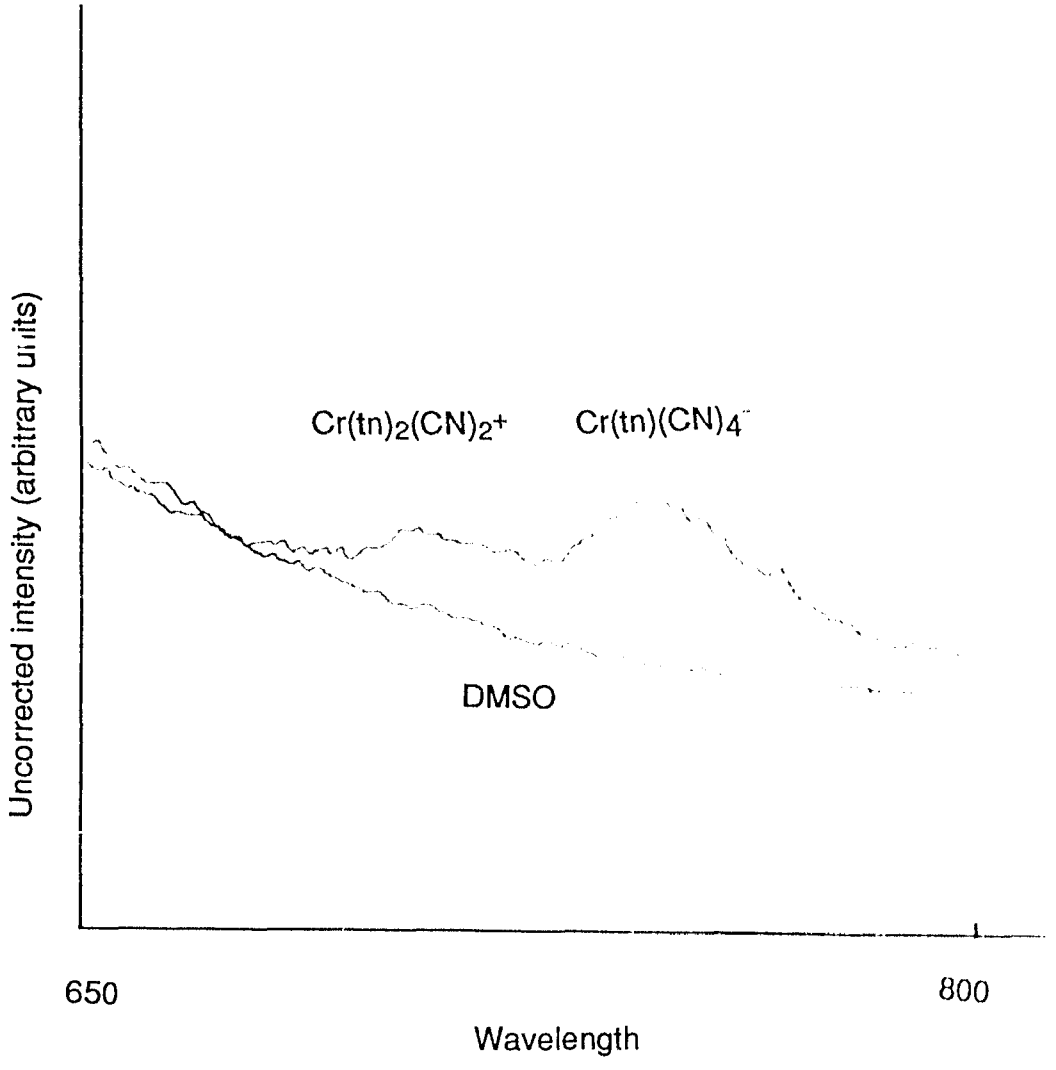


**Fig. 4.3.2** Emission spectrum of $[Cr(tn)_2(CN)_2][Cr(tn)(CN)_4]$ upon excitation at 460 nm. (See section 4.3.3.)

The experiment was performed in an attempt to characterize a sample of $[Cr(tn)_2(CN)_2][Cr(tn)(CN)_4]$ synthesized by Dr. D. A. House.

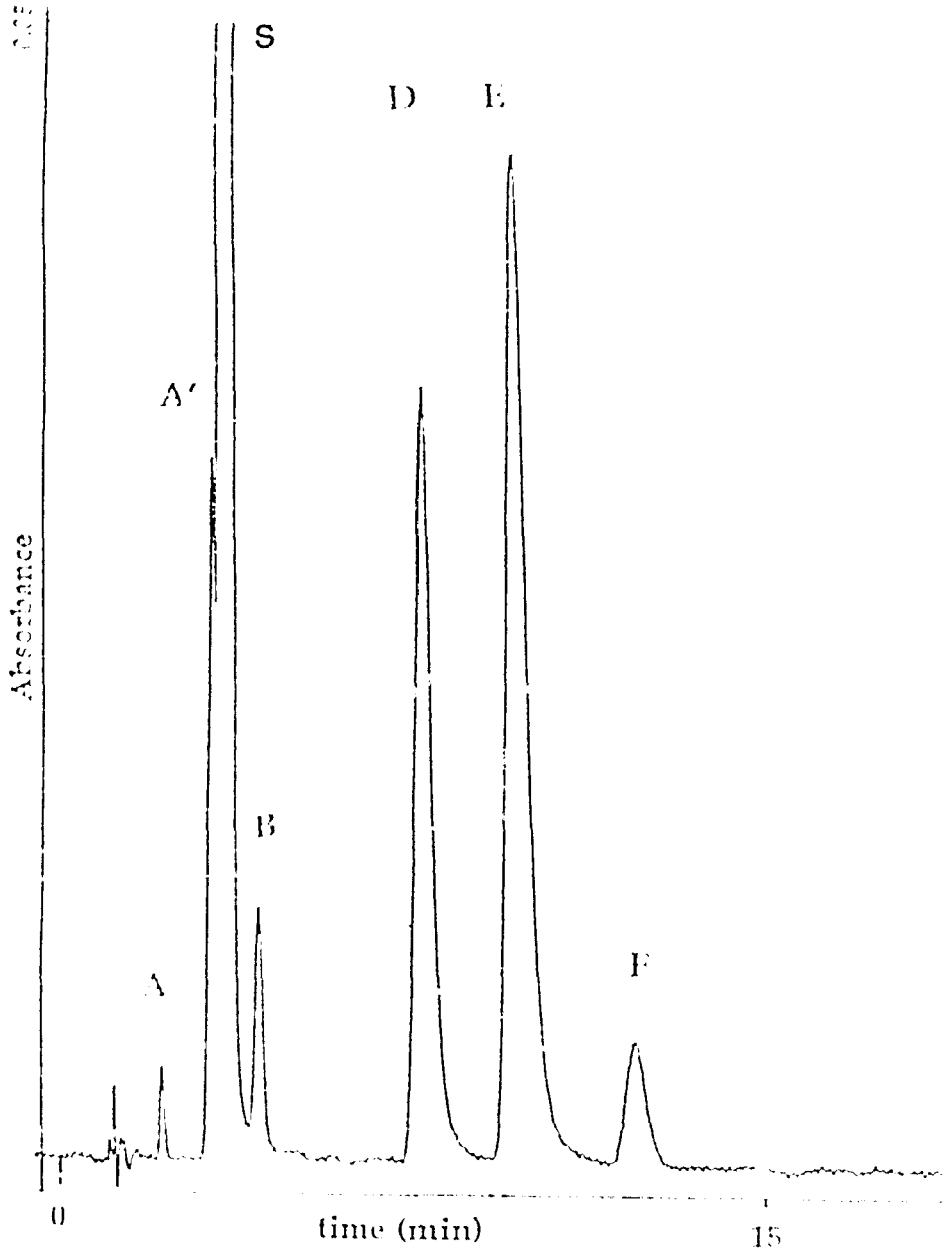


**Fig. 4.4.1** Chromatogram (HPLC) of $Cr(tn)_3^{3+}$ at 20% photolysis.

**Key :** S = $Cr(tn)_3^{3+}$ (starting complex), D = *cis*-$Cr(tn)_2(tnH)(H_2O)^{4+}$, E = *trans*-$Cr(tn)_2(tnH)(H_2O)^{4+}$, F = $Cr(tn)(tnH)_2(H_2O)_2^{5+}$, B = secondary photoproduct, A, $A^1$ are artifact peaks.

**Conditions** : eluents; 25 mM sodium butanesulfonate and 25 mM triethylamine in 18% methanol at pH 3.0; Flow rate 2 mL $min^{-1}$; Detection wavelength 228 nm.

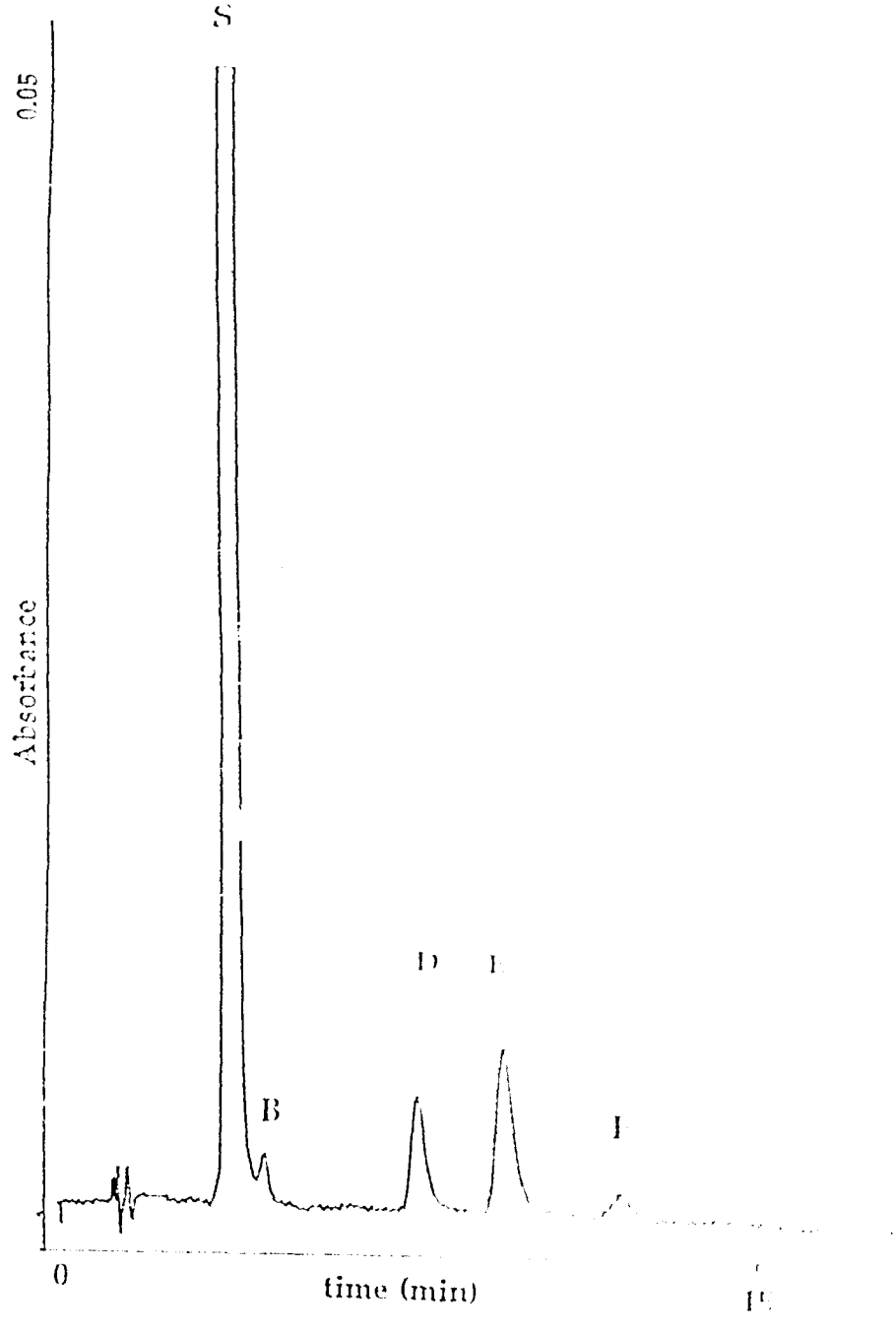


**Fig. 4.4.2** HPLC chromatogram of $Cr(tn)_3^{3+}$ at 3 % photolysis.

**Key :** same as for Fig. 4.4.1

**Conditions** : same as for Fig. 4.4.1

present chromatograms isocratic eluent compositions were used making the repetitive analysis quicker than previously where eluent gradients were used. Thus, the results based on the present chromatograms are expected to be more sensitive, accurate and precise.

Interestingly, photolysis of $Cr(tn)_3^{3+}$ produced two additional peaks (B, and F), not reported under previous conditions. Several attempts were made to identify these additional peaks.@

(i) A thermal blank for photolysis does not develop B, D, E, F or any other peaks.

(ii) Peaks were developed approximately linearly with time of photolysis for 3 to 12% conversion. Peak areas of B and F are, however, much smaller than D and E (e.g. in a 10% photolysed sample, the peak areas of B and F were about 4 and 6% of (D + E) respectively) and therefore the high uncertainty of small peak areas does not allow us to determine the exact pattern of variation.

(iii) Heating of a solution of S at 60°C for 30 min produced minor amounts of B and E in addition to the major product D. F was not detected.

(iv) If a photolysed (10%) sample was allowed to stand for another ~30 min, longer than the time scale of a photophysics experiment, under photolysis conditions, no detectable change in peak areas was observed.

@ The conditions used were: $8 \times 10^{-3}$ M $Cr(tn)_3^{3+}$ solutions (Absorbance = ~0.3 at 436 nm) in $3 \times 10^{-2}$ M $HClO_4$, unless otherwise stated. Photolysis was carried out at 436 nm ($I = 7 \times 10^{-8}$ einsteins $s^{-1}$). Samples thermostated at 10°C unless specified.

(v) If a photolysed (10%) sample was heated at 60°C for ~30 min, the areas of S, D and E were gradually decreased, greatly developing B, another peak that elutes just before S, and to a small extent F. It can also be seen that the D/E ratio was increased from 0.63 to 1.0. This latter phenomenon is most probably because D was thermally developed from S, while D and E deplete at a faster rate.

(vi) Photolysis in water (without $HClO_4$) also produced similar chromatograms with all the peaks.

(vii) At higher extent of photolysis, a new small peak C, started to appear between B and D peaks (retention time = 5 min, under the conditions used in Fig. 4.4.1).

The above observations lead to the following conclusions about the species corresponding to B and F peaks.

(i) They are all photoproducts.

(ii) At higher temperature B can also be a minor thermal product of S.

(iii) At higher temperature B is the major and F is the minor, thermal products of D and E.

(iv) Photochemical formation of A, B and F are not assisted by $HClO_4$.

The results indicate that $Cr(tn)_3^{3+}$ most probably undergoes secondary photolysis from the very early stage of the photoreaction (at least from 3% conversion). Considering the structure of prirnary photoproducts, the most likely secondary photoproducts are $Cr(tn)_2(H_2O)_2^{3+}$ and $Cr(tn)(tnH)_2(H_2O)_2^{5+}$. The above results and usual guidelines for assigning the RP-HPLC peaks (see section 4.2.2.4), are consistent with the assignment that B and F correspond to these two species respectively. Test runs with authentic samples, however,

show that both *cis*- and *trans*-$Cr(tn)_2(H_2O)_2^{3+}$ species are not resolved from S and therefore B is not $Cr(tn)_2(H_2O)_2^{3+}$. While it is reasonable to assign the peak F to $Cr(tn)(tnH)_2(H_2O)_2^{5+}$, the peak assignment of B is more subtle than expected.

Despite these small additional peaks, we observe the same D/E ratio reported, up to 12% conversion (section 4.4.2b). Therefore, our wavelength dependence study can be carried out without establishing the exact origin or the identity of the B and F species.

An advantage of using $Cr(tn)(CN)_4^-$ as a quencher is that it is expected to be free from interference with the chromatographic analysis of the photoreaction of $Cr(tn)_3^{3+}$. Since $Cr(tn)(CN)_4^-$ is a negative ion, it elutes as a column unretained peak (1 min). Any of its primary products would be neutral, and would have very short retention times. To confirm this, the HPLC peak development due to the thermo- and photoreaction of $Cr(tn)(CN)_4^-$ was studied under the eluent conditions used for $Cr(tn)_3^{3+}$ analysis.

When $Cr(tn)(CN)_4^-$ was allowed to stand in $3 \times 10^{-2}$ M $HClO_4$ at ~28°C for 2 hours, three peaks were observed, two of which were barely resolved from S while the third peak has a retention time of 1.6 min. If the solution was allowed to stand for 24 hours, a fourth peak was developed at 2.2 min (Fig. 4.4.3). We believe this fourth peak is $Cr(tn)(H_2O)_4^{3+}$, produced as a result of acid catalyzed loss of all four cyanides. No peak development was observed when the compound is allowed to stand in $1 \times 10^{-3}$ M $HClO_4$ at 28°C for one hour. Also no peaks were detectable upon photolysis of $Cr(tn)(CN)_4^-$, under this chromatographic condition presumably due to overlapping of such peaks with $Cr(tn)(CN)_4^-$.

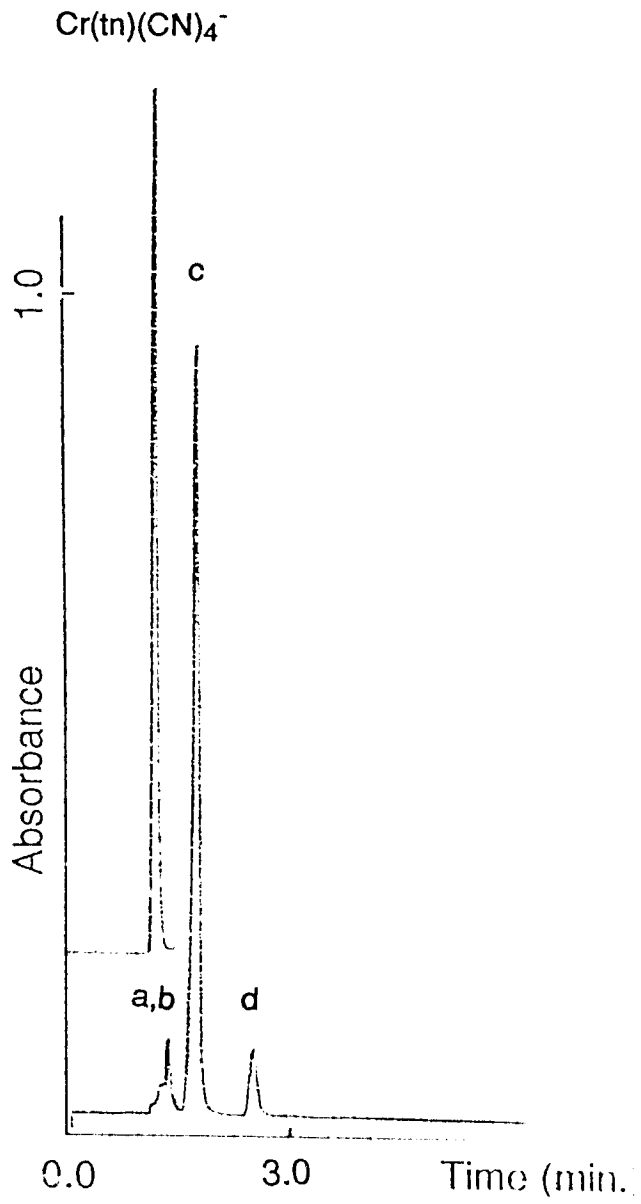


**Fig. 4.4.3** Chromatogram of $Cr(tn)(CN)_4^-$ and its products under the HPLC conditions used for the analysis of the photoreaction of $Cr(tn)_3^{3+}$.

**Key :** upper (off set) = before thermolysis, lower = after thermolysis. a,b,c,d = thermal products

**Conditions** : same as for Fig. 4.4.1

Thus all the peaks that may develop from $Cr(tn)(CN)_4^-$ during the time scale of our experiments elute with a retention time ≤1.6 min whereas all the peaks from $Cr(tn)_3^{3+}$ have retention times ≥2.2 min. Therefore, the above study shows that chromatographic analysis of the photoreaction of $Cr(tn)_3^{3+}$ is not affected by the $Cr(tn)(CN)_4^-$ quencher or its products.

### 4.4.2 Quenching with $Cr(tn)(CN)_4^-$

4.4.2a Experimental Aspects

In order to obtain reliable values for photoproduct ratio (D/E), it is necessary to suppress thermal reactions of any species which would have an effect on D/E ratio. We have observed that the thermal reactions of photolysed sample ($1 \times 10^{-2}$ M), upon standing at room temperature, occur in such a way that the net effect on D/E (=*cis/trans*) ratio is dependent on the pH of the medium.

(a) At pH ~1.5 ($3 \times 10^{-2}$ M $HClO_4$) D/E ratio increases. This was attributed to the thermal generation of D from S, in addition to thermal depletion of D and E. (Section 4.3).

(b) In pH values between 5 and 7, D/E ratio decreases due to rapid thermal depletion of peak D. This is presumably due to the recoordination of the *cis* isomer, similar to the manner discovered for the photoproduct of $Cr(2,3,2\text{-tet})(CN)_2^+$ (section 3.2.5b).

(c) At pH 13 (0.11 M NaOH) D/E ratio increases.

All these effects are significant during the time scale of our experiments, at room temperature, but their effect on the D/E ratio is negligible at 10°C. For instance, at pH 10, the peaks A, B and F stay stable at 10°C for at least 40 min.

We find that it is essential to maintain the solutions at low temperature during this wavelength dependence study, especially at high concentrations.

We have also observed that the species corresponding to B and F are unstable in base (pH ≥12) even at 10°C. If the pH of a sample photolysed in acid (pH = 1.5), where all the peaks are seen (Figure 4.4.1), is adjusted to 12, peaks B and F disappear rapidly. Peak F is the fastest to disappear (<10 min). These thermal reactions, however, do not alter the D/E ratio.

The absorbance of $Cr(tn)_3^{3+}$ samples at the wavelength of photolysis was about 0.3 at the wavelength of photolysis. It corresponds to about $9 \times 10^{-3}$, $7 \times 10^{-3}$ and $2.1 \times 10^{-2}$ M sample concentrations at 436, 488 and 514 nm wavelengths. At the latter concentration, photoproducts can be detected if the sample is exposed to background light for more than 5 minutes. Therefore samples were prepared carefully in the dark.

Experiments without a quencher or with $Na[Cr(tn)(CN)_4]$ quencher were performed in $3 \times 10^{-2}$ M $HClO_4$ and/or $1 \times 10^{-3}$ $HClO_4$ acid. For a given extent of quenching, an estimated (using SV equation, $k_q = 3 \times 10^8$ $M^{-1}$ $s^{-1}$) amount of quencher is used and the emission lifetime of $Cr(tn)_3^{3+}$ was measured before and after adding the quencher. One example for an 90% estimated quenching, the measured lifetimes of $Cr(tn)_3^{3+}$, before and after photolysis were 2.3 ± 0.03 and 0.25 ± 0.02 μs respectively at 20°C. Calculation, assuming linear quenching shows that 90% of emission is indeed quenched. For higher extents (>90%) of quenching, emission lifetime measurements cannot be measured accurately but such measurements confirmed that ≥95% was quenched. Therefore the extent of quenching was estimated using SV equation only. For 99 and 100% quenching in $OH^-$, $1.1 \times 10^{-3}$ and $1.1 \times 10^{-1}$ M NaOH solutions were used ($k_q = 6 \times 10^{10}$ $M^{-1}$ $s^{-1}$).

If the samples in 1.1 x $10^{-1}$ M NaOH were directly injected into HPLC, under our eluent conditions (pH = 3.0), the chromatograms were somewhat distorted and broader peaks were observed. Therefore, the solutions were acidified, by mixing 400 μL of the solution with 20 μL of 2M $HClO_4$, prior to injection. The solution in 1.1 x $10^{-3}$ M NaOH, however, can be injected directly, without the acidification.

In most of the experiments the product ratio (D/E) was determined at different extents of conversion, usually between 3 and 8%. The total exposure times were less than 15 min, except in the case of quenched photolysis at 436 nm where the exposure time was ~35 min. The laser power at 488 and 514 nm was about 25 mW.

4.4.2b Results

488 and 514 nm are well separated wavelengths along the edge of the lowest energy quartet band of $Cr(tn)_3^{3+}$ (Fig. 4.4.4) whereas 436 nm is in the usual region of quartet excitation. Therefore, these wavelengths of excitation are suitable to test the "red edge" effect. The results corresponding to unquenched and quenched photolysis at these wavelengths are presented in Table 4.4.1.

At all three wavelengths, we get the same photoproduct distribution, ~38% D of (D + E) for the unquenched photoreaction. It was shown[63] that peak area ratio of D : E represents true D : E product ratio. Therefore, our chromatograms show that the ratio of major photoproducts is *cis* : *trans* = 38 : 62%. This is in agreement with the reported value (40 : 60%), within the experimental uncertainties.

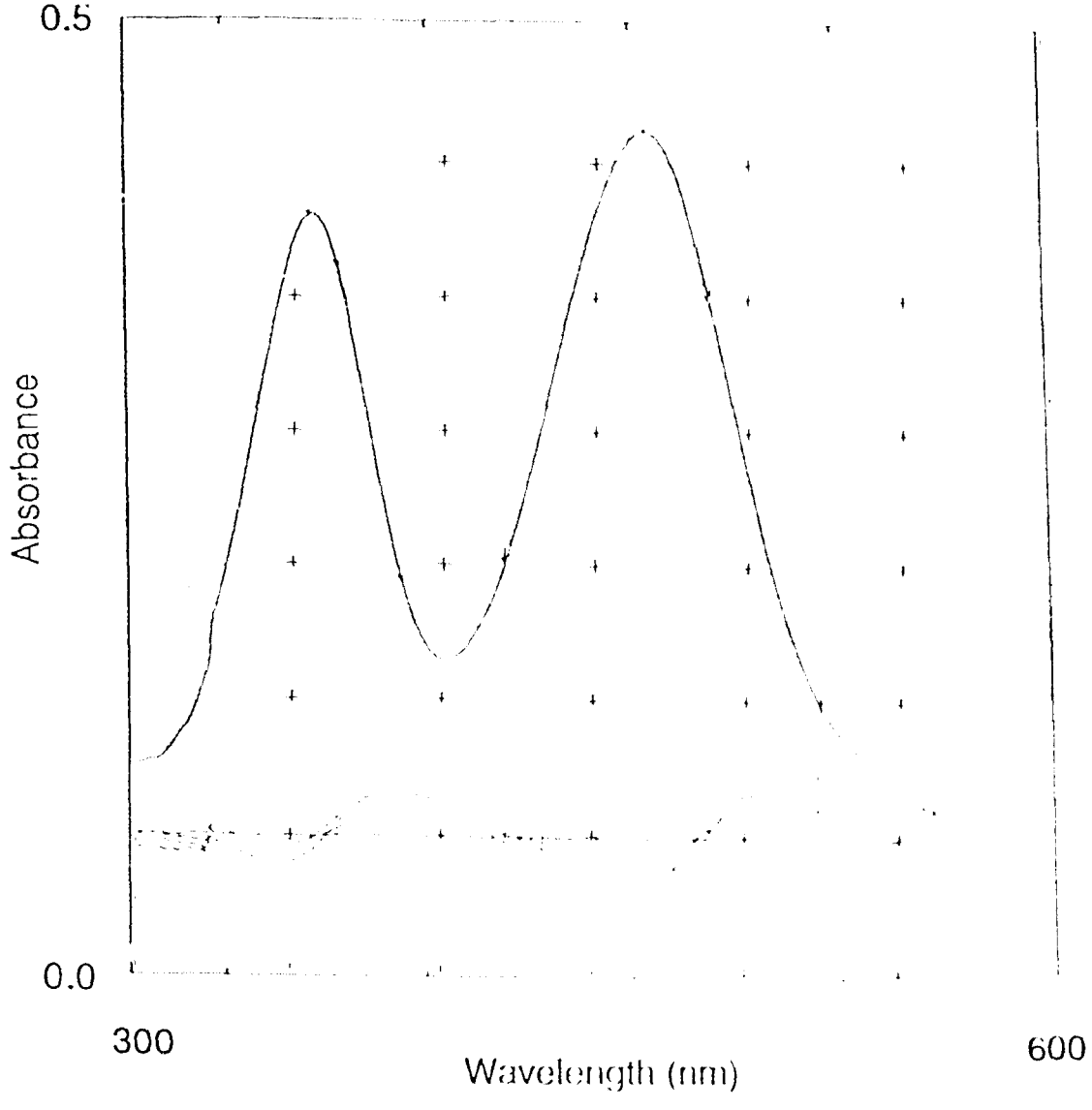


**Fig. 4.4.4** UV/Vis absorption and difference spectra on the photolysis of $Cr(tn)_3^{3+}$ in acidic aqueous solution at room temperature.

**Table 4.4.1** Results of the wavelength dependence studies of the prompt photoaquation of $Cr(tn)_3^{3+}$ with $Cr(tn)(CN)_4^-$ and $OH^-$ quenchers.

| Quencher | % quenching | % *cis* product | | |
|---|---|---|---|---|
| | | 436 nm | 488 nm | 514 nm |
| -- | 0 | 38 ± 1 (5) | 38 ± 1 (4) | 39 ± 1 (4) |
| -- | 0 | 40 ± 3[a] | 40 ± 3[a] | |
| $Cr(tn)(CN)_4^-$ | 97 | 45 ± 1 (3) | # | # |
| | 90 | 43 ± 1 (3) | 43 ± 1 (7) | # |
| $OH^-$ | 100 | 48 ± 2 (8) | 48 ± 2 (10) | 48 ± 2 (7) |
| | 100 | 62 ± 2[a] | | 73 ± 2[a] |
| | 99 | 48 ± 1 (4) | # | # |

[a] Kirk and Ibrahim's results.[97]

# These results could not be obtained due to the failure of the Argon ion laser. The number of runs corresponding to the mean and standard deviation of each run is given in parenthesis.

Photoreaction, where the doublet pathway is mostly quenched with $Cr(tn)(CN)_4^-$ (Fig. 4.4.5) shows an increase in percentage *cis* isomer in photoproducts . This increase is much smaller than the change from 40 to 62% cis product observed by Kirk and Ibrahim for hydroxide quenching. We also find no change in product distribution by changing the excitation wavelength to 488 nm for the photoreaction where 90% of the doublet pathway is quenched by $Cr(tn)(CN)_4^-$. Also if the quencher is added after the photolysis, the percentage cis isomer in photoproducts is equal to the value obtained for unquenched photoreaction (38 ± 1% *cis* isomer), confirming the product ratio measurement

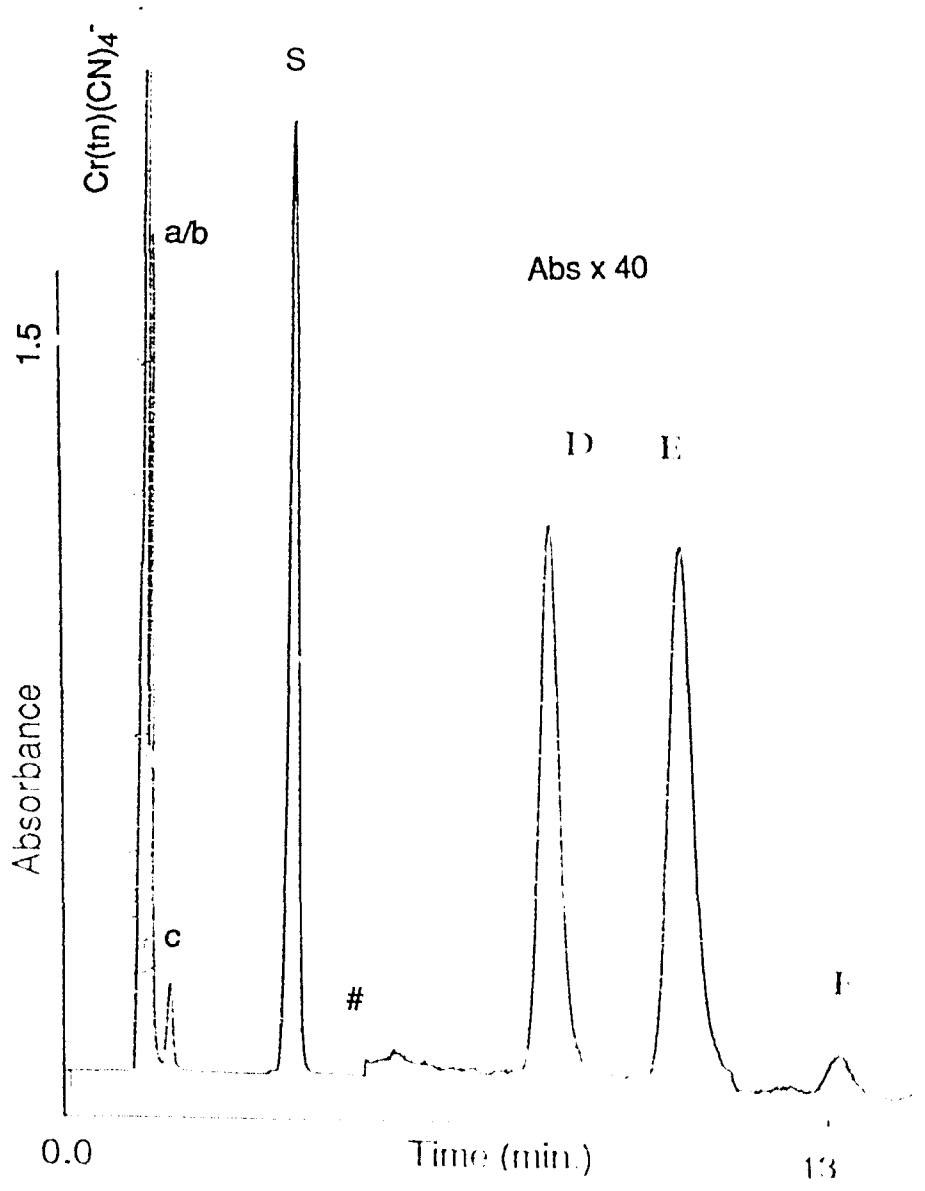


**Fig. 4.4.5** Chromatogram (HPLC) of $Cr(tn)_3^{3+}$ for 7 % photolysis with $Cr(tn)(CN)_4^-$ to quench 90 % of the doublet reaction.

**Key :** same as for Fig. 4.4.1 except that the first three peaks (< ? min) correspond to $Cr(tn)(CN)_4^-$ and its products (a, b, c of Fig. 4.4.3), # = scale change

**Conditions** : same as for Fig. 4.4.1.

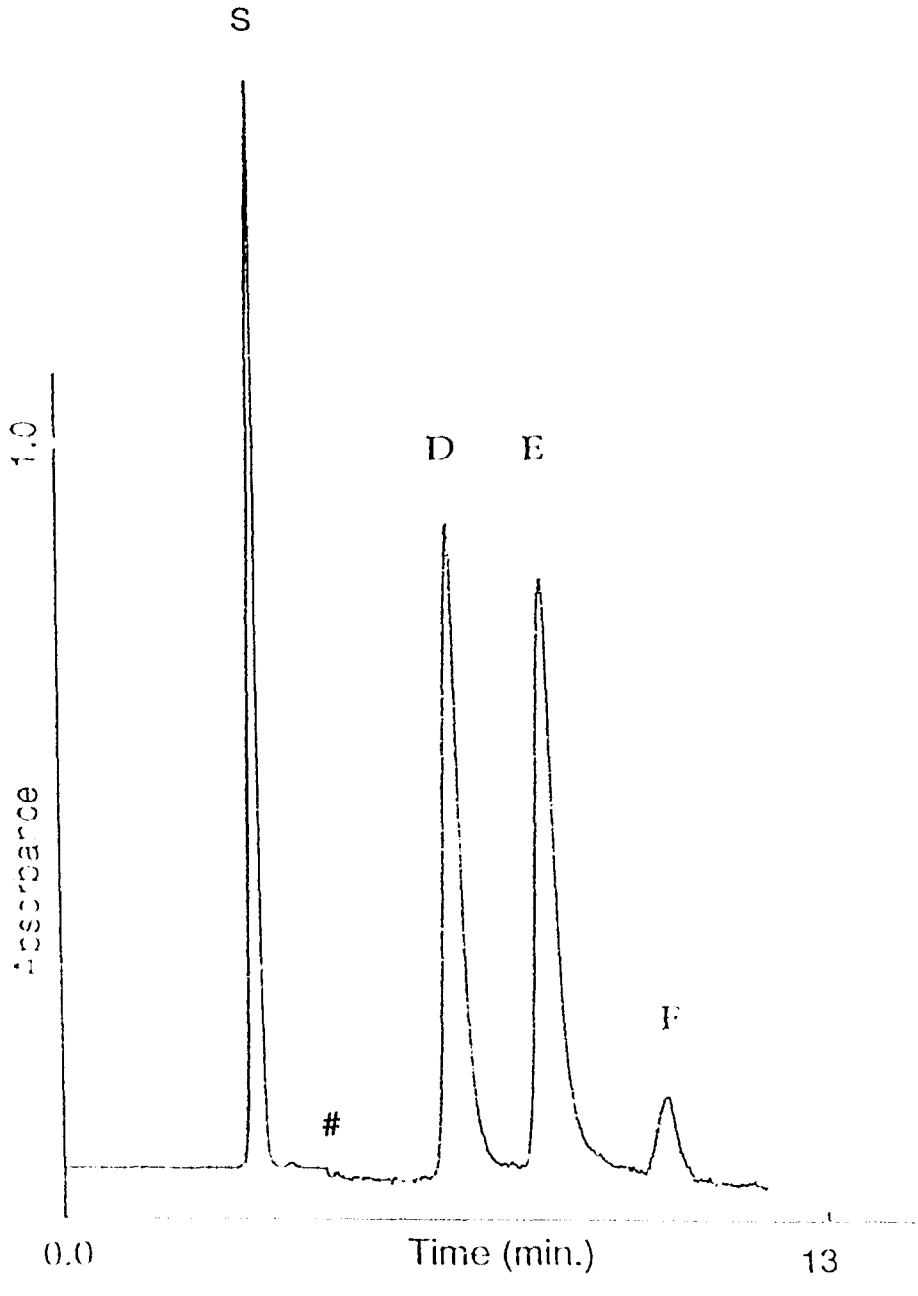


**Fig. 4.4.6** HPLC chromatograms of $Cr(tn)_3^{3+}$ for 6 % photolysis with $OH^-$ to quench 99 % of the doublet reaction.

**Key :** same as for Fig. 4.4.1

**Conditions** : same as for Fig. 4.4.1

with quenching is not complicated by effects like differential precipitation of photoproducts with the quencher.

With this background we reinvestigated Kirk and Ibrahim's results with $OH^-$ quenching, using our chromatographic conditions (Fig. 4.4.6). We find only 48 ± 2% *cis* isomer at all three wavelengths.

Therefore the increase in percentage *cis* isomer in photoproducts upon quenching the doublet pathway is smaller than reported, and a further increase of *cis* isomer upon increasing the excitation wavelength along the red edge of the UV/Vis spectrum ("Red edge effect") was not observed.

Due to technical reasons (breakdown of the Argon Ion Laser) it was not possible to measure the photoproduct distribution with $Cr(tn)(CN)_4^-$ quencher at 514 nm excitation. Despite this result it is notable that the percent cis isomer due to $OH^-$ and $Cr(tn)(CN)_4^-$ are the same with the experimental uncertainty. The latter is on the lower side, presumably because the extent of quenching is somewhat smaller than 100%. Therefore, it is reasonable to believe that the percent *cis* isomer in photoproducts of $Cr(tn)_3^{3+}$ due to the prompt reaction is about ~47%, independent of the quencher. Since slow component of $Cr(tn)_3^{3+}$ is about 78%, calculations# show that the percent cis isomer from the slow reaction only, is about 35%. Hence, there is a small (12%) change in photoproduct isomer distribution between the "prompt" and the "slow" reactions.

### 4.4.3 Discussion

A point of interest in our chromatographic conditions for analyzing $Cr(tn)_3^{3+}$ and its products is that it gives baseline resolved peaks for cationic

---

# If the % cis due to "slow" reaction is a, 0.78a + 0.22 x 47 = 38. Therefore a = 35%

species from 2+ to 5+ (inclusive) in one chromatogram. It is not usual for one chromatographic condition to separate ions with this much of a charge difference. The reason for this ability is precumably due to the presence of tnH+ ligands in all the species with ≥4+ overall charges. This "dangling" positive charge, residing on the non coordinated end of the amine, does not contribute fully to the charge seen by the chromatographic process (section 4.2.2.4). Therefore, "chromatographically effective charge" of tnH+ ligand can be considered as "(1/2)+". Hence, "chromatographically effective overall charge" on our 4+ (D and E), and 5+ (F) species would be "3(1/2)+" and "4+". Therefore it is feasible for these 4+ and 5+ species to appear under chromatographic conditions suitable for separating ions of 3+ and 4+.

Chromatographic (Ion Exchange) separation of 3+ ions from 4+ ions has been previously reported.[113] To our knowledge, however, this is the first occasion of the chromatographic appearance of a nicely separated 5+ ion from species with lower charge.

The observations of the additional photoproduct peaks (B and F) could have been considered as a simultaneous multimode photoreaction. The only instance a multimode photoreaction has been reported, is the proposal that $Cr(tn)_3^{3+}$ photochemically looses both ends of tn with a quantum yield of 0.04 . This work has since been disputed in literature.[63] We do not have data to eliminate the possible multimode reaction, but the analogy with other systems suggests that the likely situation is that secondary photolysis is occuring in the early stages of the reaction.

It was, however, not expected to have significant secondary photolysis at 436 or 488 nm photolysis since the absorbance of photoproducts at 436 nm is slightly less than $Cr(tn)_3^{3+}$ and at 488 nm their absorbance is the same

(Fig. 4.4.4). This indicates that photoproducts should have high quantum yields, to undergo secondary photolysis at low extents of photolysis.

The quantum yields of photoproducts can be estimated using the theory developed by Wirth and Linck.[128] They showed that, for the reaction (eq. 4.4.2)

$$A \xrightarrow{h\upsilon} B \xrightarrow{h\upsilon} C \qquad (4.4.2)$$

the following relationships can be derived

$$[C]_t / [B]_t = (T - 1 + f^T - Tf) / (f - f^T) \qquad (4.4.3)$$

where,

$$T = (\varepsilon_B \Phi_B) / (\varepsilon_A \Phi_A) \qquad (4.4.4)$$

and

$$f = [A]_t / [A]_0 \qquad (4.4.5)$$

In these expressions $[A]_t$, $[B]_t$ and $[C]_t$ are the concentrations of A, B and C at the photolysis time t. $[A]_0$ is the concentration of A before photolysis, $\varepsilon_A$ and $\varepsilon_B$ are molar absorptivities of A and B at the wavelength of excitation. $\Phi_A$ and $\Phi_B$ are quantum yields of A and B. Therefore f represents the unphotolysed fraction of A.

The equation 4.4.3 can be used in an iterative procedure using a computer program (written by Dr. A. D. Kirk) to find values of T and f that fit an observed $[C]_t / [B]_t$ ratio. Once a suitable T value is found for the observed f, $\Phi_B$ can be calculated using the equation 4.4.4 if $\Phi_A$ and $\varepsilon_B/\varepsilon_A$ ratio is known. The results based on these equations are independent of the sample absorbance at the excitation wavelength and the time of photolysis.[129]

Using HPLC analysis, a $Cr(tn)_3^{3+}$ sample photolysed to 12% conversion (f = 0.88) shows that the peak area ratio of all the secondary photoproducts to

the area of primary photoproducts, (B+F) / (D+E), is ≤ 0.13. If we assume the molar absorptivities of all B, D, E and F species at 228 nm detection wavelength are equal, this ratio corresponds to $[C]_t$ / $[B]_t$ ratio in equation 4.4.3. The computer iteration shows that the T value (corresponding to $[C_t]$ / $[B]_t$ = 0.13 (the upper limit) and f = 0.88) is 1.95. Assuming this molar absorptivity ratio is one and substituting $\Phi_A = \Phi(Cr(tn)_3^{3+}) = 0.14$ we get $\Phi_{photoproducts} = 0.27 \approx 0.3$.

It shows the observed extent of secondary photolysis is feasible, if the quantum yield of each photoproduct is ~0.3. This is a reasonable value for a Cr(III) complex. Therefore Worth & Link model predicts that the observed extent of secondary photolysis is favorable. (Further supporting data may be obtained if the photoproducts D and E are isolated and their thermo- and photolysis studied chromatographically)

This result indicates that, the usual expectation that secondary photolysis occurs only at high extents of photolysis is not always true. The photoproducts of $Cr(tn)_3^{3+}$, however, contrasts the photoreaction of *trans*-$Cr(2,3,2\text{-tet})(CN)_2^{+}$, where no significant photoproducts were observed up to a very high (50%) of photolysis.

Our results support that the percentage *cis* isomer in the photoproducts of $Cr(tn)_3^{3+}$ increases upon quenching the doublet pathway. However, the change we observe is much smaller than reported. The reason for Kirk and Ibrahim's results being different from ours is most probably because they did not have baseline resolved peaks and therefore the absolute value of the peak area ratio could be misleading. Since we had baseline resolved peaks and more sensitive chromatograms, we believe that the present results are more reliable.

Our experiments did not show any measurable increase in percentage *cis* isomer along the red edge, when the doublet pathway was quenched by $OH^-$ or $Cr(tn)(CN)_4^-$ quenchers. Therefore, we conclude that there is no red edge effect in the prompt photoaquation of $Cr(tn)_3^{3+}$. There is, however, a 12% difference, though small, in the percentage cis product due to the reaction from the doublet and the quartet pathways. Therefore, the result is still consistent with the claim "The difference arises because of the specific vibrational excitation of the Franck-Condon quartet state." Due to the absence of the red-edge effect, however, the above 12% difference in the percentage cis isomer can also be accounted for the fact that the doublet and quartet pathways do <u>not</u> necessarily go via the same precessor state.

# CHAPTER FIVE

## Conclusion

In this work we have used the stereochemical behavior of Cr(III) photoaquation reactions to investigate several mechanistic aspects of excited state processes. The new compound *trans*-[Cr(2,3,2-tet)$(CN)_2$]$ClO_4$ was used to investigate whether the stereochemical change is a requirement for equatorial ligand loss. Our attempts to investigate the prompt photoaquation of $[Cr(tn)_3]Cl_3$ in competition with the vibrational relaxation, were based on the new compounds *trans*-$[Cr(tn)_2(CN)_2]ClO_4$ and $Na[Cr(tn)(CN)_4]$. The ion pair RP-HPLC method was developed as the major analytical tool in all these investigations. The method was successful in establishing isomeric identity, and in qualitative and quantitative analysis of products. The major conclusions of the study are given below.

Despite our initial expectation, *trans*-Cr(2,3,2-tet)$(CN)_2^+$ complex is photolabile. It undergoes a stereoretentive photoreaction ($\Phi = 0.09$) with loss of a terminal primary amine end of the 2,3,2-tet ligand to produce *trans*-Cr(2,3,2-tetH)$(H_2O)(CN)_2^{2+}$ in acidic aqueous solutions. Therefore we conclude that stereochemical change is **not** a requirement for equatorial ligand loss.

The application of Vanquickenborne and Ceulemans theory and their Jahn-Teller approach to photostereochemistry show that the observed unusual stereoretentive photoreaction can be attributed to the presence of the 2,3,2-tet ligand in the molecule. The specific feature of the ligand causing this behavior could be the fact that the coordinated atoms are primary and secondary amines with different ligand field strengths and / or the coordinated amines are linked with short carbon chains. The ligand hinders usual reaction involving stereochemical change and consequently promotes a stereoretentive pathway.

Since the above result is attributed to the specific structure of the molecule, it cannot be used to draw any conclusions about the general behavior of equatorial ligand substitution of Cr(III) complexes. In order to investigate this aspect and to study the questions emerged during this study, the following future work can be proposed.

It is important to study the photostereochemistry of other similar complexes. *Trans*-Cr(3,2,3-tet)$(CN)_2^+$ [130] is an ideal example for this purpose. The number of molecules suitable for this purpose is, however, limited. The following experiments are suitable in principle but they could be difficult synthetically and analytically. It will be interesting to use a complex analogous to the title compound, but with linking carbon chains long enough to allow the ligand motion for stereochemical change. Moreover, It would be interesting to study the photochemistry of analogous compounds that do not have the linkage between coordinated am(m)ines at all. While *trans*-Cr$(NH_3)_4(CN)_2^+$ has already been investigated, the following compounds; *trans*-Cr$(CH_3NH_2)_4(CN)_2^+$, 1,6-CN-2.4-$NH_3$-Cr$(CH_3NH_2)_2(NH_3)_2(CN)_2^+$ and 1,6-CN-2,5-$NH_3$-Cr$(CH_3NH_2)_2(NH_3)_2(CN)_2^+$; which are close unlinked analogs to the title compound, are yet to be studied.

It would be possible to check whether the presence of primary and secondary amines in 2,3,2-tet ligand would have any effect on driving the stereoretentive reaction, by using analogous compounds where the terminal ends are also secondary amines ( e.g. 2,3,2-tet$(CH_3)_2$ ligand).

The photoreaction of *trans*-Cr(2,3,2-tet)$(CN)_2^+$ goes completely via the doublet excited state and, in contrast to the analogous *trans*-Cr$(NH_3)_4(CN)_2^+$, it does not produce the ***cis***-Cr(2,3,2-tet)$(H_2O)(CN)_2^+$ product expected to arise from the higher lying $^4E$ state. We have attributed this behavior to the high

doublet/quartet and $^4B_2/^4E$ energy gaps perhaps implying that $^4E$ reaction for analogous compounds is observable only if they show a prompt reaction. This can be investigated by measuring the percentage slow component of *trans*-$Cr(NH_3)_4(CN)_2^+$. Depending on this result, a quenching experiment [as was done for *trans*-$Cr(NH_3)_4(CN)(NCS)^+$,[58]] to investigate the photoproduct ratio arrising by the "slow" and "fast" components of the reaction, in parallel with the title compound, may provide further information on the mechanistic pathway of the photochemical reaction. Also the comparison of photoproducts and the percentage reactions via the doublet states of $Cr(CH_3NH_2)_2(NH_3)_2(CN)_2^+$ complexes described above, for the title compound and *trans*-$Cr(NH_3)_4(CN)_2^+$ would be informative.

Another aspect, important with respect to interpretation of results presented here, is to investigate whether the reaction takes a dissociative or associative pathway. This problem can be studied by volume of activation measurements for the photoreaction of the title molecule.

The observed new phenomena of the pH dependence of the rate constant of recoordination was studied only at three pH values. In order to investigate this behavior, it is desirable to obtain a complete curve of k(recoordination) versus pH. Further work on this can be done for complexes with mono-coordinated en or tn type ligands. While such species are difficult to make thermally, they can be obtained easily by photolysing compounds like $Cr(en)_3^{3+}$ or $Cr(tn)_3^{3+}$.

We have chosen *trans*-$[Cr(tn)_2(CN)_2]ClO_4$ as a suitable molecule to carry out wavelength dependence studies. This compound undergoes photoaquation of both cyanide and tn ligands in acidic aqueous media to produce *trans*-$Cr(tn)(tnH)(H_2O)(CN)_2^{2+}$ (A). *cis*-$Cr(tn)(tnH)(H_2O)(CN)_2^{2+}$ (B),

and *cis*-$Cr(tn)_2(H_2O)(CN)^{2+}$ (C) with a total quantum yield of 0.09. The major (A) and minor (B and C) photoproducts were assigned to the products via $^4B_2$ and $^4E$ states respectively. The compound shows a strong emission band centered at 703 nm, with a very long lifetime of 185 μs at room temperature aqueous solutions.

The cyanide loss mode is about 35% of the total reaction and this mode is not predicted by Vanquickenborne and Ceulemans theory of ligand labilization. We have attributed this behavior to the poor leaving ability of tn which promotes the other reaction modes.

The photoreaction is non-linear, where the apparent total quantum yield decreases with the extent of photolysis. This interesting new phenomenon was shown to be caused by quenching of the doublet reaction pathway by its own thermo- and photoproducts. The reasons for this behavior have been attributed to the long emission life-time, the presence of conducting ligands and low charges on the reactants and products. We believe this phenomenon could be rather general, especially for complexes with long lifetimes. Such a complication may affect other systems and may have been overlooked due to analytical difficulties. This quenching behavior, though novel and interesting, makes *trans*-$Cr(tn)_2(CN)_2^+$ rather unsuitable for the intended wavelength dependence studies.

We have shown that $Na[Cr(tn)(CN)_4]$ shows the necessary thermo- and photostability, high efficiency of quenching, high solubility and nominal analytical interference, to be a good quencher for energy transfer quenching studies of transition metal complexes. Also we have found that the light absorption by $Cr(tn)(CN)_4^-$ in the wavelength region of interest corresponding to

the lowest energy quartet excitation band of $Cr(tn)_3^{3+}$, is minimal and therefore it is a suitable quencher to investigate the "red-edge effect."

The chromatograms for the analysis of the photoreaction of $Cr(tn)_3^{3+}$ were improved to obtain well base-line resolved peaks. They are sensitive in detecting peaks and can be used conveniently to produce more accurate and precise results of the photoproduct peaks ratio. Our chromatograms also show the separation of a 5+ ion from complexes with lower charge.

HPLC analysis shows that the photoaquation of $Cr(tn)_3^{3+}$ undergoes secondary photolysis from the very early stages of the reaction. Assuming equal molar absorptivities at the detection wavelength (228 nm), it was shown that photoproducts present at 10% conversion of $Cr(tn)_3^{3+}$, have undergone about ~10% of secondary photolysis. This result indicates that the usual expectation for secondary photolysis to occur only at high extents of photolysis is not always true.

We find the percentage *cis* isomer of photoproducts produced by the prompt reaction is about 12% higher than for the reaction via the doublet state. This difference is, however, much smaller than the earlier reported value. Despite this discrepancy (which could be due to the use of chromatograms with incompletely resolved peaks in the previous report), we observe the same directional variation supporting the previous finding. Therefore, this result is consistent with the previous interpretation that the photoreaction is competitive with vibrational relaxation. Our data, however, failed to reproduce the "red-edge effect" reported for photoaquation of $Cr(tn)_3^{3+}$. Therefore, the above 12% difference in the percentage cis isomer can also be accounted for the fact that the doublet and quartet pathways do <u>not</u> necessarily go via the same precessor state.

Our success in using the ion pair RP-HPLC technique to study many aspects described in this dissertation, along with most of the recent work in our research group, demonstrates the power of this method. Due to the use of the UV/Vis detector, however, the peak area ratio of all the peaks does not reflect the real ratio of chemical species since the molar absorptivities can be different. This makes peaks identification and quantitative analysis more uncertain. Therefore, developing a detection method which would provide a good correlation with the peak area ratio with the chemical species will enhance the value of this method. An excellent approach would be use of Atomic Absorption detector for chromium.

In conclusion, our investigation of the photochemistry of *trans*-Cr(2,3,2-tet)$(CN)_2^+$ and the wavelength dependence of $Cr(tn)_3^{3+}$ photoreaction provides additional insights on the mechanism and the excited state participation of Cr(III) complexes. Overall, the present work, demonstrates the value of the use of stereochemistry to investigate the mechanistic aspects of the photoaquation reactions of Cr(III) complexes.

# REFERENCES


(1) Balzani, V.; Moggi, L., *Coord. Chem. Rev.* **1990**, *97*, 313.

(2) Carassiti, V., *Coord. Chem. Rev.* **1993**, *125*, 351.

(3) Sykora, J.; Sima, J., *Coord. Chem. Rev.* **1990**, *107*, 1.

(4) Balzani, V., *Tetrahedron* **1992**, *48*, 10443.

(5) Balzani, V.; Ballardini, R.; Bolletta, F.; Gandolfi, M.T.; Juris, A.; Maestri, M.; Manfrin, M.F.; Moggi, L.; Sabbatini, N., *Coord. Chem. Rev.* **1993**, *125*, 75.

(6) Kirk, A.D., *Comments Inorg. Chem.* **1993**, *14*, 89.

(7) Moensted, L.; Moensted, O., *Coord. Chem. Rev* **1989**, *94*, 109.

(8) Endicott, J.F.; Ramasami, T.; Tamilarasan, R.; Lessard, R.B.; Ryu, C.K., *Coord. Chem. Rev.* **1987**, *77*, 1.

(9) Jamieson, M.A.; Serpone, N.; Hoffman, M.Z., *Coord. Chem. Rev.* **1981**, *39*, 121.

(10) Hollebone, B.R.; Langford, C.H.; Serpone, N., *Coord. Chem. Rev.* **1981**, *39*, 181.

(11) Kirk, A.D., *Coord. Chem. Rev.* **1981**, *39*, 225.

(12) Zinato, E. "Substitutional Photochemistry of First-Row Transition Elements." Concepts of Inorganic Photochemistry. Adamson, A. W. ; Fleischauer, P. D. ed. **1975** John Wiley & Sons, Inc. New York, London, Sydney, Toronto.

(13) Balzani, V.; Carassiti, V. *Photochemistry of Coordination Compounds*; Academic Press: London and New York, **1970.**

(14) Lever, A.B.P. *Inorganic Electronic Spectroscopy*; Elsevier: Amsterdam, Oxford, New York, Tokyo, **1984.**

(15) Zinato, E., *Coord. Chem. Rev.* **1993**, *00*, 00.

(16) Kirk, A.D.; Guedel, H.U., *Inorg. Chem.* **1992**, *31*, 4564.

(17) Ricciori, P.; Zinato, E.; Prelati, M., *Inorg. Chem.* **1981**, *20*, 1432.

(18) Vanquickenborne, L.G.; Ceulemans, A., *J. Am. Chem. Soc.* **1977**, *99*, 2208.

(19) Adamson, A.W. "Photochemistry and Chemiluminescence." Concepts of Inorganic Photochemistry. Adamson, A. W. , Fleischauer, P. D. ed. **1975** Wiley-Interscience. New York, London, Sydney, Toronto.

(20) Zinato, E., *J. Am. Chem. Soc.* **1969**, *91*, 1076.

(21) Adamson, A.W., *J. Phys. Chem* **1967**, *71*, 798.

(22) Pribush, R.A.; Poon, C.K.; Bruce, C.M.; Adamson, A.W., *J. Am. Chem. Soc.* **1974**, *96*, 3027.

(23) Kirk, A.D.; Frederick, L.A., *Inorg. Chem.* **1981**, *20*, 60.

(24) Pyke, S.C.; Link, R.G., *J. Am. Chem. Soc.* **1971**, *93*, 5281.

(25) Zink, J.I., *J. Am. Chem. Soc.* **1972**, *94*, 8039.

(26) Zink, J.I., *Mol. Photochem.* **1973**, *5*, 151.

(27) Wrighton, M.; Gray, H.B.; Hammond, G.S , *Mol. Photochem.* **1973**, *5*, 165.

(28) Zink, J.I., *J. Am. Chem. Soc.* **1974**, *96*, 4464.

(29) Vanquickenborne, L.G.; Ceulemans, A., *Coord. Chem. Rev.* **1983**, *48*, 157.

(30) Riccieri, P.; Zinato, E.; Damiani, A., *Inorg. Chem.* **1988**, *27*, 3755.

(31) Kirk, A.D., *J. Am. Chem. Soc.* **1971**, *93*, 283.

(32) Manfrin, M.F.; Moggi, L.; Balzani, V., *Inorg. Chem.* **1971**, *10*, 207.

(33) Kirk, A.D.; Moss, K.C.; Valentin, J.G., *Can. J. Chem.* **1971**, *49*, 1525.

(34) Rosebush, W.J.; Kirk, A.D., *Can. J. Chem.* **1976**, *54*, 2335.

(35) Gandolfi, M.T.; Manfrin, M.F.; Moggi, L.; Balzani, V., *J. Am. Chem. Soc.* **1972**, *94*, 7152.

(36) Kirk, A.D., *Mol. Photochem.* **1973**, *5*, 127.

(37) Vanquickenborne, L.G.; Ceulemans, A., *J. Am. Chem. Soc.* **1978**, *100*, 475.

(38) Vanquickenborne, L.G.; Ceulemans, A., *Inorg. Chem.* **1978**, *17*, 2730.

(39) Vanquickenborne, L.G.; Coussens, B.; Postelmans, D.; Ceulemans, A.; Pierloot, K., *Inorg. Chem.* **1992**, *31*, 539.

(40) Zinato, E.; Riccieri, P.; Adamson, A.W., *Inorg. Chem.* **1974**, *96*, 375.

(41) Wong, C.F.C.; Kirk, A.D., *Inorg. Chem.* **1976**, *15*, 1519.

(42) Vanquickenborne, L.G.; Coussens, B.; Postelmans, D.; Ceulemans, A.; Pierloot, K., *Inorg. Chem.* **1992**, *31*, 539.

(43) Ceulemans, A. "Orbital Models and the Photochemistry of Transition-Metal complexes." Vibronic Processes in Inorganic Chemistry. Flint, C. D. ed. **1988** Kluwer Academic. Dordrecht, Boston, London.

(44) Krause, H.H.; Wasgestian, F., *Inorg. Chim. Act.* **1978**, *29*, 231.

(45) Krause, H.H.; Wasgestian, F., *Inorg. Chim. Act.* **1981**, *49*, 231.

(46) Langford, C.H.; Tong, J.P.K., *J. Chem. Soc. Chem. Commun.* **1977**, 138.

(47) Angermann, K.; Eldik, R.V.; Kelm, H.; Wasgestian, F., *Inorg. Chem.* **1981**, *20*, 956.

(48) Angermann, K.; Eldik, R.V.; Wasgestian, F., *Inorg. Chem. Act.* **1981**, *49*, 247.

(49) Waltz, W.L.; Lee, S.H.; Friesen, D.A.; Lilie, J., *Inorg. Chem.* **1988**, *27*, 1132.

(50) Vincze, L.; Friesen, D.A.; Mezyk, S.P.; Waltz, W.L., *Inorg. Chem.* **1992**, *31*, 4950.

(51) Riccieri, P.; Zinato, E., *Inorg. Chem.* **1980**, *19*, 3279.

(52) Zinato, E.; Riccieri, P.; Prelati, M., *Inorg. Chem.* **1981**, *20*, 1432.

(53) Kirk, A.D.; Porter, G.B., *Inorg. Chem.* **1980**, *19*, 445.

(54) Kane-Maguire, N.A.P.; Crippen, W.S.; Miller, P.K., *Inorg. Chem.* **1983**, *22*, 696.

(55) Kane-Maguire, N.A.P.; Wallace, K.C.; Corbranchi, D.P.; Derrick, J.M.; Speece, D.G., *Inorg. Chem.* **1986**, *25*, 2101.

(56) Riccieri, P.; Zinato, E., *Inorg. Chem.* **1990**, *29*, 5035.

(57) Riccieri, P.; Zinato, E., *Polyhedron* **1992**, *11*, 71.

(58) Riccieri, P.; Zinato, E.; Damiani, A., *Inorg. Chem.* **1987**, *26*, 2667.

(59) Forster, L.S., *Chem. Rev.* **1990**, *80*, 331.

(60) Forster, L.S., *Adv. Photochem.* **1991**, *16*, 215.

(61) Walters, T.T.; Adamson, A.W., *Acta Chem. Scand. A* **1979**, *33*, 53.

(62) Zinato E.; Riccieri, P., *Coord. Chem. Rev* **1993**, *125*, 35.

(63) Kirk, A.D.; Ibrahim, A.M., *Inorg. Chem.* **1988**, *27*, 4567.

(64) Kirk, A.D.; Porter, G.B., *J. Phys. Chem.* **1980**, *84*, 887.

(65) Zinato, E.; Adamson, A.W., *J. Phys. Chem.* **1985**, *89*, 839.

(66) Kane-Maguire, N.A.P.; Crippen, W.S.; Miller, P.K., *Inorg. Chem.* **1983**, *22*, 2972.

(67) Kirk, A.D.; Fernando, S.R.L., *Coord. Chem. Rev.* **1993**, *00*, 00.

(68) Kirk, A.D.; Fernando, S.R.L., *Inorg. Chem.* **1991**, *31*, 656.

(69) Garner, C.S.; House, D.A. "Amine Complexes of Chromium(III)." Transition Metal Chemistry. Carlin, R. L. ed. **1970** Marcel Dekker Inc. New York.

(70) House, D.A., *Coord. Chem. Rev.* **1977**, *23*, 223.

(71) Colton, R., *Coord. Chem. Rev.* **1985**, *62*, 85.

(72) Colton, R., *Coord. Chem. Rev.* **1988**, *90*, 1.

(73) Riccieri, P.; Zinato, E., *Inorg. Chem.* **1980**, *19*, 853.

(74) Riccieri, P.; Zinato, E., *Inorg. Chem.* **1981**, *20*, 3722.

(75) Riccieri, P.; Zinato, E., *Inorg. Chem.* **1985**, *24*, 441.

(76) Edwards, J.O.; Monacelli, F.; Orgatti, G , *Inorg. Chim. Acta* **1974**, *11*, 47.

(77) Riccieri, P.; Zinato, E., *Inorg. Chem.* **1981**, *20*, 3722.

(78) Kane-Maguire, N.A.P.; Bennett, J.A.; Miller, P.K., *Inorg. Chim. Acta* **1983**, *76*, L123.

(79) Kutal, C.; Adamson, A.W., *J. Am. Chem. Soc.* **1971**, *93*, 5581.

(80) Kutal, C.; Adamson, A.W., *Inorg. Chem.* **1973**, *12*, 1990.

(81) Ferraudi, G.J. *Elements of Inorganic Photochemistry*; Wiley-Intersciences: New York, Chichester, Brisbane, Toronto, Singapore, **1988**.

(82) Waltz, W.L.; Lilie, J.; Lee, S.H., *Inorg. Chem.* **1984**, *23*, 1768.

(83) Kirk, A.D.; Scandola, M.A. ., *J. Phys. Chem.* **1982**, *86*, 4141.

(84) Kirk, A.D.; Frederick, L.A.; Wong, C.F.C., *Inorg. Chem.* **1979**, *18*, 448.

(85) Kane-Maguire, N.A.P.; Wallace, K.C.; Miller, D.B., *Inorg. Chem.* **1985**, *24*, 597.

(86) Riccieri, P.; Zinato, E., *J. Am. Chem. Soc.* **1975**, *97*, 6071.

(87) Rosebush, W.J.; Kirk, A.D., *Can. J. Chem.* **1976**, *54*, 2335.

(88) Kirk, A.D.; Heyd, D., *Inorg. Chem.* **1991**, *30*, 2453.

(89) Hollebone, B.R., *Theor. Chim. Acta* **1980**, *56*, 45.

(90) Chen, S.N.; Porter, G.B., *Chem. Phys. Lett.* **1970**, *6*, 41.

(91) Langford, C.H., *Can. J. Chem.* **1972**, *50*, 887.

(92) Ballardini, R.; Varani, G.; Wasgestian, H.F.; Moggi L.; Balzani, V., *J. Phys. Chem.* **1973**, *77*, 2947.

(93) Wasgestian, H.F., *J. Phys. Chem.* **1972**, *76*, 1947.

(94) Kane-Maguire, N.A.P.; Phifer, J.E.; Toney, C.J., *Inorg. Chem* **1976**, *15*, 193.

(95) Kirk, A.D.; Hoggard, P.E.; Porter, G.B.; Rockley, M.G.; Windsor, M.W., *Chem. Phys. Lett.* **1976**, *37*, 199.

(96) Rojas, G.E.; Dupuy, C.; Sexton, D.A.; Magde, D., *J. Phys. Chem.* **1986**, *90*, 87.

(97) Kirk, A.D.; Ibrahim, A.M., *Inorg. Chem.* **1990**, *29*, 4848.

(98) Vaughn, J.W.; Stvan, O.J.; Magnuson, V.E., *Inorg. Chem.* **1968**, *7*, 736.

(99) Fee, W.W.; Harrowfield, J.N.M.B.; Jackson, W.G., *J. Chem. Soc. A* **1970**, 2612.

(100) Nakano, M.; Kawaguchi, S., *Inorg. Chem.* **1979**, *74*, 179.

(101) House, D.A.; Yang, D., *Inorg. Chim. Acta.* **1983**, *74*, 179.

(102) Kirk, A.D.; Hewavitharana, A.K., *Anal. Chem.* **1988**, *60*, 797.

(103) Demas, J.N. *Excited State Lifetime Measurements*; Academic Press: New York and London, **1983**.

(104) Parker, C.A. "Measurement of Light by Chemical Methods." Photoluminescence of Solutions. **1968** Elsevier Publishing Company. Amsterdam, London, New York.

(105) Kirk, A.D.; Namasivayam, C., *Anal. Chem.* **1983**, *55*, 2428.

(106) Demas, J.N.; Bowman, W.D.; Zalewoski, E.F.; Velapoldi, R.A., *J. Phys. Chem.* **1981**, *85*, 2766.

(107) Hamai, S.; Hirayama, F., *J. Phys. Chem.* **1983**, *87*, 83.

(108) Gowin, E.; Wasgestian, F., *Inorg. Chem.* **1985**, *24*, 3106.

(109) Press, W.H.; Flannery, B.P.; Teukolsky, S.A.; Vetterling, W.T. "Modelling of Data." Numerical Recipes in Pascal. **1989** Cambridge University Press. Cambridge, New York, Port Chester, Melbourne, Sydney.

(110) Riccieri, P.; Zinato, E., *Inorg. Chim. Acta* **1990**, *177*, 147.

(111) Kaizaki, S.; Hikada, M.J.; Shimura, M.J., *Bull. Chem. Soc. Jpn.* **1975**, *48*, 902.

(112) Sattelberger, A.P.; Darsow, A.; Schaap, W.D., *Inorg. Chem.* **1976**, *15*, 1412.

(113) Cimolino, M.C.; Shipley, N.J.; Linck, R.G., *Inorg. Chem.* **1980**, *19*, 3291.

(114) Vanquickenborne, L.G.; Ceulemans, A., *Inorg. Chem.* **1979**, *18*, 3475.

(115) Wong, C.F.C.; Kirk, A.D., *Inorg. Chem.* **1977**, *16*, 3148.

(116) Jamieson, M.A.; Serpone, N.; Hoffman, M.Z., *J. Am. Chem. Soc.* **1983**, *105*, 2933.

(117) Kirk, A.D., *Private communication* **1993**.

(118) Kirk, A.D.; Wong, C.F.C., *Inorg. Chem.* **1979**, *18*, 593.

(119) Sasseville, R.; Langford, C.H., *J. Am. Chem. Soc.* **1979**, *101*, 5835.

(120) Kirk, A.D.; Frederick, L.A.; Glover, S.G., *J. Am. Chem. Soc* **1980**, *102*, 7120.

(120b) Cimolino, M.C.; Link R.G., *Inorg. Chem.* **1981**, *20*, 3499

(120c) Zinato, E.; Adamson, A.W.; Reed J.L., *Inorg. Chem.* **1984**, *23*, 1138

(120d) Sandrini, D.; Gandolfi, M. T.; Juris, A.; Balzani, V., *J. Am. Chem. Soc.* **1977**, *3*, 4324

(121) Kirk, A.D.; Namasivayam, C.; Ward, T., *Inorg. Chem.* **1986**, *25*, 2225.

(122) Hughes, M.N.; McWhinnie, W.R., *J. Chem. Soc. A* **1967**, 592.

(123) Wong, C.F.C.; Kirk, A.D., *Can. J. Chem.* **1975**, *53*, 3388.

(124) Kirk, A.D., *J. Chem. Edu.* **1983**, *60*, 853.

(125) Pfeil, A., *J. Am. Chem. Soc.* **1971**, *93*, 5395.

(126) Chiang, A.; Adamson, A.W., *J. Phys. Chem.* **1968**, *72*, 3827.

(127) Spees, S.T.; Adamson, A.W., *Inorg. Chem.* **1962**, *1*, 531.

(128) Wirth, G.; Linck, R.G., *J. Am. Chem. Soc.* **1973**, *95*, 5913.

(129) Wong, C.F.C.; A.D.Kirk, *Inorg. Chem.* **1976**, *15*, 1519.

(130) Kaizaki, S.; Takemoto, H., *Inorg. Chem.* **1990**, *29*, 4960.